Flückiger, Matthias; Larch, Mario; Ludwig, Markus; Pascali, Luigi

Working Paper

The Dawn of Civilization: Metal Trade and the Rise of Hierarchy

CESifo Working Paper, No. 10929

Provided in Cooperation with:
Ifo Institute – Leibniz Institute for Economic Research at the University of Munich

Suggested Citation: Flückiger, Matthias; Larch, Mario; Ludwig, Markus; Pascali, Luigi (2024) : The Dawn of Civilization: Metal Trade and the Rise of Hierarchy, CESifo Working Paper, No. 10929, Center for Economic Studies and ifo Institute (CESifo), Munich

This Version is available at:
https://hdl.handle.net/10419/296018

CESifo WORKING PAPERS

10929
2024

January 2024

The Dawn of Civilization: Metal Trade and the Rise of Hierarchy

Matthias Flückiger, Mario Larch, Markus Ludwig, Luigi Pascali

CESifo

Impressum:

CESifo Working Papers
ISSN 2364-1428 (electronic version)
Publisher and distributor: Munich Society for the Promotion of Economic Research - CESifo GmbH
The international platform of Ludwigs-Maximilians University's Center for Economic Studies and the ifo Institute
Poschingerstr. 5, 81679 Munich, Germany
Telephone +49 (0)89 2180-2740, Telefax +49 (0)89 2180-17845, email office@cesifo.de
Editor: Clemens Fuest
https://www.cesifo.org/en/wp
An electronic version of the paper may be downloaded
· from the SSRN website: www.SSRN.com
· from the RePEc website: www.RePEc.org
· from the CESifo website: https://www.cesifo.org/en/wp

CESifo *Working Paper No. 10929*

The Dawn of Civilization: Metal Trade and the Rise of Hierarchy

Abstract

In the latter half of the fourth millennium BC, our ancestors witnessed a remarkable transformation, progressing from simple agrarian villages to complex urban civilizations. In regions as far apart as the Nile Valley, Mesopotamia, Central Asia, and the Indus Valley, the first states appeared together with writing, cities with populations exceeding 10,000, and unprecedented socio-economic inequalities. The cause of this "Urban Revolution" remains unclear. We present new empirical evidence suggesting that the discovery of bronze and the ensuing long-distance trade played a crucial role. Using novel panel data and 2SLS techniques, we demonstrate that trade corridors linking metal mines to fertile lands were more likely to experience the Urban Revolution. We propose that transit bottlenecks facilitated the emergence of a new taxing elite. We formally test this appropriability theory and provide several case studies in support.

JEL-Codes: D020, F100, H100, N400, O430.

Keywords: urban civilizations, long-distance trade, metal trade, transit bottlenecks.

Matthias Flückiger
University of York / United Kingdom
matthias.flueckiger@york.ac.uk

Mario Larch
University of Bayreuth / Germany
mario.larch@uni-bayreuth.de

Markus Ludwig
TU Braunschweig / Germany
markus.ludwig@tu-braunschweig.de

Luigi Pascali
Universitat Pompeu Fabra
Barcelona / Spain
luigi.pascali@upf.edu

January 25, 2024
We thank seminar audiences at Autonoma Barcelona, Autonoma Madrid, Bocconi, Boston College, Bayreuth, CEMFI, Dartmouth, Drexel, George Mason University, Georgetown, Harvard, LUISS, Maastricht University, University of Michigan, New York University, University of Pennsylvania, Pompeu Fabra University, Princeton, Stanford, University of Southern California, Toulouse, UCLA, Yale, and University of York. We also thank participants at the following workshops: CEPR Political Economy and Institutions workshop (2023), USC Trade Miniconference (2023), Princeton IES Summer Trade Workshop (2023). For helpful comments we would like to thank Ran Abramitzky, Treb Allen, Jim Anderson, Costas Arkolakis, Gojko Barjamovic, Sascha Becker, Daniel Bernhofen, Leah Boustan, Thomas Chaney, Kerem Cosar, Mark Dincecco, James Fenske, Raquel Fernandez, Martin Fiszbein, Jeffry Frieden, Teresa Fort, Elhanan Helpman, Oded Galor, Edward Glaeser, Claudia Goldin, Gene Grossman, Stephan Heblich, Leander Heldring, Elhanan Helpman, Noel Johnson, John McLaren, Stelios Michalopoulos, Omer Moav, Mushfiq Mobarak, Ian Morris, David Nagy, Josh Ober, Giacomo Ponzetto, Lorenz Rahmstorf, Steve Redding, Jose-Antonio Espin-Sanchez, Michael E. Smith, Mara Squicciarini, Robert Staiger, Guido Tabellini, Jaume Ventura, Jesus Fernandez-Villaverde, Joachim Voth, and Yoto Yotov, Romain Wacziarg, David Weil. Finally, we thank an incredible team of research assistants: Maria Jose Aguirre Gomez, Anastasia Bunke, Beth Finlaysochikova, Oliver Hanney, Frederic Heise, Alla Iaguadeva, Marina Lizano, Carlos Maroto, Jospeh Moeschl, Florian Mueller, Precious Odusanya, Jiaxuan Ren, and Sebastian Thiem. Luigi Pascali acknowledges financial support from the EU through the ERC Consolidator (ROOTS_101088889) and from the Spanish Ministry of Economy and Competitiveness, through the Severo Ochoa Programme for Centres of Excellence in R&D (CEX2019-000915-S).

1 Introduction

During the latter half of the fourth millennium BC, a remarkable transformation in human societal structures took place. Simple agrarian villages evolved into complex, urban civilizations. The seeds of this transformation can be traced back to around 9000 BC, when the advent of agriculture set off a demographic explosion and spurred the rise of the first large farming settlements. Yet, it wasn't until the fourth millennium BC that state-level societies began to emerge, marked by the emergence of monumental buildings, the appearance of writing, and the rise of bustling urban centers housing over 10,000 residents. This dramatic shift was eloquently encapsulated by Childe's term the "Urban Revolution" (see Childe, 1950). Within less than a millennium, the defining elements of this revolution materialized in far apart regions, stretching from the Nile Valley and Mesopotamia to the distant landscape of Central Asia and the Indus Valley. Not long after, a comparable transition happened in Anatolia, China, Greece, and the broader Mediterranean basin. The emergence of the Urban Revolution raises intriguing, fundamental questions. What caused this transition? Why did it emerge in some regions but not in others? These are fundamental questions in the social sciences. In fact, modern social sciences, from the work of the moral philosophers Thomas Hobbes, John Locke and Jean-Jacques Rousseau, started by investigating the origins of political inequalities and complex hierarchies. But these are also key questions in the comparative development literature as an early start in the civilization process has been posited as an important determinant in explaining the relative economic success of nations today[1]. The objective of this paper is to propose a theory aimed at addressing these research questions in the context of the Old World and to test this theory using novel data and a series of natural experiments of history.

We conjecture that the turning point is the invention of bronze in the fourth millennium BC onwards. The discovery of bronze enabled our ancestors to create metal tools, which made farming and hunting more efficient, and metal weapons. Rapidly, bronze became a fundamental material for the survival of farming societies and elaborate arrangements had to be made to ensure a continuous supply of it for essentially two reasons. First, metals were generally scarce in densely populated areas. Second, bronze is an alloy made primarily with copper and tin, two metals that are naturally to be found in regions far away from each other. The result was an explosion of long-distance trade. Some of the trade routes connecting large

[1]Recent research in the field of comparative development has highlighted an exceptional persistence in the levels of economic, technological, and political development around the world until 1500 AD (Comin, Easterly and Gong, 2010; Ashraf and Galor, 2011; Maloney and Valencia Caicedo, 2016; Davis and Weinstein, 2002; Olsson and Paik, 2020). Although the European colonization seems to have created a "reversal of fortune" among European colonies (Acemoglu, Johnson and Robinson, 2002), once accounting for migration between countries, ancient economic disparities are still explaining a large portion of current economic disparities (Putterman and Weil, 2010; Chanda, Cook and Putterman, 2014). See Galor (2011) and Galor (2022) for an exhaustive review of the main theories and narratives behind the long-term persistence of economic outcomes. Matranga and Pascali (2021) provide a review of the empirical work.

populations with far-away mining regions were constrained by natural topography to pass by some regional bottlenecks. Traders could not avoid these bottlenecks unless they were willing to face disproportionate transportation costs. We posit that it is precisely in these bottlenecks that a new elite, relying on taxing these transit traders, could emerge, leading eventually to the city-states and the great civilizations of the antiquity.

To test this theory, we proceed in three steps: 1) identify the transit regions in the metal trade network, 2) estimate the causal impact of transit metal trade on the emergence of the Urban Revolution, and 3) elucidate the mechanism by which transit metal trade precipitated the rise of the Urban Revolution.

After summarizing the related literature in Section 2 and describing our data in Section 3, we identify the transit regions in the Bronze Age metal trade network in Section 4. We use a definition that goes back to Ramsay (1890), who proposed the concept of "road-knots": the passages in which a series of routes, dictated by natural topography and the distribution of natural resources, intersect. To locate these areas, we start by constructing the Bronze Age natural transportation network. Specifically, we combine standard methodologies in the trade literature with data on natural topography and ancient bilateral trade relationships to identify the least-cost paths between any two grid cells (1×1 degree) in the Old World. Long-distance trade during the Bronze Age is essentially an effort to bring metals, mainly copper and tin, in the densely populated farming areas. We identify the "road-knots" in the resulting trade network by counting the least-cost paths that transit each grid cell in the Old World, while connecting the cells with tin and copper mines with all the other reachable cells, weighted by their respective cropland areas.

In Section 5, we test the causal impact of transit metal trade on the rise of the Urban Revolution. Our research question does not allow for one perfect randomized controlled trial that could prove and disprove our thesis. Plus, to our knowledge, there does not exist an ideal global database that coherently measures the different defining aspects of the Urban Revolution: the emergence of states, the rise of socio-economic inequalities and the explosion of large settlements. We therefore perform multiple imperfect tests based on different datasets. We present our empirical analysis in four subsections, each using different data, that capture different aspects of the Urban Revolution, and different identification strategies, as dictated by the nature of the underlying data.

The first subsection focuses on the emergence of large cities. We use two readily available datasets to capture the evolution of urban settlements over time: Reba, Reitsma and Seto (2016) and Klein Goldewijk, Beusen and Janssen (2010) provide data on cities' location and urban population from the fourth millennium BC. Figure 1 illustrates the grid cells we identified as road-knots in the metal trade network and all recorded settlements with 10,000+ inhabitants dating before the Bronze Age collapse (1300 BC). Nearly all cities in the sample arose in potential transit areas in the metal trade routes, a result confirmed by

our cross-sectional OLS estimates. Still, several factors prevent a causal interpretation of this correlation. In particular, our measure of transit trade potential is likely to be affected by the rise of cities and the Urban Revolution itself as it depends on the distribution of mines and cropland areas around the globe, which are clearly endogenous to the location of cities and complex hierarchies. To get closer to a causal link between metal transit trade and the rise of cities, we use a 2SLS estimation framework. The instrumental variable is an alternative measure of transit trade potential, which does not rely on the endogenous distribution of metal mines and cropland, is not affected by human intervention, and is purely driven by geography and climate. It is constructed by counting the number of least-cost paths that transit a certain cell, while connecting the cells with tin and copper natural deposits (not the Bronze Age mines) to the other cells in the Old World, weighted by their approximate net primary production (NPP), a measure of the maximum potential biomass that can be produced in a certain region, given the local geo-climatic conditions[2,3]. The 2SLS regressions confirm the results of the OLS panel regressions. Doubling the number of least-cost metal trade paths transiting a certain cell, translates into an increased probability of a city being located in that cell by more than half of the average value of the dependent variable. Furthermore, we observe that while the transit regions in the copper trade played a crucial role from the fourth millennium BC, the significance of transit areas in the tin trade only became apparent from the latter half of the third millennium BC. This development mirrors the transition from arsenic bronze, an alloy of arsenic and copper, to tin bronze, an alloy of tin and copper, which occurred during the third millennium BC.

The results based on ancient cities have certain limitations. First, due to the cross-sectional nature of the data we cannot exclude potential omitted geographic factors that might be driving the 2SLS results (though we do control for a large set of potential confounders). Furthermore, an evaluation of pre-trends is challenging given that, barring a few exceptions, urban settlements prior to bronze usage are scarce. Secondly, the emergence of cities represents merely one facet of the Urban Revolution, failing to encapsulate other pivotal aspects such as the escalation in socioeconomic disparities and hierarchical complexity.

To address these limitations, in the second subsection, we employ two additional data sources, which report the locations of radiocarbon-dated archaeological sites in the Old World, which presumably indicate social and political hierarchy. The first is an historical atlas of the most relevant archaeological sites (Atlas of World Archaeology, Bahn, 2000) and the second is a gazetteer for ancient history (the Pleiades Project, Bagnall, 2022). Using a difference-in-differences approach, we show that road-knots are associated with a relative increase in settle-

[2]To estimate the NPP, we used a paleoclimate simulator, which reconstructs past climate conditions in a high-resolution manner (Karger et al., 2021) in conjunction with a well-established model of habitat development in response to climate (Miami model, see Lieth, 1975).

[3]Using the NPP to measure land productivity comes with important advantages: it is unaffected by human intervention and it captures land productivity for both hunter-gatherers and farmers, independently from the mix of crops and animals (domesticated or not) used for subsistence.

ments and archaeological sites during the Bronze Age (as compared to the Stone Age). This result is corroborated by both OLS and 2SLS estimates and is not explained by pre-trends. Our estimates suggest that metal trade accounts for approximately a third of the increase in sites indicative of complex social hierarchies. Admittedly, these back-of-the-envelope calculations are very crude estimates and should be taken with a grain of salt as they assume that the roll out of the metallurgical techniques was uniform across the globe. Nevertheless, our estimates suggest that the invention of bronze was definitely not just a by-product of the Urban Revolution but an important driver.

The two sources used to capture the rise of social and political hierarchies in this subsection have some caveats: one is dated and the second one is skewed towards Europe, the Middle East and Mediterranean Africa. For this reason, we move to high-quality regional data in the following two empirical subsections (at the cost of losing a global perspective).

In the third subsection, we use the Atlas of Chinese Relics, a 31-volume atlas published by the Chinese National Heritage Administration with detailed information on 500,000+ archaeological sites dating from the Paleolithic onwards. We digitize the atlas and use a Naïve Bayesian text algorithm to identify sites indicative of the rise of the Urban Revolution. Specifically, the algorithm recognizes those sites that are indicative of some of the criteria that Gordon Childe uses to define the Urban Revolution: large settlements, monumental public works, specialized ruling class exempt from manual tasks, a system of recording used in the production process, written documents, and artistic expression. Once again, using both an OLS and 2SLS difference-in-differences design, we find that metal trade led to a statistically significant relative increase in all these six elements defining the Urban Revolution.

In the fourth subsection, we examine Bronze Age Europe. With the exception of the Southeast region, which we do not include in our analysis, Europe did not witness the emergence of political states or large cities during the Bronze Age. However, the continent did experience an evolution in political hierarchies, transitioning from tribes to chiefdoms in various regions. This is evidenced by the development of larger polities characterized by a hierarchical settlement structure and the appearance of elite burials. One of the advantages of focusing on Europe is that we can date the majority of copper and tin mines serving the continent, depending on whether they were operating during the middle or late Bronze Age. We can thus study how changes in the road-knots, induced by new mineral discoveries, affected social hierarchy. To capture the transition towards chiefdoms, we digitize the Prähistorische Bronzefunde, a collection of monographs on metal artifacts dating from 3000 to 500 BC. This allows us to trace the spread of elite burials. Our findings indicate that a doubling of least-cost paths through a grid cell correlates with a threefold increase in the likelihood of finding metal weapons in Bronze Age graves within that cell.

The results so far suggest that metal trade was an essential driver of the rise of complex hierarchies during the Bronze Age: substantial political inequality was much more likely to

emerge in the trade road-knots compared to other regions. But - why were road-knots so crucial to the emergence of complex hierarchies? We propose a simple theory that emphasizes the appropriability of transit trade. When long-distance trade exploded following the invention of bronze, a new elite relying on taxing transit trade could emerge. Transit trade is appropriable not just by a would-be elite, composed of organized stationary bandits, but also by unorganized rowing bandits. The fundamental difference between the two groups is that stationary bandits can commit to a tax rate. Although, in our theory, elites are not benign, the shift from rowing bandits to stationary bandits is a Pareto improvement: as in Olson (1993) and Mayshar, Moav and Pascali (2022), the commitment of bandits to a tax rate serves both the bandits (which can choose a tax rate that maximizes their revenues) and the productive group (which benefit from the deterrence of unorganized rowing bandits).

In Section 6, we test for this appropriability mechanism. Guided by a theoretical model, we construct a grid-cell measure of the potential revenues from taxing the local transit trade. For each grid cell in the Old World, we compute the increase in global transportation costs in the metal trade network if that cell is removed from the network. The intuition is that fiscal revenues from taxing transit trade in a certain location cannot exceed the transportation costs traders would incur to bypass that location. Essentially, this variable identifies the bottlenecks in the metal trade network. We then study whether the Urban Revolution is predicted by our measure of potential transit trade (i.e., the road knots) or our measure of potential fiscal revenues (i.e., the bottlenecks). It turns out that, when both variables are included as regressors, only the latter one consistently predicts the rise of cities, settlements and archaeological sites produced during the Bronze Age. This result points towards our appropriability theory as the main candidate to explain the impact of transit trade on the rise of the Urban Revolution, although a series of caveats, that we discuss in detail in a dedicated subsection, apply.

To provide further evidence in support of the appropriability theory, in Section 7, we provide a series of case studies that illustrate the role of trade in spurring the rise of political states, socio-economic inequalities, and cities in Mesopotamia, Anatolia, Indus Valley, Aegean Sea, and China.

The city-state of Assur, the capital of what would become the Assyrian Empire, provides an example of how trade in metals fostered the rise of cities and states in the Bronze Age. Originally, Assur was a small settlement lying on the least productive edge of Mesopotamia. Its fate changed when bronze metallurgy diffused in the Near East. Anatolia had a dense population supported by productive agriculture but lacked an indigenous tin source. The most feasible method for the Anatolians to import tin was engagement with Assyrians, who, in turn, obtained it from merchants coming from the South and the East of Assur. Assur became a nodal point in this trade route. The chiefs of Assur promoted this transit trade by guaranteeing a series of privileges and protection to the traders passing by the city (see Section

7.3 for further details). By the dawn of the second millennium, Assur became the capital of a trade civilization. Assyrian chiefs established a series of trading colonies along the trade routes connecting Assur with the small Anatolian city-states. These trade posts reproduced Assur's legal and financial institutions and played a crucial role in fostering the economic, institutional, and demographic development of Anatolian city-states. In particular, they were instrumental to the rise of a local elite of Anatolian kings, who were both guaranteeing protection for passing merchant caravans and maintaining roads and bridges in exchange for tolls and taxes on transit trade.

Let us emphasize here that complex hierarchies and trade pre-date the invention of Bronze. The circulation of prestige goods in the Neolithic indicates both the presence of chiefs, who were able to control the surplus produced in areas with storable crops, and the existence of a system of exchange within a limited territory, with occasional short-lived long-distance connections. What is fundamentally different in the Bronze Age is the scale in both hierarchical complexity and long-distance exchanges[4]. During the Neolithic, there were no states and no long-distance trade networks of the kind that provided all Bronze Age communities, on a regular basis, with metals coming from mines thousands of miles away. The shift from local exchange to high-end international trade created, especially through rivers, seacoast and valleys, some clear bottlenecks. Controlling these bottlenecks allowed the rise of a new elite, which was based on the control (or ownership) of passage routes, rather than agricultural land for storable crops. An example of such a shift from the Neolithic to the Bronze Age is provided by the distribution of tells in Hungary. In the Neolithic, tells were concentrated in the highly fertile lowlands along the Tsiza. Archaeological findings of the prestige goods, dating from the period, are found with a typical fall-off curve from the tell indicating a regional economy with sporadic long-distance exchanges. During the Bronze Age, new tells formed in vacant areas, lined up along the Danube. These locations were not suited for agriculture: villages on the bank of a large river have access to only half of the circular catchment area of villages in the middle of productive land. They were ideal, however, in the eyes of a new elite that could easily tax the metals transiting the river. This link between the elite and the metal trade is confirmed by the presence of metal hoards in the palaces and bronze objects in the elite burials. These objects also testify the development of regular interregional economic interactions and division of labor (see Kristiansen and Suchowska-Ducke, 2015).

The paper is organised as follows. Section 2 describes the previous literature. Section 3 provides a detailed description of the data used for the empirical analysis. Section 4 lays out the empirical strategy to identify the passage routes in the metal trade network. Section 5 identifies the impact of metal trade on the rise and diffusion of cities and inequality in the Old World. Section 6 describes and tests the appropriability mechanism. Section 7 presents

[4] Meller and Michel (2020)'s book offers a rich and evocative depiction of the connections spanning from the ancient city of Babylon to the British Isles during the Bronze Age.

six case studies that are consistent with a metal trade theory of the Urban Revolution. Some concluding remarks close the paper.

2 Previous Literature

Our work contributes to two separate bodies of literature in the social sciences.

First, it contributes to a large empirical literature in economics that studies the role of international connections and market access for comparative development. To our knowledge, our work is a first attempt, within this literature, to go back to the very beginning of the civilization process, it has a global scope and it provides some empirical validation to the view that trade might have been the *raison d'être* of the Urban Revolution. The closest work is Barjamovic et al. (2019), which shows that natural transportation networks are critical in explaining the hierarchy of ancient city sizes in Central Turkey during the Middle Bronze Age (2000-1650 BC)[5].

Second, our findings contribute to the body of literature that emphasizes the role of geography in explaining the emergence of political states. Within this literature, three sets of theories have emerged. The first set of theories associate the rise of hierarchy with the increased productivity of labor that came with farming. As farmers could produce surplus beyond survival needs, a non-working elite could emerge. Diamond (1998) provides a notable example of this "productivity" theory and argues that early state formation in Eurasia was due to a range of environmental factors that led to an earlier transition to farming and more productive agriculture[6]. The second set of theories links the development of complex hierarchies to the increased ability of a rising elite to appropriate the fruits of labor: in essence, complex societal structures are more likely to form in areas where it's easier to tax or seize farmers' produce. Mayshar, Moav and Pascali (2022) recently formalize this concept and show that regions where geographical constraints led farmers to cultivate cereal grains – crops that are relatively simple to tax or confiscate compared to others – also tended to be the regions that first transitioned from tribal societies to chiefdoms and states.[7] The third set of theories

[5] A recent literature has documented the role of trade in ancient development during the Iron Age. See Bakker et al. (2021) on Phoenician cities and Adamson (2021) on Greek city-states.

[6] The productivity theories on the rise of early complex hierarchies have a long pedigree in social sciences. Adam Smith argued that the Neolithic transition produced in some regions large farming surpluses. These surpluses made it possible to have a class of bureaucrats, as a result of labor specialization, and increased the demand for an extended role of government (Smith, 1978, p. 65). Friedrich Engels (1942) argued similarly that the surplus generated by the adoption of agriculture was a prerequisite for the transition to a class society. More recently, a growing empirical literature in comparative development has shown that a richer prehistoric availability of domesticates is an important predictor of the timing of the Neolithic transition (Ashraf and Galor, 2011), the early emergence of macro-level polities (Borcan, Olsson and Putterman, 2018; Petersen and Skaaning, 2010), independence from colonial powers post 1500 AD (Ertan, Fiszbein and Putterman, 2016) and higher per-capita GDP today (Bleaney and Dimico, 2011; Hibbs and Olsson, 2004).

[7] An influential "appropriability" theory goes back to Carneiro (1970)'s circumscription theory, which contends that supranational polities emerge in areas with high agricultural productivity surrounded by geographic barriers that prevented farmers from escaping from an expropriating elite. Mayoral and Olsson (2020) and

relates the emergence of complex hierarchies with a series of functions that a powerful elite can provide. Prominent "functionalist" theories focus on the demand for the construction and maintenance of hydraulic infrastructures[8] or storage facilities[9] and the demand for stability and security[10] as means to increase the productivity of workers. These three sets of theories provide different mechanisms through which the alluvial lowlands of the Tigris and the Euphrates in Mesopotamia, the Nile in Egypt, the Indus and the Ghaggar-Hakra in India, and the Yellow River in China became the cradles of civilization. The productivity theories highlight the agricultural productivity of alluvial lands, the appropriability theories emphasize the circumscription of these areas or the relatively high productivity of cereal grains, and the functionalist theories point towards the higher scope for a series of infrastructures, like dams or irrigation systems. We propose a different mechanism, which speaks to both the appropriability and the functionalist approaches. Rivers were the highways of the Bronze Age: long-distance trade in metals and grains was forced to transit these rivers, thus creating local demand for a state, able to guarantee the welfare gains from trade, and making it possible to have a state, as transit trade could be easily taxed. Cities in the Bronze Age, with few exceptions, were located on either alluvial valleys or, after 2000 BC, in coastal regions. One clear advantage of our proposed mechanism is that it can explain not only cities along the rivers but also cities along the coast, as coastal navigation provides an alternative to river navigation to move bulky materials. None of these first coastal cities was located in areas where agriculture was exceptionally productive, while all of them were located in strategic trade nodes. For instance, in the Mediterranean, the Aegean cities related with the Minoan (from 1900 BC) and the Mycenaean (from 1600 BC) civilizations emerged on a crucial passing point between Europe and the Near East, while the city of Troy (from 1400 BC), on the Bosporus Strait, could control all trade in and out of the Black Sea. Notice that the long-distance trade explanation of the origin of the Urban Revolution also provides some rationality for a fascinating hypothesis that relates the invention of ironworking with the collapse of the Bronze Age civilizations[11].

The idea that long-distance trade in metals was a fundamental driver of the civilization

Schönholzer and François (2023) provide systematic evidence in support for the circumscription theory of state formation. See also Allen, Bertazzini and Heldring (2022).

[8] See Wittfogel (1957) and Bentzen, Kaarsen and Wingender (2017).

[9] See Testart et al. (1982).

[10] See Dal Bó, Hernández-Lagos and Mazzuca (2022).

[11] In the 13th century BC, ironworking began spreading from present-day Bulgaria and Romania, while all major civilizations in Europe, West Asia and Africa collapsed. Within five decades, almost all cities were destroyed, trade relations were severed, writing systems vanished and populations living along the coast moved to the interior. Palmer (1962) suggested that spread of ironworking might be the reason behind the Bronze Age collapse. Iron is superior to bronze for weapons and agricultural tools and can be found almost anywhere in the Old World. The diffusion of the ironworking technology might have been detrimental for the Bronze Age main civilizations for two reasons. First, it undermined the role of Bronze Age cities as it nullified their locational advantage on the trade routes towards copper and tin mines and it made obsolete a series of city-institutions constructed to protect interregional trade. Second, it undermined an elite based on the control of metal trade and it allowed newly formed peripheral armies with iron weapons to quickly destabilize entire states.

process is of course not new. Metal trade has been cited repeatedly as a factor in primary state development (Childe, 1930; Sanders, 1968; Polanyi, Pearson and Ahrensburg, 1957). Our theory is particularly close to recent works of Timothy Earle and Kristian Kristiansen[12]. These authors argue that constriction points in the Bronze Age trade network created the potential for social segments to control the production and flows of critical metal goods: this eventually led to more complex and ranked societies and the rise of networks of integrated polities. For instance Earle et al. (2015) conjecture that "chiefdoms probably arose at mountain passes, river crossings, and other constriction points, where moving metal and other wealth would have then required payments for safe passage through each local polity".[13]

Other authors have emphasized the role of long-distance trade in metals in fostering the development of specific civilizations. Famously, Gordon Childe suggested that the origins of the Egyptian states could be found in the copper long-distance trade between the Nile region and the Red Sea[14]. In Section 7, we review the literature on the link between metal trade and the Urban Revolution with reference to a series of Bronze Age civilizations that arose in Mesopotamia, Anatolia, the Indus Valley, the Aegean Sea, and China. With respect to this literature, our approach has two advantages. First, we do not focus on a particular region or society: we test a general theory on the role of Bronze and trade in metals on the rise of the first urban civilizations using data covering the entirety of the Old World. Second, we use a natural experiment of history to infer causality.

3 Data

3.1 The Urban Revolution

The Urban Revolution is a multifaceted process and capturing it in the archaeological data in a consistent manner across space and time is difficult. Gordon Childe (1950) defined ten specific criteria, all deducible from archaeological data, to distinguish the earliest instances of the Urban Revolution from any older or contemporary Neolithic village: 1) population density higher than in any previous settlements, 2) a class of full-time specialists (craftsmen, merchants, officials, priests, etc.) that do not work directly to procure their food and live on-site, 3) a system of transfers (through taxes or donations) of the primary surplus from producers to the elite, 4) truly monumental buildings which symbolize the concentration of

[12] See Earle (2002, 2013); Earle and Spriggs (2015); Earle et al. (2015); Kristiansen and Suchowska-Ducke (2015); Kristiansen and Earle (2015).

[13] With reference to the rise of hierarchy along rivers, Earle et al. (2015) argue "When analysing water-based transport, the number of alternative routes is critical to define bottlenecks. The more options (of equivalent cost) that were available, the less constrained was the a bottleneck".

[14] In the words of Childe (1930): “Some favorably situated villages grew into real towns, and the chief of one of them, Abydos, that commanded one main caravan route to the Red Sea and the East, was eventually able to master the whole land to the Mediterranean coasts, founding what is termed the First Dynasty (about 3100 BC).”

social surplus, 5) a ruling class exempt from all manual tasks, 6) systems of recording and exact sciences, 7) scripts and calendars, 8) artistic expressions, 9) regular long-distance trade relationships, 10) state organization based on residency rather than kinship. Unfortunately, to our knowledge, a dataset that perfectly captures the emergence of these ten criteria in archaeological sites across the Old World does not exist. We rely, instead, on several datasets that each capture some of these criteria.

3.1.1 Urban settlements

We use two readily available datasets to capture the first of Childe's criteria identifying the Urban Revolution: the increase in village size.

The first dataset captures the location of ancient cities and was assembled by Reba, Reitsma and Seto (2016) using two principal sources: Chandler (1987) and Modelski (2003). Both Chandler and Modelski define a city, distinct from a village, based upon population estimates. Specifically, for the years before 1000 BC, a city is defined as a concentration of at least 10,000 inhabitants. The dataset is developed using archaeological records, historical works, census data, and applying rank-order principles, like Zipf's law. Data are generally sparse over time. Some cities have several population data points before 1000 BC, while others only have one or two observations; some missing values in the time series are imputed using different methodologies. The sparse nature of the data does not allow us to measure the spread of urban settlements over time; we only use the information on whether there is *any* evidence of a certain city at *any* point in time before the Bronze Age collapse (1300 BC).[15] The location of these cities is depicted by the grey-shaded dots in Figure 1. Based on this information, we construct a dummy variable that identifies 1×1-grid cells in the Old World for which there is evidence of at least one ancient city. As an alternative outcome, we use the number of ancient cities located in each grid cell. The first two rows of Table A.1 (Panel A) report summary statistics for these two outcome variables. There are a total of 64 pre-1300 BC cities, which fall into 46 separate grid cells. There is evidence of ancient cities in only 0.42 percent of the grid cells, while the maximum number of ancient cities in a cell is 7 (at the delta of the Tigris and Euphrates).

A clear shortcoming of Reba, Reitsma and Seto (2016)'s dataset is that it is based on sources that date back to the early 2000s, thus omitting the most recent advances in urban archaeology. For this reason, we also run a series of robustness checks using a more recent dataset, HYDE 3.1 (Klein Goldewijk, Beusen and Janssen, 2010). This data source offers spatially explicit urban population estimates every millennium after 10000 BC. For our analysis, we use the estimates for 2000 BC, the latest available year before the Bronze Age Collapse.[16]

[15] Results are not sensitive to the exact choice of the cutoff date. We obtain similar results when we use any date between 1500 BC and 500 BC as a cutoff.

[16] Using estimates for the year 1000 BC leaves our results unchanged.

Admittedly, most of the information provided by HYDE 3.1 are the results of state-of-the-art imputation techniques based on relatively few data points.

3.1.2 Archaeological sites

In an attempt to capture the increase in large settlements, the rise of monumental buildings, and the increase in political and economic inequality—three essential elements of the Urban Revolution—we rely on two archaeological data sources.

The first source is Bahn (2000)'s Atlas of World Archaeology, a collection of detailed maps and descriptions of the world's most relevant archaeological sites. The Atlas covers 7,708 archaeological sites spanning from the Paleolithic to the Classical antiquity. We use the geocoded version of the atlas provided in Schönholzer and François (2023) and extract the sites that fall into the Paleolithic, Neolithic as well as the Bronze Age.[17] The result is a list of 560 sites that emerged during the Paleolithic, 664 sites that belong to the Neolithic, and 1,419 associated with the Bronze Age. Figure B.1 shows the location of these sites. For the empirical analysis, we create a panel dataset which counts both the total number of sites and the number of sites classified as settlements in each Old-World 1×1-degree grid cell during the Paleolithic/Mesolithic, Neolithic, and Bronze Age. Table A.1 (Panel B)reports summary statistics for these two outcome variables. Only 4.9 (0.7) percent of grid cells have at least one site (one settlement), while the maximum number of sites (settlements) in a grid cell is 43 (16).

A drawback of the Atlas is that it does not represent a systematic collection of all globally known archological sites. Furthermore, it is somewhat outdated and does not reflect the archaeological discoveries and progress in the last 20 years. For this reason, we also use a second source: the Pleiades Project, an open-source gazetteer of ancient sites (Bagnall, 2022).[18] We limit our analysis to sites where the location is precisely known and categorize these sites into two groups: settlements and other archaeological sites.[19] The first group is restricted to those places labeled as 'settlement' or 'urban' in the database. The second group includes all sites characterized by the presence of man-made structures. The spatial distribution of the sites used in our analysis is depicted in Figure B.2. To assign these sites to a time period, we use two alternative approaches. First, we use the (textual) description in the Pleiades database to identify the pre-Bronze and the Bronze Age sites. This leaves us with a total of 897 sites, 245 of which predate the invention of Bronze. We then count the sites that fall into a grid cell in each of these two eras. The result is a two-period grid-cell level panel dataset. Alternatively, we exploit the (numeric) estimates of the start and end date of a site, which are reported in the Pleiades database. On the basis of these dates we

[17] Data downloaded on 27 July 2023 from `davidschonholzer.com`.

[18] See `pleiades.stoa.org/docs` for detailed documentation.

[19] Bakker et al. (2021) refer to these two classes as 'wide' and 'narrow'. See Bakker et al. (2021, p.658) for more details.

construct a panel dataset that covers the years 7000–1300 BC at 1,000 year intervals.[20] For each millennium we determine how many settlements and archaeological sites lie within a grid cell. This gives us a six-period grid-cell level panel dataset.

3.1.3 China

Data on the rise and spread of the Urban Revolution in China are drawn from the Chinese Cultural Heritage Atlas, the most comprehensive catalog of Chinese archaeological sites. This source is based on joint efforts between the Chinese central and provincial cultural heritage bureaus to compile a mapping of all excavated monuments and remains in China. The catalog is completed for 28 out of 34 provinces (data for the provinces of Taiwan, Macau, Hong Kong, Jiangxi, Guizhou and Hainan are still under construction). Each archaeological site is geocoded, dated and described in detail. We OCR the 31 volumes that compose the Atlas and focus on the 85,000+ sites dating Before the Common Era. The spatial distribution of these sites is illustrated in Appendix Figure B.3. Each site contains a long description (on average 58 words). For a tenth of the sample, we manually coded whether this description makes any reference to one of the following features: 1) urban settlements, 2) ruling class exempt from manual tasks, 3) monumental building, 4) a standardized system of measures and recordings used in exchange and production, 5) writing, 6) highly developed art forms. After developing this training sample, we use a naïve Bayesian classifier to classify all sites in the Atlas according to these six criteria. Appendix Figure B.4 reports a correspondence plot, which details the words that are overused to describe the sites classified according to each criterion. For instance, in the top right, we can see that words such as "city", "township", "wall", and "village" are disproportionally associated with the criteria "Urban Settlements", while words like "Han", "dynasty", "state", are associated with the criteria "Ruling Class". Once each site has been classified, we then count the sites associated with criteria indicative of the Urban Revolution in each 1×1 grid cell in the Paleolithic, Neolithic and Bronze Age. Table A.1 (Panel C) reports the summary statistics of the dataset.

3.1.4 Europe

Except for the Southeast region, Europe did not witness the emergence of political states or large cities during the Bronze Age. However, the continent did experience an evolution in political hierarchies, transitioning from tribes to chiefdoms in various regions. To measure this political development, we gathered data on Bronze Age elite burials, focusing specifically on those containing bronze weapons. Such burials are a significant archaeological indicator of the presence of local chiefdoms (Earle et al., 2015, Renfrew and Bahn, 2016, pp. 175).

To capture the diffusion of burials with metal weapons, we digitized the Prähistorische

[20] The time intervals are: [7000, 6000), [6000, 5000), [5000, 4000), [4000, 3000), [3000, 2000), [2000, 1300].

Bronzefunde (PBF). This project systematically compiles information on archaeological metal artifacts found in Europe. Since 1966, it has published 186 volumes systematically recording individual metal finds from 3000 to 500 BC. The PBF organizes these into book series, or *Abteilungen* (divisions), by artifact type. For instance, *Abteilung IX*, covering axes and hatchets, comprises 29 volumes, each focusing on a specific region. An expert archaeologist from the respective region usually compiles this information from various sources, such as museum catalogs [21].

We focus on weapons, specifically those classified as 'axes and hatchets' and 'swords' (*Abteilung IX* and *Abteilung IV*, for a total of 39 volumes). We augment this data with artifacts from the "Bronze und urnenfelderzeitliche Schwerter" database (Hahnekamp, 2011)[22]. Combined, the PBF volumes and Hahnekamp's data encompass Central and Western Europe. Figure B.5 illustrates the find locations and the spatial scope of our Bronze Age analysis. Appendix C offers more details on the data sources and construction.

For each artifact in our database, we note three key details: (i) the coordinates of excavation site's, (ii) the site's nature (e.g., burial site), and (iii) the artifact's archaeological type or family (e.g., Pădureni axe type). Using (ii) we identify the elite burials, while using (iii) we link the burial to a specific time periods (Early-, Middle-, and Late Central Europe Bronze Age). For example, entry 13 from *Prähistorische Bronzefunde, Abteilung IV, Book 2*, is a "hilt plate short swords of the Sauerbrunn type", a sword associated with the Göggenhofen culture and thus dating back to the Central Europe Middle Bronze Age (Schauer, 1971, p. 22). Figure C.1 presents a book excerpt to illustrate the entry structure.

For our empirical analysis, we create a 1×1-degree grid-cell panel data set comprising two time periods, which correspond to the Central Europe Early/Middle Bronze Age [3000 BC, 1300 BC) and Late Bronze Age [1300 BC, 750 BC]. For each period and grid cell, we count the number of elite burials. Table A.1 (Panel D) reports the summary statistics of the dataset.

3.2 Bilateral trade flows

We reconstruct trade flows for prehistoric periods using archaeological artifacts. For artifacts to be included in our analysis, two requirements have to be fulfilled. A first prerequisite is that an artifact's find site and provenance can be identified. This allows us to reconstruct trade flows by defining the archaeological excavation site as the destination and the production site as the origin. The second prerequisite is that the period of production is known. In the main analysis, we will focus on goods produced and traded during the Bronze Age. For robustness checks, we will alternatively use goods predating the invention of bronze.

Combining existing databases with results from our own literature review, we identified

[21] For example, the volumes on bronze axes and hatchets excavated in Romania (*Abteilung IX: Äxte, Beile—Die Äxte und Beile in Rumänien I–II*) were written by Alexandru Vulpe, a Romanian archaeologist.

[22] http://chc.sbg.ac.at/schwerter/map.php.

approximately 7,500 artifacts that fulfill the two inclusion requirements. These artifacts vary in type and range from weapons, to jewelry, and utensils. For the Bronze Age, we estimate trade costs based on 3,744 metal-based artifacts. These data are compiled from a variety of academic sources. For pre-bronze periods, we can draw on around 3,700 artifacts. Data are taken from two existing databases (Pétrequin et al., 2012; Schauer et al., 2020). A more detailed description, including figures depicting the spatial extent of the trade data, is presented in Appendix D.

Based on the geocoded information on the provenance and excavation site, we assign the artifacts to their respective 1×1-degree grid cell of origin and destination. We then aggregate this information to the grid-cell-pair level, giving us the number of artifacts excavated in grid cell j and produced in grid cell i for the pre-Bronze and Bronze Age, respectively.

3.3 Cropland and productive land

We use data from Klein Goldewijk, Beusen and Janssen (2010) to determine the distribution of cropland over time. This dataset estimates land use at 1000-years intervals from 9,000 BC. It is worth noting that the distribution of farming populations may have been influenced by the great civilizations of the time. To isolate an exogenous component in this variable, we use a specific measure of land productivity, the net primary production (NPP). This measure gauges the potential biomass that can be produced in a region based on local geo-climate conditions, and is therefore unaffected by human intervention. We utilize the Miami model (Lieth, 1975) to determine the NPP for given local climatic conditions, and the CHELSA-TraCE21k12 simulator (Karger et al., 2021) to reconstruct climatic conditions at a high-resolution manner every millennium from 9000 BC onward. This measure of land productivity has several advantages for our analysis, compared to other measures previously used in the literature. Firstly, it captures land productivity for both hunter-gatherers and farmers. Secondly, it is independent of the mix of crops and animals used for subsistence, whether domesticated or not.

In robustness checks, we also exploit two alternative measures of the productivity of the land which have been widely used in the comparative development literature. The first is the Caloric Suitability Index developed in Galor and Özak (2016), which captures the highest attainable caloric yields from subsistence farming, given the set of crops available in the Old World before the Columbian exchange. The second one is an index developed by Ramankutty et al. (2002), which captures the fraction of land that is suitable for agriculture.

3.4 Metal mines and deposits

We conducted a thorough review of the archaeological literature to compile a new dataset on Bronze Age metal mining sites. The requirement for the inclusion of a mining site in the

dataset is that both the location of the mine, as well as its activity during the Bronze Age, are identifiable. The final dataset comprises 47 tin mines and 121 copper mines, distributed across 32 and 80 separate grid cells, respectively. For mines supplying Europe, we distinguish between those operating before and after 1300 BC.

We face two significant challenges in using the mining data for our empirical analysis. Firstly, the location of mines is endogenous to the spatial distribution of cities and states. Secondly, the archaeological record of Bronze Age mines may not accurately reflect the actual metal deposits exploited during that era. In particular, the sources of tin during the third millennium remain uncertain: Bronze Age miners did not have access to veins running through granite, and instead relied on cassiterite, which leaves no trace of its former contents. The resulting measurement error is not random, as archaeological findings on ancient metal sources are more likely to appear in regions that have been extensively excavated.

To address these endogeneity concerns, we also use data on the actual location of tin and copper deposits as they are known today, regardless of whether they have ever been exploited or not, sourced from the U.S. Geological Survey (2011).

3.5 Other data

We construct a range of additional grid-cell level geographical characteristics. Specifically, we extract information on coastlines and navigable rivers[23] from `naturalearthdata.com`, while elevation data come from WorldClim (v. 2.1)[24]. Additionally, we collect data on temperature and precipitation (Karger et al., 2021), length of growing season (FAO/IIASA, 2011), malaria suitability (Kiszewski et al., 2004), biomes (Olson et al., 2001), and natural harbors (NGA, 2019).

4 Bronze Age transit regions

The aim of this section is to pinpoint the transit regions within the Bronze Age metal trade network. To achieve this, we rely on Ramsay's (1890) concept of "road knots", the natural passage points where several trade routes intersect. In the first subsection, we employ established methodologies in the field of international trade to analyze Bronze Age trade data and reveal the underlying transportation network. In the second subsection, we utilize this network alongside information on the spatial distribution of cropland and metal sources to identify the road-knots in the metal trade network. To do this, we rely on the fact that long-distance Bronze Age trade is driven by the necessity to exchange agricultural crops for

[23] To account for the importance of rivers, we use the Strahler order of streams. This is an index that ranges from one to six. Navigable rivers are those that fall into categories 1–5 (Vörösmarty et al., 2000).

[24] On the basis of these elevation data, we measure terrain ruggedness using the index devised in Riley, Degloria and Elliot (1999) and in Nunn and Puga (2012).

tin and copper. Notably, the location of Bronze Age cropland and mines is likely influenced by the spatial development of the Urban Revolution. In the third subsection, we isolate an exogenous element of the road-knots by identifying the transit points that connect metal deposits and naturally productive land, which are not influenced by human intervention.

4.1 Period-specific transport costs

To our knowledge, estimates of the relative transportation costs predating the Iron Age are unavailable. We infer them using a methodology in the spirit of Donaldson (2018). Based on data from naturalearthdata.com, we start by dividing the world into transport surface grids of 0.25×0.25 degrees and assign each grid cell to one of the following shipping modes: sea, river, or land.[25] Each mode is associated with a per-unit distance transport cost: $\boldsymbol{\alpha} = \left(\alpha^{sea}, \alpha^{river}, \alpha^{land}\right)$. We impose three restrictions that reflect the technological constraints of the time. First, maritime transport is only possible along the coast (and below 60° latitude). Second, riverine transport is only feasible on navigable rivers. Third, transport is not possible across high mountain ranges (above 15,000 feet). The resulting topographical transport surface is depicted in Figure D.2.

The vector $\boldsymbol{\alpha}$ is unknown, so we treat it as a vector of parameters to be estimated. Conditional on $\boldsymbol{\alpha}$, we use the Dijkstra (1959)'s algorithm to identify the least-cost path between every grid-cell pair mf; $LC_{mf}[\boldsymbol{\alpha}]$ denotes the associated transportation cost.[26] We then estimate a standard gravity equation using the Poisson pseudo-maximum likelihood (PPML) estimator:

$$\mathcal{X}_{mf} = \exp\left(\delta \ln LC_{mf}[\boldsymbol{\alpha}] + \beta_m + \beta_f\right) + \varepsilon_{mf}, \tag{1}$$

where $\mathcal{X}_{mf}$ denotes the number artifacts, excavated in grid cell f, and originating from grid cell m. β_m and β_f are a full set of origin and destination fixed effects.

We estimate equation (1) iteratively over all relative transport cost combinations $\alpha^{sea} = [1, 20]$, $\alpha^{river} = [1, 50]$ and $\alpha^{land} = [1, 100]$ for two sets of artifacts: those dating from the Stone Age (SA)[27] and those dating from the Bronze Age (BA). For each set of artifacts, we then choose the vector $\boldsymbol{\alpha}$ that minimizes the log-likelihood of the estimated gravity equation. We normalize $\alpha^{sea} = 1$, so that $\boldsymbol{\alpha}$ captures how costly a given shipping mode is relative to maritime shipping. For the Bronze Age, this fit-maximizing transport cost vector is given by $\widehat{\boldsymbol{\alpha_{BA}}} = (1, 2, 6)$, while for the Stone Age is $\widehat{\boldsymbol{\alpha_{SA}}} = (1, 1/14, 2/7)$.

Our estimates suggest that the relative costs of shipping goods changed dramatically across modes after the invention of bronze. Sea shipping shifted from being the most to the least

[25] The relatively coarse size of cells is chosen to account for the fact that coastlines as well as river courses can shift over time.

[26] We assume that transshipment between different transport modes is costless.

[27] Throughout, we loosely use the term "Stone Age" to describe the prehistoric period before the advent of bronze technology

costly. This aligns well with the archaeological evidence. Before the Bronze Age, waterborne transport depended entirely on dugout canoes. These canoes had shallow hulls and were propelled by men using oars or paddles. They were, therefore, neither suited for (or capable of) long-distance journeys nor large-scale cargo transport. As a result, long-distance trade took place overland. For example, goods exchanged between the Near East and Mediterranean Europe were most likely transported via the Anatolian land bridge (Rahmstorf, 2010). This pattern of overland-dominated transport changed with the development of deep-hulled boats alongside the invention of sails at the beginning of the Bronze Age. The plank boats with deep hulls could carry several tonnes of goods and were stable enough for coastal shipping. The sailing technology further contributed to reduced seaborne transport costs by increasing the maneuverability and speed of boats. These technological innovations facilitated large-scale transport of goods via sea routes, making seaborne transport the most cost-effective mode of shipping goods over long distances (e.g., Nessel, Neumann and Bartelheim, 2018). This resulted in the economic integration of the Mediterranean and Mesopotamia as well as flourishing long-distance trade between Mesopotamia and the Indus civilization via the Indian Ocean (e.g., Rahmstorf, 2010; Cunliffe, 2011, p. 189; or Vogt, 1996).

Our estimates further suggest a moderate decline in overland transport costs relative to river transport between the Stone and the Bronze Age.[28] Again, this finding aligns well with the archaeological evidence. During the Stone Age, goods were transported overland by humans or ox wagons, implying limited cargo-carrying ability and slow progress across space. Several important innovations increased speed and freight capacity during the Bronze Age. For example, the spoked wheel was invented along with chariots and other transport vehicles (Uckelmann, 2013). Furthermore, the domestication of camels made overland transport of bulk commodities in arid regions feasible. More details on the data and estimation procedure are provided in Appendix Appendix D.

4.2 Identifying the road-knots

We adopt a two-steps approach to identify the road knots within the metal trade transportation network.

In the first step, we utilize the estimated Bronze Age specific transportation costs ($\widehat{\boldsymbol{\alpha}}$) along with the topographic map of the world to infer the least-cost paths connecting each grid cell containing cropland in the year 3000 BC to the nearest tin mine and the nearest copper mine. To exclude impractically long routes, we disregard paths that are more costly than traveling a distance equivalent to 10,000 kilometers by sea. (It is important to note that this restriction does not significantly impact our empirical findings and results). In this way, we construct a comprehensive list of optimal routes connecting cropland with metal mines, which

[28] However, it is important to note that river transport is relatively cheaper (compared to overland transport) during both the Stone Age and the Bronze Age.

are illustrated in Figure B.6.

In the second step, for each grid cell k, we calculate a "transit index", T_k, as a weighted count of the optimal routes in this list that traverse through the cell. Specifically:

$$T_k = \sum_{m \in \mathcal{M} \setminus \{k\},\, f \in \mathcal{F} \setminus \{k\}} \mathcal{I}_{P^\star_{mf}}[k] \times Crop_f, \tag{2}$$

where $\mathcal{M}$ and $\mathcal{F}$ are the sets of all tin and copper mines and croplands, respectively, $P^\star_{mf}$ denotes the least-cost path from a tin or copper mine m to farmers in cell f, $\mathcal{I}_{P^\star_{mf}}[k]$ is an indicator function taking value one if $k \in P^\star_{mf}$, and zero else, and $Crop_f$ is the extent of cropland (measured in square kilometers) in grid cell f in the year 3000 BC. In other words, T_k is the number of least-cost paths transiting k that connect one square kilometer of cropland to a metal mine. It is worth noting that T_k is very similar to the concept of betweenness centrality in the network[29].

Figure 1 shows the spatial distribution of the transit index, with darker shading indicating the road-knots. The black dots indicate the location of Bronze Age cities. We observe a clear correlation: most cities emerged in metal trade road knots.

4.3 Transit trade: isolating an exogenous component

The finding above does not necessarily imply a causal link: the Bronze Age distribution of both mines and cropland, which are used to infer T_k, was likely influenced by the spatial distribution of cities and advanced civilizations. To isolate exogenous variation in the transit index, we construct an alternative measure of centrality, D_k, which captures the transit regions connecting metal deposits (rather than Bronze Age mines) with productive land measured by net primary production (rather than Bronze Age cropland), two components that are unaffected by human intervention. We use the following formula:

$$D_k = \sum_{d \in \mathcal{D} \setminus \{k\},\, p \in \mathcal{P} \setminus \{k\}} \mathcal{I}_{P^\star_{dp}}[k] \times Prod_p. \tag{3}$$

where $\mathcal{D}$ and $\mathcal{P}$ are the sets of all metal deposits and productive land cells, respectively, $P^\star_{dp}$ denotes the least-cost path from deposit d to productive land in cell p, $\mathcal{I}_{P^\star_{dp}}[k]$ is an indicator function taking value one if $k \in P^\star_{dp}$, and zero else, and $Prod_p$ is the the net primary production of cell o in the year 3000 BC. Figure B.7 illustrates the distribution of tin and copper deposits and the net primary production measure (panel A) along with the resulting values of D_k (panel B).

It is important to note that the estimation of D_k relies on the relative transport costs estimated for the Bronze Age. The available technology during the time might have also been

[29] The betweenness centrality of a node in a network is defined as the number of least-cost paths that pass through that node connecting all node-pairs within the network. See for details Appendix E.

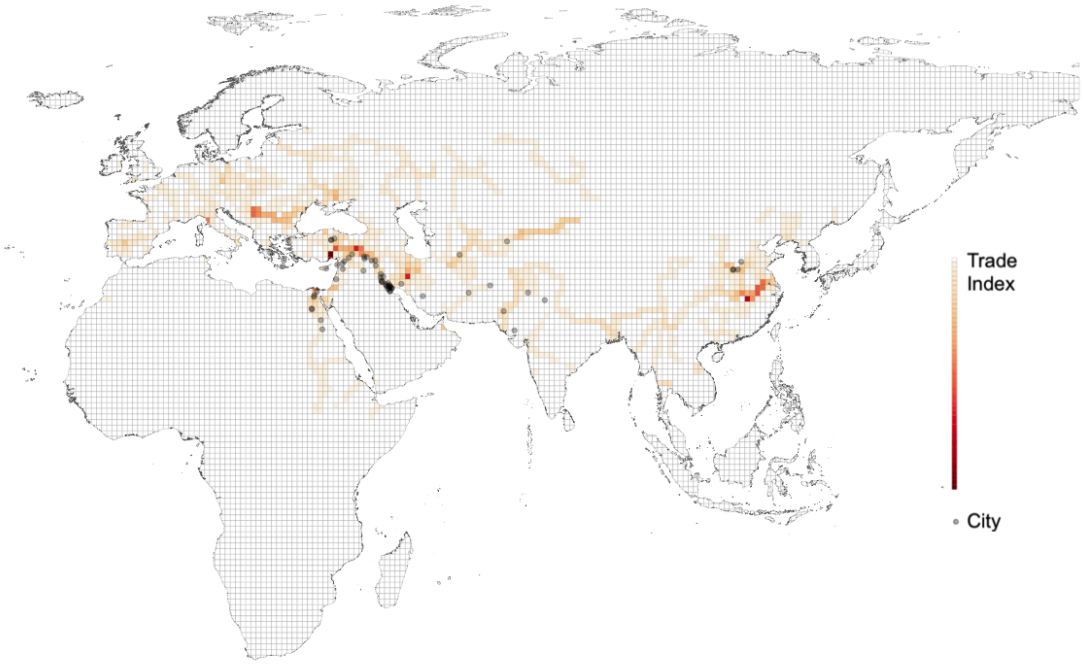

Figure 1: Geographic scope of analysis, Bronze-Age cities and transit index.
Figure depicts the location of cities up to 1300 BC (source: Reba, Reitsma and Seto (2016)) along with the transit index (as defined by equation (3)).

influenced by the Urban Revolution itself. To account for this, we also calculate an alternative value for D_k, which is based on the relative transport costs estimated for the Stone Age.

5 Metal trade and Urban Revolution

5.1 Cross-sectional evidence: Bronze Age cities

This subsection examines the link between metal trade and Bronze Age urban settlements. As we have seen, a visual inspection of Figure 1 provides a first clue of the positive correlation between the location of Bronze Age road knots and cities. We formally test for this relationship by estimating the following equation:

$$y_k = \theta \, IHS(T_k) + X_k' \, \phi + \varepsilon_k, \tag{4}$$

y_k is a dummy indicating whether a city had emerged in grid cell k during the Bronze Age.[30] The main regressor of interest is T_k, the transit trade index of grid cell k, transformed using

[30] For ease of interpretation, we multiply the dummy by 100.

the inverse hyperbolic sine (IHS) transformation. The IHS transformation behaves like a log (thus filtering out scale effects), but it allows to retain the zero-value observations. The vector X_k represents a set of geographical controls.

To correct for the spatial autocorrelation of the error term, we estimate standard errors in two different ways: we allow either for clustering at the 5×5 grid cell level or for spatial autocorrelation, using Conley (1999) standard errors, with distance cutoffs of 1000 km. In Appendix Figures B.8a–B.8b, we show how results are affected by varying the size of the clustering grid (from 1×1 to 20×20) or the Conley cutoff (from 100km to 2,000km). The takeaway is that the size of standard errors are only slightly affected by these changes.

Table 1 reports the estimates. The data source for the Bronze Age cities is Reba, Reitsma and Seto (2016). Column (1) reports the baseline OLS estimate, controlling solely for continent fixed effects. The estimated coefficient of T_k is positive and statistically significant: doubling the number of least-cost paths transiting a certain cell translates into an absolute increase in the probability of a Bronze Age city emerging in that cell by 0.26 percentage points This is a large number, considering that cities are found in just 0.42 percent of the cells in the sample.

The OLS estimates reported in column (1) are far from having a causal interpretation. The transit index is influenced by various factors, including the spatial distribution of croplands and mines, which themselves may be affected by the spatial distribution of Bronze Age cities and civilizations. To get closer to a causal relationship between the metal transit trade and the emergence of cities, we employ a 2SLS estimation framework. The instrumental variable, described in detail in the previous section, is an alternative measure of potential transit trade, which captures the passage regions connecting mineral deposits and productive land, two objects unaffected by human intervention (unlike mines and cropland). We will thereafter refer to this variable as the "natural transit index". We remind the reader that the specific measure of land productivity used in constructing this variable reflects the potential biomass that can be produced in each region as dictated by climate factors: it is independent of the land's exploitation strategy, including both hunting-gathering and agriculture. The first stage is the following:

$$IHS(T_k) = \delta \, IHS(D_k) + X_k' \, \eta + \zeta_k, \tag{5}$$

where D_k is the instrumental variable.

The 2SLS estimates are reported in columns (2) to (8) of Table 1. Column (2) displays the most parsimonious specification, accounting solely for continent fixed effects. The first-stage results indicate that the instrument is positively correlated with the transit index and is powerful, with F-statistics ranging from 51 to 228. The second-stage results point towards an estimated θ of similar magnitude to the OLS estimates. In the next six columns, we control for all those geographical features that are mechanically correlated with the transit

Table 1: Transit trade and Bronze Age cities. OLS and 2SLS cross-sectional evidence using Reba, Reitsma and Seto (2016) city data

	Any City by 1300 BC (×100)							IHS #Cities
	OLS (1)	2SLS (2)	2SLS (3)	2SLS (4)	2SLS (5)	2SLS (6)	2SLS (7)	2SLS (8)
	OLS	**Panel A: Second stage**						
Transit index	0.379	0.437	0.440	0.406	0.397	0.411	0.403	0.005
	(0.090)***	(0.137)***	(0.157)***	(0.143)***	(0.123)***	(0.132)***	(0.148)***	(0.002)**
	[0.141]***	[0.203]**	[0.225]*	[0.204]**	[0.176]**	[0.191]**	[0.203]**	[0.003]*
Proximity mines			-0.009				-1.178	-0.014
			(0.077)				(0.484)**	(0.007)**
			[0.095]				[0.691]*	[0.010]
Proximity croplands				0.118			1.510	0.018
				(0.070)*			(0.553)***	(0.008)**
				[0.096]			[0.810]*	[0.011]
Sea					0.220		0.222	0.002
					(0.183)		(0.176)	(0.002)
					[0.184]		[0.179]	[0.002]
River					0.285		0.189	0.004
					(0.289)		(0.292)	(0.003)
					[0.377]		[0.346]	[0.004]
Mountains					-0.377		-0.405	-0.005
					(0.190)**		(0.260)	(0.003)
					[0.246]		[0.351]	[0.004]
Centrality						-0.045	-0.045	-0.001
						(0.026)*	(0.026)*	(0.000)
						[0.037]	[0.035]	[0.000]
		Panel B: First stage						
IV Transit index		0.714	0.616	0.648	0.623	0.689	0.518	0.518
		(0.047)***	(0.045)***	(0.046)***	(0.049)***	(0.048)***	(0.048)***	(0.048)***
		[0.073]***	[0.069]***	[0.070]***	[0.074]***	[0.074]***	[0.072]***	[0.072]***
Continent fixed effects	Yes	Yes	Yes	Yes	Yes	Yes	Yes	Yes
Area grid cell	Yes	Yes	Yes	Yes	Yes	Yes	Yes	Yes
Observations	10,970	10,970	10,970	10,970	10,970	10,970	10,970	10,970
Mean dependent variable	0.419	0.419	0.419	0.419	0.419	0.419	0.419	0.004
First-stage F-stat (5×5 grids)		228.2	186.1	198.8	159	205.9	115.6	115.6
First-stage F-stat (Conley 1000km)		94.31	79.31	84.67	70.40	86.39	51.60	51.60

Notes: Panel A reports cross-sectional OLS and 2SLS estimates of equation (4). Panel B reports the corresponding first-stage estimates (equation (5)). The unit of observation is a 1×1-degree grid cell k. 'Any city by 1300 BC' equals 100 if a city was present in grid cell k by 1300 BC (and 0 otherwise), while 'IHS #Cities' is the total number of cities that emerged before 1300 BC transformed using the inverse hyperbolic sine function. 'Transit index' is defined by equation (2), while 'IV Transit index' is defined by equation (3). Footnotes 31, 32, and 34 describe the construction of the controls: 'Proximity mines,' 'Proximity croplands,' and 'Centrality.' 'Sea' identifies coastline cells. 'River' identifies cells intersected by a river. 'Mountains' identifies cells with mean elevation above 15,000 feet (4,500 meters). Standard errors clustered at the level of 5×5 degree grid cells are reported in parentheses. Standard errors computed using the approach of Conley (1999) (cut-off 1000km) are reported in square brackets. * $p < 0.10$, ** $p < 0.05$, *** $p < 0.01$.

index measure. Specifically, in column (3), we control for proximity to mines[31], in column (4) for proximity to cropland[32], in column (5) for topography[33], and in column (6) for the centrality in the natural transportation network[34]. In column (7), we simultaneously add all aforementioned controls. Including these controls, separately or together, has minimal effect on the estimates of θ. The final column of Table 1 focuses on the intensive margin, indicating that the transit index not only affects the emergence of cities during the Bronze Age but also the number of cities that arise within each cell.

Appendix Figure B.9 provides the estimates for the benchmark 2SLS regressions (controlling exclusively for continent fixed effects) but, instead of focusing on cities established before 1300 BC, it examines cities established every 500 years from 3300 BC to 1300 BC. The figure shows that while the estimated coefficient for the transit index is consistently positive, it rises between 3300 BC and 2300 BC, then remains stable thereafter. Notably, it only becomes statistically significant from 2300 BC onwards. In Appendix Figures B.10 and B.11, the analysis differentiates between transit routes leading to copper and tin mines. The estimated coefficients for both transit indexes are positive in each millennium and increasing from 3300 BC to 2300 BC. However, while the estimated coefficient on the copper transit index is statistically significant already in the fourth millennium, the estimated coefficient on the tin transit index is statistically significant only from the latter half of the third millennium. This finding might reflect the transition from arsenic bronze, a copper-arsenic alloy, to tin bronze, a copper-tin alloy during the third millennium BC.

In Appendix Table A.2 we repeat the benchmark 2SLS analysis but control for the various measures of land productivity that have been employed in the comparative development literature. As discussed in Section 2, land productivity is commonly mentioned as a determinant of early urbanization and social hierarchy. However, conditional on the transit trade index, land productivity is negatively associated with the presence of cities. This suggests that the data do not support the conventional productivity theories explaining the rise of the Urban Revolution. Furthermore, including land productivity as a control does not affect the point estimate of θ.

A potential concern, related to the excluded instrument, comes from the mode-specific relative transportation costs used for its construction. As explained in Section 4.1, these costs are

[31]Formally proximity to mines M_k is defined as: $M_k = 1/\sum_{m \in \mathcal{M}} LC_{m,k}$, where $LC_{m,k}$ is the cost associated with shipping metal from the cost-minimising mine producing metal m to grid k.

[32]Formally, the proximity to cropland (PC) is given by $PC_k = \sum_{f \in \mathcal{F} \setminus \{k\}} \frac{1}{TC_{f,k}} \times Crop_f$, where $TC_{f,k}$ are the transport cost from grid cell f to cell k and $Crop_f$ is the croplands area of cell f.

[33]We include separate dummy variables for each of the topographical characteristics that influences the estimated transport cost to transit a cell. More specifically, making land the reference category, we include an indicator for the adjacency to the sea, the presence of a navigable river, and the presence of very high mountains.

[34]Network centrality is measured as the eigenvector centrality in the natural transportation network.

estimated from Bronze Age trade relationships in Europe and the Middle East. This might pose a threat to our identification strategy since Bronze Age transportation technologies might have been specifically tailored to the needs of civilizations in Europe and the Middle East: cities might be central in the metal trade network not because they initially emerged in natural passage regions between mines and cropland but because they acquired this centrality by developing specific transportation technologies to gain easy access to cropland and mines. To address this concern, we conduct two robustness checks, which are reported in the first two columns of Appendix Table A.3. First, we document that our estimates remain stable if we restrict the spatial extent of our analysis to areas that are not used in the estimation of the relative transportation costs (column (1)). Second, we employ relative transportation costs estimated for the Stone Age, rather than the Bronze Age, in constructing our instrument (column (2)). In both cases, the results are virtually unchanged although, as expected, the instrument exhibits slightly less statistical power in the latter case. In column (3) of Table A.3, we demonstrate that our estimates remain robust when accounting for a wide range of observable characteristics. To tie our hands, we extend the set of controls to include all natural characteristics employed in Henderson et al. (2018)'s article, which investigates the historical and current determinants of the spatial distribution of economic activity worldwide.[35] Additionally, we demonstrate that our results remain stable when controlling for transit trade indices constructed for all other metals traded during the Bronze Age: gold, lead, and silver (Murr, 2015).[36] This specifically speaks to the concern that metal deposits could be spatially clustered, in which case the bronze transit index could capture the effects of trade in other metals (column (4)).

A concern related to our main results comes from the data sources on Bronze Age cities. As discussed in the data section, the data in Reba, Reitsma and Seto (2016) are constructed from two rather old sources. For this reason, in Appendix Table A.4, we repeat the analysis using an alternative, more modern source: HYDE 3.1 (Klein Goldewijk, Beusen and Janssen, 2010). Rather than capturing the cities, this source reports the urban population in each grid-cell in each BC millennium since the Neolithic. The dependent variable is now the (IHS of) of the urban population in 2000 BC (the latest data point available before the Bronze Age collapse). Once again, all main results are confirmed.

Table A.5 (Panel A) delves deeper into identifying the specific components of the centrality measure that underpin the Urban Revolution. Column 1 mirrors our standard OLS regression, identifying road knots in the trade network via our benchmark transit index, which captures the least-cost paths linking square kilometers of farmland to the nearest tin and copper mines.

[35] Specifically, we control for average temperature, precipitation, (absolute) latitude, distance to coastline the length of growing period, ruggedness, Kiszewski et al. (2004)'s malaria index, 14 biome indicators, and dummy variables indicating whether a natural harbour lies within the grid cell.

[36] In analogy to our instrumental variable approach, we construct transit trade measures for gold, lead, and silver. That is, for each metal we combine the location of primary deposits with the climate-based net primary production to construct the transit trade measure according to Equations (5) and (7).

Subsequently, we explore three alternate transit indices. First, we consider a transit index that counts the least-cost paths passing through a cell, connecting every grid cell in the Old World to the nearest farmland (column 2). Second, we consider a transit index that counts the least-cost paths passing through a cell, connecting every grid cell in the Old World to the nearest tin and copper mine (column 3). Third, we consider a transit index that is similar to our benchmark but considers not the least-cost paths but the shortest paths connecting farmland with mines (i.e., it assumes that the cost of transportation is the same for sea, river, and land) (column 4). The estimates reveal that while these alternative transit indices are somewhat linked to urban presence, including them as control variables (alone or jointly) doesn't notably change the association between our primary transit index and the existence of Bronze Age cities (see columns 5-8). Panel B of Table A.5 corroborates this insight for the reduced form, using analogous variations of the exogenous natural transit index rather than the transit index. The conclusion from this table is that during the Bronze Age, the key factor for urban development was not simply being in a well-connected area with easy access to farmlands, mines, or other territories. Rather, it was crucial to be a transit hub that linked agricultural areas with tin and copper mines while using Bronze Age transport technologies.

Overall, the results presented in this subsection provide some evidence supporting the hypothesis that transiting long-distance metal trade played an important role in explaining the emergence of the Urban Revolution. Cities were much more likely to be established along trade corridors connecting cropland with tin and copper mines. The 2SLS estimates suggest a causal link but, due to the cross-sectional nature of the data, we cannot exclude that other potential omitted geographic factors might be driving the results (though we do control for a large number of confounders). To overcome this limitation, we next turn to panel data, which allows us to account for time-invariant geographic factors.

5.2 Difference-in-Differences evidence: Archaeological sites

In this subsection, we employ two additional data sources, which report information on the location of archaeological sites and ancient settlements in the Old World pre-dating the Bronze Age collapse. The first is an historical atlas of the most relevant archaeological sites (Bahn, 2000), and the second is a gazetteer for ancient history (the Pleiades Project, Bagnall, 2022). We use a difference-in-differences design to study whether, moving from the Stone Age to the Bronze Age, there was a shift in archaeological sites and settlements towards the passage regions in the Bronze Age metal trade. More specifically, we estimate the following equation:

$$y_{k,p} = \beta \; IHS(T_k) \times I_p^{BA} + X'_{k,p}\,\Phi + \mu_k + \mu_p + \psi_{k,p}, \tag{6}$$

where $y_{k,p}$ captures either archaeological sites or settlements dating from period p in grid cell k; I_p^{BA} is an indicator for the Bronze Age; T_k is the transit index; $X_{k,p}$ is a set of

time-varying control variables. Cell fixed effects, μ_k, control for time-invariant factors, while continent×period fixed effects, μ_p, control for any time pattern in the number of archaeological sites. We rely on a 2SLS framework to isolate an exogenous variation in the difference-in-differences regressor. Specifically, the first stage is:

$$IHS(T_k) \times I_p^{BA} = \sigma \, IHS(D_k) \times I_p^{BA} + X'_{k,p} \, \psi + \rho_k + \rho_p + \xi_{k,p}. \tag{7}$$

Table 2 presents the difference-in-differences results. In Panel A we use the Bahn (2000) data as outcomes, in Panel B the data from the Pleiades Gazetteer.

The first five columns of Table 2 report the OLS results for different outcomes and different sets of time-varying controls $X'_{k,p}$. We start by focusing on archaeological sites and using a parsimonious specification, in which we only control for regional trends by including continent×period fixed effects ρ_p. For both, the Bahn (2000) and the Pleiades data, we find that road knots, as captured by our transit index, are associated with an increase in archaeological sites. Specifically, doubling the number of least-cost paths passing by a grid cell is associated with an absolute increase in the likelihood of observing an archaeological site in the cell from the Stone Age to the Bronze Age in the order of 0.55 percent in the Bahn (2000)'s dataset (compared to a mean of 4.92 percent) and 0.45 percent in the Pleiades dataset (compared to a mean of 1.96 percent). In column (2), we see that these estimates are robust to the inclusion of a list of geographical controls interacted with period fixed effects. These controls include the full list of geographical features that are mechanically correlated with our transit index measure and that are already discussed in the previous subsection: proximity to mines, proximity to cropland, topography, and centrality in the transportation network. In columns (3)–(5), we replace the dependent variable with the (IHS-transformed) number of archaeological sites, the presence of settlements, and the (IHS-transformed) number of settlements, respectively. Our transit trade measure is associated with an increase in all these three alternative outcomes, thus confirming previous results.

In keeping with the structure of the previous analysis, we re-run all regressions using our 2SLS approach (columns (6)–(10)). The first-stage F-statistics range between 114 and 319, documenting the relevance of our instrument. Throughout, we find that bronze transit trade intensity increases the probability of discovering an archaeological site established during the Bronze Age, relative to a site established in the Stone Age (columns (6)–(8)). Similarly, we find a positive effect on the establishment of settlements in the next two columns. As in the cross-sectional analysis, the size of the IV estimates are close to their OLS counterparts.

In Appendix Table A.6 we conduct robustness tests in analogy to those presented in the previous subsection. Specifically, we show that our estimates are robust if (i) we restrict our sample to cells not used in the estimation of the relative transport cost vector $\boldsymbol{\alpha_{BA}}$, (ii) use relative transport costs estimated for the Stone Age (rather than the Bronze Age)

Table 2: Transit trade and archaeological sites. Difference-in-differences (Stone Age vs Bronze Age)

	OLS					2SLS				
	Any Site (×100)		IHS #Sites	Any Settlement (×100)	IHS #Settlements	Any Site (×100)		IHS #Sites	Any Settlement (×100)	IHS #Settlements
	(1)	(2)	(3)	(4)	(5)	(6)	(7)	(8)	(9)	(10)
Panel A: Second stage Bahn (2000) archaeological sites										
Transit index×Bronze Age	0.799	1.177	0.022	0.385	0.004	0.834	1.526	0.019	1.059	0.012
	(0.245)***	(0.259)***	(0.004)***	(0.116)***	(0.001)***	(0.348)**	(0.607)**	(0.008)**	(0.306)***	(0.003)***
	[0.259]***	[0.249]***	[0.004]***	[0.113]***	[0.001]***	[0.371]**	[0.585]***	[0.008]**	[0.294]***	[0.003]***
Panel B: Second stage Pleiades Gazetteer (Bagnall, 2022)										
Transit index×Bronze Age	0.645	0.606	0.011	0.482	0.009	0.421	0.419	0.008	0.421	0.008
	(0.117)***	(0.127)***	(0.003)***	(0.111)***	(0.002)***	(0.127)***	(0.222)*	(0.003)**	(0.192)**	(0.003)***
	[0.130]***	[0.134]***	[0.003]***	[0.117]***	[0.002]***	[0.130]***	[0.193]**	[0.003]**	[0.163]***	[0.002]***
Panel C: First stage										
IV Transit index×Bronze Age						0.626	0.448***	0.448	0.448	0.448
						(0.035)***	(0.039)	(0.039)***	(0.039)***	(0.039)***
						[0.041]***	[0.042]***	[0.042]***	[0.042]***	[0.042]***
Geography controls×Bronze Age	No	Yes	Yes	Yes	Yes	No	Yes	Yes	Yes	Yes
Grid cell fixed effects	Yes	Yes	Yes	Yes	Yes	Yes	Yes	Yes	Yes	Yes
Continent×Bronze Age	Yes	Yes	Yes	Yes	Yes	Yes	Yes	Yes	Yes	Yes
Observations	21,940	21,940	21,940	21,940	21,940	21,940	21,940	21,940	21,940	21,940
Mean dependent variable Panel A	4.923	4.923	0.066	0.670	0.007	4.923	4.923	0.066	0.670	0.007
Mean dependent variable Panel B	1.964	1.964	0.026	1.541	0.020	1.964	1.964	0.026	1.541	0.020
First-stage F-stat (5×5 grids)						319.1	135.4	135.4	135.4	135.4
First-stage F-stat (Conley 1000km)						231.1	114	114	114	114

Notes: This table reports difference-in-differences OLS and 2SLS estimates of equation (6). The unit of observation is a 1×1 grid-cell k in period p (Stone Age or Bronze Age). 'Any Site' ('Any Settlement') equals 100 rather than 0 for a grid cell k in period p if there is at least one archaeological site (settlement) dating from period p and located in grid cell k. 'IHS #Sites' ('IHS #Settlements') is the inverse hyperbolic sine function of the number of archaeological sites (settlements) dating from period p and located in grid cell k. 'Transit index' is defined by equation (2), while 'IV Transit index' is defined by equation (3). Geography controls include proximity to mines, proximity to croplands, sea dummy, river dummy, mountains dummy, and centrality. Panel A uses archaeological data from Bahn (2000), while Panel B uses data from Bagnall (2022). Panel C reports first-stage estimates (equation (7)). Standard errors clustered at the level of 5×5 degree grid cells are reported in parentheses. Standard errors computed using the approach of Conley (1999) (cut-off 1000km) are reported in square brackets. * $p < 0.10$, ** $p < 0.05$, *** $p < 0.01$.

in the construction of our instrumental variable, (iii) extend the set of control variables, and (iv) account for transit trade in other metals. Finally, as in the previous subsection, in the Appendix Figures B.12a–B.12d, we show the sensitivity of our estimates to different estimation methods for the standard errors.

Pre-trends

To trace out the impact of transit trade over time and test for pre-trends, we construct two panel datasets (see Section 3 for details). The first is a three-period panel. Based on information reported in Bahn (2000), we count the number of archaeological sites that fall within each grid, separately for the Paleolithic/Mesolithic, Neolithic, and Bronze Age. The second dataset is based on the dated sites in the Pleiades Project and reports the number of archaeological sites in each grid cell, dated at 1,000 year intervals from 7000 BC to 1300 BC.

To investigate if our transit trade index exerts different effects over time, we interact the (time-invariant) index with time period fixed effects. In the subsequent analysis, we use the period preceding the Bronze Age as the reference category. For the three-period panel this is the Neolithic, for the six-period panel we take the time period [5000,4000) as the reference category. The time-period interacted coefficients of the transit trade index thus capture the differential effect of the transit trade on the outcome in a given period relative to the base period. The inclusion of grid cell fixed effects and time period dummies implies that time-invariant cell-specific differences as well as general time-specific changes are washed out.

Formally, the second stage can be represented as:

$$y_{k,p} = \sum_{p=1}^{P} \psi_p \, T_k \times I_p + X'_{k,p} \, \lambda + \tau_k + \tau_{c(k),p} + \varepsilon_{k,p}. \tag{8}$$

The dependent variable $y_{k,p}$ indicates the presence of any archaeological site in grid cell k in period p. Grid-cell-level fixed effects are represented by τ_k, continent×time-period fixed effects by $\tau_{c(k),p}$, and the idiosyncratic error term by $\varepsilon_{k,p}$. In keeping with the previous analysis, we also include the full set of (time-period interacted) controls, $X_{k,p}$. The coefficients ψ_p capture the additional effect of the transit trade index in each period relative to the reference period.

Figure 2 visualizes the resulting 2SLS point estimates and the 90 percent confidence intervals. In panel (a) we use the data from Bahn (2000), in panel (b) the information from the Pleiades Project. In both cases, we find that the transit trade only starts to exert a differential effect on the probability of finding an archaeological site after the onset of the Bronze Age. Point estimates for earlier periods are not statistically significantly different compared to the reference period. This absence of pre-trends provides further evidence that our estimates capture the Bronze Age-specific effects of transit trade in input metals.

Taken together, the estimates reported in this subsection corroborate the hypothesis that

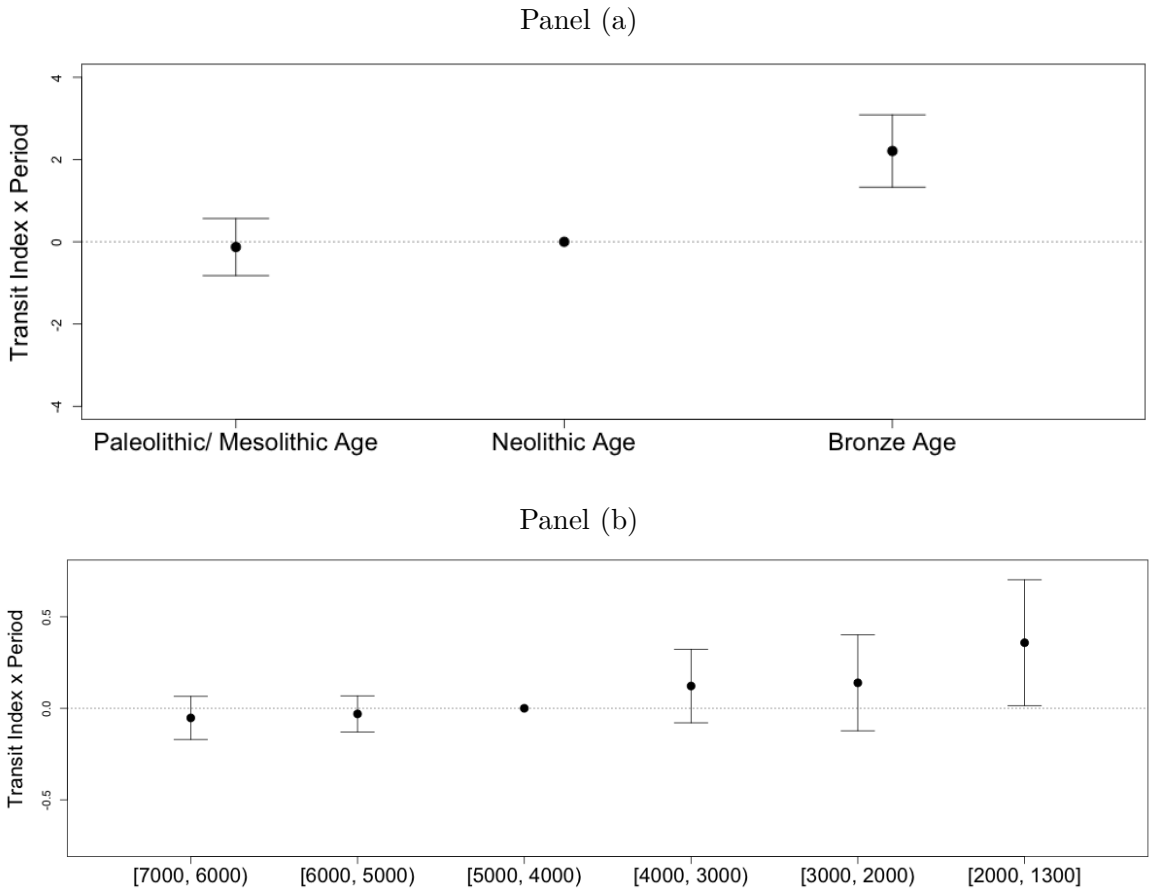

Figure 2: Estimated impact of the transit index on the spatial location of archaeological sites over time

Figure depicts 2SLS point estimates and 90% confidence intervals of ψ_p in equation (8). Standard errors are clustered at the level of 5×5 degree grid cells. Dependent variable equals 100 if an archaeological site is present in a given 1×1 grid cell k dating from period p and 0 otherwise. Panel (a) uses data on archaeological sites from Bahn (2000); the reference period is the Neolithic Age. Panel (b) uses data from Bagnall (2022); the reference period is the time span $[5000, 4000)$ BC. See Section 3 for details on definition and construction of variables.

regions located along metal trade corridors were more likely to see the emergence of settlements and large built-up areas during the Bronze Age. Still, an important note of caution relates to the quality of our outcome variables employed so far. As outlined in Section 3, these come with various caveats. Specifically, the Bahn (2000) data are rather outdated, while the Pleiades data are skewed towards Europe, the Middle East, and Mediterranean Africa.

In the last part of this empirical section, we reproduce our main insights focusing on two regions for which high-quality data are available: China and Europe.

5.3 China

Bronze metallurgy in China originated around 2000-1900 BC and it probably developed inside China separately without outside influence. The archaeological site of Erlitou is the largest among the sites dating from these years. As explained in detail in subsection 7.6, Erlitou is located at the center of an intricate network of rivers connecting metal-rich mountains to the fertile Chinese lowlands. Essentially, a recent archaeological literature argues that Erlitou took advantage of this strategic position to direct the metal trade in the region, eventually becoming the capital of a trade civilization (and probably the first state in Chinese history). In this subsection, we show that the link between trade and the Urban Revolution in China extends beyond the Erlitou civilization.

The advantage of focusing on China is that we can rely on a comprehensive and detailed catalog of Chinese archaeological sites, which we digitized to capture the rise and spread of the Urban Revolution in the Chinese context. As described in the data section, we use a text algorithm to identify sites indicative of (1) urban settlements, (2) ruling class exempt from manual tasks, (3) monumental building, (4) a standardized system of measures and recordings used in exchange and production, (5) writing, and (6) highly developed art forms.

We aggregate these artifacts at 1×1 degree grid-cells for three periods: Paleolithic, Neolithic, and Bronze Age. We assume that the Bronze Age starts in 2070 BC with the first Chinese dynasty (Xia) and ends in 771 BC with the Western Zhou dynasty. The result is a panel dataset that illustrates the rise of different aspects that have been associated with the Urban Revolution in China.

Empirical analysis

To study how metal trade fostered the Urban Revolution in this context, we estimate the difference-in-differences regression model in equation (6). The main results are illustrated in Table 3. In this table we use three variables to capture the Urban Revolution. The first one is an indicator variable, which identifies the presence of archaeological sites that feature at least one of the six Childe's criteria associated with the Urban Revolution; the second one is a variable that counts the number of criteria; the third is a principal component of the six criteria.

Both the OLS and 2SLS estimates point towards a large and statistically significant association between the transit index measure and the Chinese relics indicative of the Urban Revolution. The 2SLS estimates imply that an exogenous doubling of the number of transiting paths connecting metal mines with cropland implies an increase in the probability of featuring sites indicative of the Urban Revolution during the Bronze Age in the order of 600 log points. The magnitude of the estimated coefficient does not change if we run the parsimonious specifications, with only grid-cell and period fixed effects, or if we consider our

Table 3: Transit trade and archaeological sites in China. Difference-in-differences (Stone Age vs Bronze Age)

	OLS				2SLS			
	Any Criteria (×100)		IHS #Criteria	Principal Component (SD)	Any Criteria (×100)		IHS #Criteria	Principal Component (SD)
	(1)	(2)	(3)	(4)	(5)	(6)	(7)	(8)
	Panel A: Second stage							
Transit index×Bronze Age	4.461	3.315	0.106	0.113	6.373	7.215	0.205	0.232
	(0.676)***	(0.753)***	(0.023)***	(0.029)***	(1.179)***	(2.682)***	(0.071)***	(0.078)***
	[0.376]***	[0.390]***	[0.018]***	[0.022]***	[0.892]***	[2.112]***	[0.059]***	[0.065]***
	Panel B: First stage							
IV Transit index×Bronze Age					1.134	0.578	0.578	0.578
					(0.115)***	(0.129)***	(0.129)***	(0.129)***
					[0.122]***	[0.108]***	[0.108]***	[0.108]***
Geography controls×Bronze Age	No	Yes	Yes	Yes	No	Yes	Yes	Yes
Grid cell fixed effects	Yes	Yes	Yes	Yes	Yes	Yes	Yes	Yes
Period fixed effects	Yes	Yes	Yes	Yes	Yes	Yes	Yes	Yes
Observations	2,138	2,138	2,138	2,138	2,138	2,138	2,138	2,138
Mean dependent variable	17.91	17.91	0.378	0	17.91	17.91	0.378	0
First-stage F-stat (5×5 grids)					98.02	19.94	19.94	19.94
First-stage F-stat (Conley 1000km)					85.29	28.30	28.30	28.30

Notes: Panel A reports difference-in-difference OLS (columns (1)–(4)) and 2SLS (columns (5)–(8)) estimates of equation (6), while panel B reports the first-stage estimates (equation (7)). The unit of observation is a 1×1 grid-cell k in period p (Stone Age or Bronze Age). 'Any Criteria' equals 100 (rather than 0) if there is any archaeological site in grid cell k dating from period p that displays some evidence of at least one of the following features: large settlement, monumental building, a ruling class exempt from manual tasks, a system of recording, writing, art. 'IHS #Criteria' is the IHS transformation of the number of these features. 'Principal Component (SD)' is the standardized principal component. 'Transit index' is defined by equation (2), while 'IV Transit index' is defined by equation (3). Geography controls include proximity to mines, proximity to croplands, sea dummy, river dummy, mountains dummy, and centrality. Standard errors clustered at the level of 5×5 degree grid cells are reported in parentheses. Standard errors computed using the approach of Conley (1999) (cut-off 1000km) are reported in square brackets. * $p < 0.10$, ** $p < 0.05$, *** $p < 0.01$.

benchmark specifications with the usual full set of controls.

The richness of the data further allows us to investigate if transit trade differentially fostered specific aspects of the Urban Revolution. To this end, we define six dummy variables, each capturing if a specific urban revolution criterion is present in a given grid cell and period. We then separately run our 2SLS difference-in-differences regressions with the full set of controls using these dummies as outcomes. Figure 3 visualizes the results: metal transit trade seems to affect almost every aspect of the Urban Revolution.

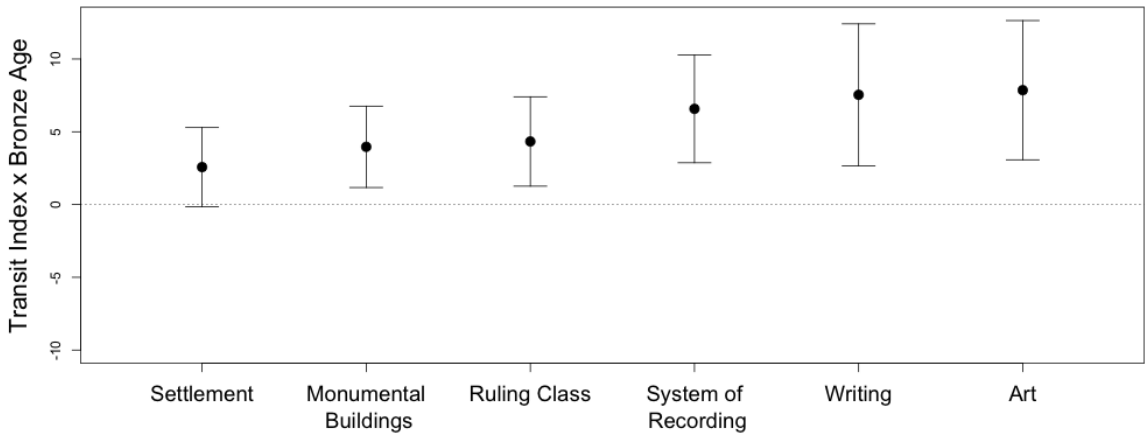

Figure 3: Estimated impact of the transit index on the rise of the Urban Revolution in China
Figure depicts 2SLS point estimates of β in Equation (6) and 90% confidence intervals. Each data point corresponds to a regression with a different depedent variable. The depedent variables equals 100 (rather than 0) if there is any archaeological site in 1×1 degree grid cell k dating from period p (Stone Age or Bronze Age) that displays some evidence of: large settlements, monumental buildings, a ruling class exempt from manual tasks, a system of recording used in the production process, writing, figurative art. Standard errors are clustered at the level of 5×5 degree grid cells.

The results presented in this subsection corroborate the findings of our previous 'global' analysis for the case of China, where very detailed outcome variables are available. In a final step, we provide further evidence for the general validity of our results by testing for the existence of pre-trends. In analogy to the main part, we analyze if metal transit trade had a differential impact during the Bronze Age by interacting the transit trade index with time period fixed effects (see Section 5.2 for more details). Figure 4 depicts the results. Reassuringly, we fail to detect any pre-trends. The transit index measure produces a differential increase in the sites indicative of the Urban Revolution only in the Bronze Age.

5.4 Europe

This subsection delves into the Bronze Age in Western and Central Europe. The advantage of focusing on this area is that the European Bronze Age is the most extensively studied episode in world archaeology, and the rich archaeological record, combined with radiocarbon dating, makes it possible to trace changes in both the transit regions in the metal trade network

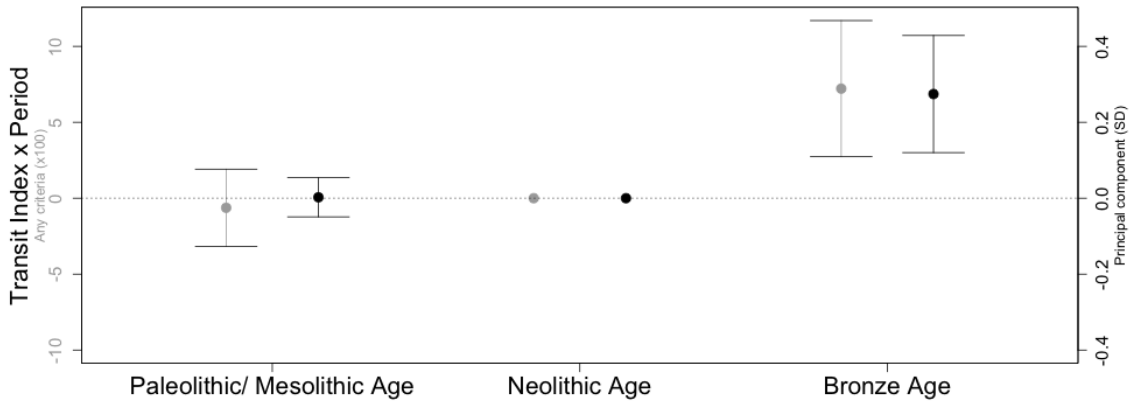

Figure 4: Estimated impact of the transit index on the rise of the Urban Revolution in China over time

Figure depicts 2SLS point estimates of ψ_p in equation (8) and 90% confidence intervals. Standard errors are clustered at the level of 5×5 degree grid cells. Grey: Dependent variable equals 100 (rather than 0) if at least one of the following features is present in sites in 1×1 degree grid cell k dating from period p: large settlements, monumental buildings, evidence of a ruling class exempt from manual tasks, a system of recording used in the production process, writing, figurative art. Black: Dependent variable is the (standardized) first principal component obtained from pooling these six features. The reference period is the Neolithic.

and the socio-economic dynamics that unfolded during this period. Specifically, we track the changes in the transit index generated by the discovery of new mines (and the depletion of old ones) that occurred in the period [1300 – 750 BC] - the Central-Europe Late Bronze Age. We then study how these changes affect the development of complex hierarchies. As previously acknowledged, Central and Western Europe did not experience the emergence of full-fledged civilizations or cities during the Bronze Age. Nonetheless, this region did witness the shift from classless bands and tribes to hierarchically structured societies, i.e., chiefdoms, where local leaders wielded a degree of centralized decision-making authority. We capture this development with data on carbon-dated Bronze Age elite burials.

Empirical analysis

As described in Section 3.1.4, we construct a two-period grid-cell panel data set that spans the Central-Europe Early/Middle Bronze Age [3000 BC, 1300 BC) and Late Bronze Age [1300 BC, 750 BC]. On these data, we run the following difference-in-difference OLS regression model:

$$y_{k,p} = \beta\ IHS(T_{k,p}) + X_{k,p}\,\chi + \mu_k + \tau_p + \psi_{k,p}, \tag{9}$$

The dependent variable, $y_{k,p}$, is either an indicator for the presence of elite burials dating from period p in the grid cell k or is an IHS transformation of the number of elite burials. The main explanatory variable is the IHS transformation of the transit trade index for cell k in period p. The vector $X_{k,p}$ represents control variables. Grid cell fixed effects and period

fixed effects are symbolized by μ_k and τ_p, respectively.

Table 4 reports the results of regression model (9). The point estimate in column (1) implies that it becomes 2.6 percentage points more likely to find evidence of an elite when transit trade increases by one percent. This translates into a 26 percent increase when moving from a cell without transit trade to one cell intersected by a path that connects a mine to a cell that devotes all of its area to crop cultivation. The size of the point estimate drops slightly from 2.6 to 2.1 when we control for proximity to mines—the other variable that exhibits within-Bronze Age variation—in column (2). The statistical significance of our results, however, is unaffected. In columns (3)–(4) we use the IHS number of elite burials as a measure of hierarchy. The qualitative pattern of results remains unchanged.

Table 4: Transit trade and elite burials in Europe

	Any Elite Burial (×100)		IHS Number of Elite Burials	
	(1)	(2)	(3)	(4)
Transit index	2.563 (1.115)** [0.892]***	2.132 (1.120)* [0.716]***	0.033 (0.018)* [0.016]**	0.020 (0.018) [0.012]*
Geography controls	No	Yes	No	Yes
Grid cell fixed effects	Yes	Yes	Yes	Yes
Period fixed effects	Yes	Yes	Yes	Yes
Observations	1,194	1,194	1,194	1,194
Mean dependent variable	23.03	23.03	0.493	0.493

Notes: This table reports OLS estimates of equation (9). The unit of observation is a 1×1 grid-cell k in period p. There are two periods: Central-Europe Early/Middle Bronze Age [3000-1300 BC) and Late Bronze Age [1300-750 BC]. 'Any Elite Burial' equals 100 if there is any elite burial (i.e., grave with metal weapon) dating from period p in grid cell k and 0 otherwise. 'Transit index' is defined by equation (2), while 'IV Transit index' is defined by equation (3). 'Geography controls' include the time-varying proximity to mines. Standard errors clustered at 1×1 degree grid cells are reported in parentheses. Standard errors computed using the approach of Conley (1999) (cut-off 1000km) are reported in square brackets. * $p < 0.10$, ** $p < 0.05$, *** $p < 0.01$.

The data on elite burials were constructed for 26 European countries. None of these countries is essential for our results. In Appendix Figure B.13 we re-run our benchmark regression (the one in column 1 of Table 4) but excluding countries one by one: in all cases the estimated coefficients are stable and statistically significant.

6 Appropriability mechanism

The results so far indicate that trade in bronze inputs was an important driver of the Urban Revolution. Social stratification, complex hierarchies, states, and cities were more likely to emerge in regions central in the metal trade network. In this section, we study one potential mechanism underlying this result. The first subsection outlines a theoretical framework which emphasizes the appropriability nature of transit metal trade. While some optimal routes connecting populations with mining regions could be easily circumvented, some others could not be avoided unless traders were willing to face a substantial increase in transportation

costs. We argue that it is exactly in these latter regions that a new elite, relying on taxing transit traders, could rise. Sufficient fiscal revenues allowed this elite to pay the fixed cost needed to establish the monopoly of power and commit to a revenue-maximizing tax rate. In turn, this arrangement was beneficial to metal traders, who avoided higher expropriation rates by unorganized roving bandits. The main insight from the model is that a trade-taxing elite, and associated civilization, is more likely to emerge in the bottlenecks to the metal trade network - regions that (a) have high transit trade volumes and (b) are costly to circumvent. In the second subsection, we bring the theory to the data. We construct a measure of the potential tax revenues that could be extracted by an elite in a grid cell, by calculating the additional trade costs to metal traders to avoid that cell. We then run a horse race between this measure, which identifies the bottlenecks in the metal trade network, and the transit trade index, which identifies the road-knots. It turns out that the bottlenecks were indeed the ultimate cradle of civilization.

6.1 Theory

In Appendix E, we present a simple model. The model is inspired by Mayshar, Moav and Pascali (2022) but features a spatial dimension. Space, mirroring our empirical setup, is structured into grid cells. Transport costs between adjacent cells are the key exogenous parameters. Grid cells can be organized as hierarchy, with a king that establishes the monopoly of violence and employs tax collectors, or as anarchy, with unorganized roving bandits.

The model includes three key agent types: farmers, foragers, and traders. Farmers are located in grid cells and produce crops using metal and cropland. Foragers are also located in grid cells and can earn a fixed exogenous income from foraging: otherwise they can choose to become bandits (under anarchy) or tax collectors employed by the king (under hierarchy). Traders transport metal from mines to farmers following a route, which traverse through grid cells and minimize trade costs. Trade costs depend on transportation costs and expropriation rates along the route. Expropriation rates in each cell are an increasing concave function of the number of bandits in cells under anarchy and of the number of tax collectors in cells under hierarchy. Specifically, in the two regimes expropriation rates are determined in the following way.

Case one: **Anarchy**. In a cell under anarchy, some foragers may turn into bandits. The expropriation rate is the one that makes bandits indifferent between entering banditry or earning an exogenous income as foragers.

Case two: **Hierarchy**. Political entrepreneurs can establish themselves as kings and establish the monopoly of violence in a grid cell by paying a fixed cost. The monopoly of violence allows states to deter bandits and to tax transit metal trade. The king hires tax collectors among foragers and pays wages set by the outside option of foraging. Kings set transport route-specific optimal tax rates to maximize net tax revenue for each least-cost route travers-

ing their territory. Optimal tax rates on a route cannot exceed the extra transportation costs that traders on that route would have to incur to avoid the king's grid cell.

The model offers three insights about expropriation rates and state formation in a grid cell. First, expropriation (tax) rates in hierarchy are lower compared to expropriation rates in anarchy. Second, in hierarchy tax revenues cannot exceed the "blockage cost" - the extra transport costs that all traders would face if the cell is removed from the network. Third, if the blockage cost is lower than the fixed cost for establishing the monopoly of violence, no hierarchy emerges. Fourth, hierarchy Pareto dominates anarchy.

Overall, the simplest insight of the model is that a state is more likely to emerge in cells characterized by high blockage costs. This prediction mirrors the conjecture that an extensive anthropological and archaeological literature, discussed in Section 2, has advanced to explain the rise of complex hierarchies during the Bronze Age. In the words of Earle et al. (2015), "In simple terms, the BA witnessed an emergence of social stratification based on control over commodity flow. [..] bottlenecks emerged in metal flows to offer emerging elites opportunities to extract surpluses".

6.2 Empirical evidence

To gauge the extent to which the rise of a tax-levying elite drives our results on the causal impact of transit trade on hierarchy, we construct a transit trade centrality measure that incorporates the scope for taxation. We build on the intuition, developed in our theoretical framework, that revenues from taxing transit trade in a certain region depend not only on the optimal routes passing by the region, but also on the absence of valid alternatives to these routes. In order to translate this insight to the data, for each grid cell in the Old World, we compute its modified efficiency centrality (Wang, Wang and Deng, 2019) in the metal trade network (see Appendix F for details). This centrality measure captures the increase in global transport costs if the cell is blocked for transit (i.e., if we do not allow paths connecting cropland with mines to intersect the cell). Subsequently, we refer to this centrality measure as the 'blockage cost' of the cell. The geographic distribution of these blockage costs, which is visualized in Figure 5, identifies the bottlenecks in the metal trade transportation network and, according to our theory, the potential for a local tax extracting elite.

We then test whether some of the impact of transit metal trade on the rise of hierarchy and the Urban Revolution, that we have documented in the previous section, can be explained by the rise of a local tax extracting elite. To do so, we re-run all the benchmark OLS specifications[37] in the previous sections, but now disentangling the role of the transit trade

[37]Subsequently, we restrict our analysis to OLS regressions. With IV regressions, we are not able to disentangle the relative importance of the trade versus taxation channel because both instruments (the one for our main transit index and the one for the blockage cost) have predictive power for both potentially endogenous variables

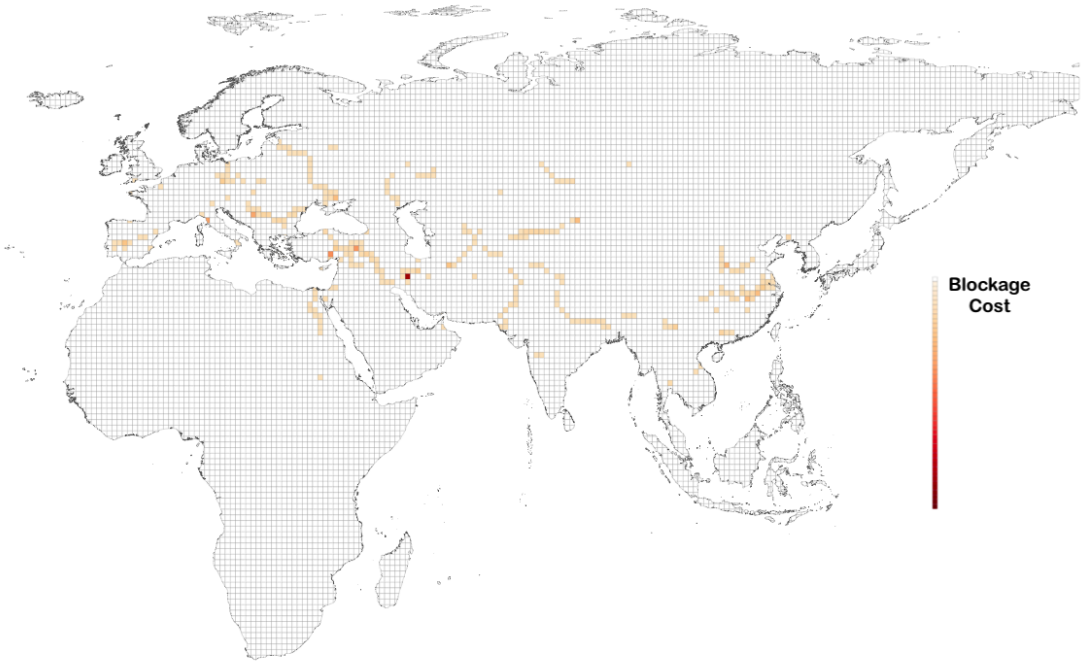

Figure 5: Blockage cost.
Figure depicts the global cost of blocking a cell for transit trade in 3000 BC (see Appendix F for more details). Darker shadings imply greater costs.

index from the role of the blockage cost. If taxation plays a role, we would expect the blockage cost coefficient to be statistically significant, positive and sizable.

Table 5 presents the findings of the horse race regressions. In analogy to the structure of Section 5 we first look at cross-sectional city data from Reba, Reitsma and Seto (2016). Column (1) reproduces the results of the OLS regression with full controls; the point estimate is 0.407. The size of the transit trade index drops by more than 60 percent (column (2)), when we account for the blockage cost. More importantly, the latter is statistically significant, positive and of considerable economic magnitude. This result is suggestive that the rise of a trade-taxing elite is a plausible mechanism to explain the relationship between transit trade and the distribution of Bronze Age cities. In columns (3)–(4) we run the OLS difference-in-difference regression using the Pleiades Gazetteer panel, while in columns (5)–(6) we do the same using the Atlas of Chinese Relics. In both cases, the estimated coefficient on the blockage cost is positive, large and statistically significant. At the same time, the estimated coefficient on transit trade drops between 24% to 32% when we control for blockage costs. In the last two columns of Table 5, we focus on Europe and run the statistical horse race exploiting only within-Bronze Age variation. The results continue to exhibit a consistent picture. When including the blockage cost as a regressor our the estimated coefficient on the

transit index drops by 60%, now even losing statistical significance at conventional confidence levels. The blockage cost coefficient, on the other hand, is statistically significant and large.

Taken together, the results presented in 5 provide suggestive evidence that the emergence of a trade-taxing elite might be the crucial link explaining the relationship between metal transit trade and the rise of civilization.

Caveats

It is important to note that these horse race regressions can only offer suggestive evidence of an appropriability mechanism linking the transit metal trade and the emergence of hierarchy. Three important caveats should be considered. First, since we could not identify exogenous variations in the blockage cost variable, we acknowledge that these OLS estimates fall short of establishing a causal relationship. Second, as is typical in OLS horse race regressions, discrepancies in measurement errors between the transit index and blockage cost variables may account for significant variations in the magnitude and statistical significance of the estimated coefficients on these two variables. Third, even in instances where we could accurately identify the causal impact of both the transit index and blockage costs, it is plausible to conceive of models wherein higher blockage costs are associated with increased transit trade for the same level of the transit index (e.g., in scenarios involving congestion costs along trade routes).

To provide further evidence in support of the appropriability theory we present a series of case studies linking metal trade with state formation in the next section.

7 Case studies

In this section, we focus on Mesopotamia, the Indus Valley, Aegean Sea and China and discuss the rise of some of the very first urbanized societies. We establish three facts that support our appropriability theory behind the rise of the Urban Revolution. First, Bronze Age urban centers are strategically located in the trade network. In fact, most cities can be found at the confluence between different rivers (e.g., Erlitou), at the delta of large rivers (e.g., Ur) or on waterways connecting different seas (e.g., Troy). Land productivity does not seem relevant: in several cases (e.g., Assur), cities are surrounded by rather infertile land. Second, a large archaeological literature has related the rise of the first urbanized core of these civilizations to the transit metal trade and has documented that the first urban elites were directly involved in the trade of metals. Third, recent work in archaeology and history has emphasized that the expansion of the core and the rise of the first empires is motivated by the need to secure trade connections and directly access metal mines.

Table 5: Horserace: transit index vs blockage costs

	Any City 1300 BC (×100) Reba, Reitsma and Seto (2016)		Any Site (×100) Bahn (2000)		Any Criteria (×100) Atlas of Chinese Relics		Any Elite Burial (×100) Prähistorische Bronzefunde	
	(1)	(2)	(3)	(4)	(5)	(6)	(7)	(8)
Transit index	0.407	0.158					2.132	0.676
	(0.093)***	(0.065)**					(1.120)*	(1.095)
	[0.145]***	[0.070]**					[0.716]***	[0.554]
Blockage cost		0.664						1.628
		(0.232)***						(0.765)**
		[0.301]**						[0.457]***
Transit index×Bronze Age			1.177	0.798	3.315	2.529		
			(0.259)***	(0.331)**	(0.753)***	(0.623)***		
			[0.249]***	[0.290]***	[0.390]***	[0.427]***		
Blockage cost×Bronze Age				1.014		2.090		
				(0.575)*		(1.578)		
				[0.383]***		[0.966]**		
Geography controls	Yes	Yes	Yes	Yes	Yes	Yes	Yes	Yes
Grid cell fixed effects	No	No	Yes	Yes	Yes	Yes	Yes	Yes
Continent×period fixed effects	No	No	Yes	Yes	Yes	Yes	Yes	Yes
Observations	10,970	10,970	21,940	21,940	2,138	2,138	1,194	1,194
Mean dependent variable	0.419	0.419	4.923	4.923	17.91	17.91	23.03	23.03

Notes: This table reports OLS estimates. Transit index' is defined by Equation (2), while Appendix F describes the construction of the variable 'Blockage cost'. The dependent variables and the 'Geography controls' are the same as in Tables 1 (for columns 1 and 2), Table 2 (for columns 3 and 4), Table 3 (for columns 5 and 6), and Table 4 (for columns 7 and 8). Standard errors clustered at the level of 5×5 degree grid cells (columns 1–6) and 1×1 degree grid cells (columns 7–8) are reported in parentheses. Standard errors computed using the approach of Conley (1999) (cut-off 1000km) are reported in square brackets. '* p < 0.10, ** p < 0.05, *** p < 0.01. * $p < 0.10$, ** $p < 0.05$, *** $p < 0.01$.

7.1 Ancient Sumer in the Early Dynastic Period (2900-2334 BC)

The Urban Revolution started with the Sumerian Civilization. After a long transition during the Uruk period, full urban life flowered during the Early Dynastic Period. At this point, all the 10 formal criteria that Childe uses to define Urban Revolution can be traced in South Mesopotamia. A thesis with a long-standing tradition in anthropology and archaeology is that long-distance trade was the main driving factor of this "Revolution." The first Sumerian cities emerged along the coast of the Persian Gulf, in the alluvial delta of the Tigris and Euphrates. These cities were located in a nodal point connecting Anatolia, Mesopotamia, and Iran with the Persian Gulf, through an enormous dendritic transportation system created by the north-to-south flowing rivers. In the words of Guillermo Algaze: *"That emergence of early cities in the southern Mesopotamian alluvium must be understood in terms of the unique ecological conditions that existed across the region during the fourth millennium, and the enduring geographical framework of the area, which allowed for the efficient movement of commodities via water transport and facilitated interaction between diverse social units alongside natural and artificial river channels. These conditions promoted evolving long-term trade patterns that, inadvertently, differentially favored the development of polities in the southern Mesopotamian alluvium over contemporary societies in neighboring regions."*

The principal commodities referred to in commercial documents during the Early Dynastic Period are copper, tin, and tin-bronze, which were usually purchased in exchange for silver, barley and wool (Lambert, 1953; Leemans, 1975; Foster, 1997; Dercksen, 1999; Prentice, 2010).

Ancient Sumerian cities were the first to show evidence of copper alloys utilization. Sumer was the birthplace of arsenic copper, which became prevalent in the second half of the 6th millennium BC, and bronze technology. The rise of bronze production coincides with the rise of the Urban Revolution among the Sumerians: tin bronze is thought to have been introduced in Mesopotamia at the very end of the 4th millennium BC, with the first known bronze object dating from around 3000 BC. Notice, however, that South Mesopotamia has no local sources of metals. The focus of much documented commercial activity of Sumerian cities is the acquisition of copper and tin, through both land routes connected to the rivers or sea routes[38].

Regarding copper, two well-documented routes were used to bring this metal to Mesopotamia. The first was a land route, which connected the mines in the Zagros (Iran) and the Taurus (Turkey) mountains with Southern Mesopotamia, and was facilitated by the rivers and canals

[38] Curiously, a famous tablet, excavated in Ur, contains the oldest known customer complaint. The complaint refers to the quality of the copper sold from a merchant coming from Dilmun, a polity almost certainly corresponding to present-day Bahrein: "When you came, you said to me as follows: I will give Gimil-Sin (when he comes) fine quality copper ingots. You left then but you did not do what you promised me. You put ingots which were not good before my messenger (Sit-Sin) and said: If you want to take them, take them; if you do not want to take them, go away! [..] Is there anyone among the merchants who trade with Dilmun who has treated me in this way? You alone treat my messenger with contempt!"

in the water system formed by the Tigris and the Euphrates (Muhly, 1973; Morr and Cattin, 2013). The second route was a sea route, which connected Ur and the other Sumerian ports in Southern Mesopotamia, through the Persian Gulf, to three exporters of copper: Magan, Dilmun and Meluhha. Magan was a polity located in present-day Oman and a major source of copper ores. Recent estimates report that approximately half of the Sumerian copper was coming from there (Giardino, 2019)[39]. Dilmun is already cited in archaic texts dealing with the copper trade in Uruk from the late fourth millennium BC. The importance of this trading post is confirmed by the fact that copper trade in the Persian Gulf was carried out by the "Dilmun boats" and transactions in Ur were conducted using the "Dilmun weight standard." Dilmun probably served only as a trading post and it was never the ultimate origin of the traded products. Based on epigraphic and archaeological evidence, it seems that the ultimate source of copper trade through Dilmun was Meluhha (Begemann et al., 2010), which is generally believed to be located in the present-day Indus Valley (Muhly, 1973), where the Harappan Civilization flourished starting from the mid-third millennium BC. Lead isotope studies have suggested that the ultimate source of copper traveling through Dilmun in Mesopotamia might be the Aravalli Hills in southern Rajasthan (Begemann and Schmitt-Strecker, 2008).

As opposed to copper, the Bronze Age sources of tin for Mesopotamia are not as well defined. The cuneiform texts seem to indicate that all the major tin sources used in the region in the early bronze age were located east of Mesopotamia. Imported tin is believed to originate mainly from western Afghanistan and the Zagros mountains in current-day Iran. Tin from Afghanistan was probably transported through a sea route passing by Magan (Cleuziou, 1982), while a land route from the Zagros mountains was probably opened later. Limited evidence of tin mining during the Bronze Age is also present in Goltepe, in Anatolia, which led to the hypothesis that some of the tin used in Mesopotamia might have also come from Anatolia (Yener and Vandiver, 1993; Yener, 2021).

The trade vocation of Sumerian cities is evidenced in the Epic of Gilgamesh, the first known piece of literature in history. The story opens with a description of Uruk (probably the first city in human history), emphasizing the beauty of its walls and its markets. The city itself is referred to as "the great market".

7.2 The Harappan civilization in the Indus Valley (2600-1900 BC)

The second half of the third millennium BC marked the birth of the first urban civilization in southern Asia, in the Indus Valley. Rather than emerging from a slow period of gradual growth and modification, as in the Sumerian case, the Harappan civilization seems to have resulted from a very short period of transformation (Green and Petrie, 2018). During the Urban Phase

[39]Moreover, excavations from the 1970s have yielded clear evidence of large-scale production of copper throughout the mountainous region of eastern Oman that can be traced back at least to the middle of the third millennium BC (Weisgerber, 1981, 1983).

(or Mature Harappan), within 100-150 years, both writing and a widely used system of weights and measures appeared, towns started displaying monumental buildings, signs of centralized urban planning (e.g., massive brick platforms, well-digging, drainage systems, gird plans) and unprecedented levels of social differentiation emerged (e.g., big/tiny houses, brick/mud houses, growth in the use of precious metals for personal adornments etc.). Starting from the seminal work of Possehl (1990) and Ratnagar (1981), several scholars have suggested that transiting trade was a major factor in the rise and maintenance of the urban centers. Trade was facilitated by two major river systems, the Indus and the Ghaggar-Hakra (now dry), which were connecting regions rich in tin and copper in Baluchistan and Afghanistan, through the Gulf of Oman, to the Persian Gulf and Mesopotamia.

In the words of Rita P. Wright (2010, p.231): *"The scale of the distribution system far outweighs anything known from previous periods and clearly was a catalyst in the growth of urbanism at mid-third millennium BC. Most revealing is the expansion of settlement into new territories located in regions strategically placed for long-distance trade linked to maritime routes."*

The foundation of some of the largest settlements in the Indus floodplains most likely reflected the growing importance of river transport. Jansen (2002) argues that this was the case for Monehjo-daro, the largest settlement in the Indus valley and one of the world's earliest major cities. Its location was unsuitable for settlement, as it was at the constant risk of flooding by the nearby Indus. Still, *"this pristine settlement was founded in key central location midway between Harappa and the mountains on the one hand and Dholavira and the sea on the other, where the great highway of the Indus met a major routes into the mountains via the Kachi plain and the Bloan pass."* (McIntosh, 2007, p.389).

An appropriability mechanism behind the link between trade and civilization has been proposed by several scholars. For instance, Jane R. McIntosh (2007, p.394) writes: *"Towns developed at communications nodes or in locations well-placed to procure resources. [..] A managerial class emerged whose role was to facilitate and organize the circulation of goods and materials. [..] Artisans and state functionaries in the towns and cities may have been sustained by agricultural produce collected as taxes, probably at the city gate, where weights are often found, suggesting the weighing of goods or materials in order to deduct fixed proportions."*

Archaeological traces of the pivotal role of the Harappan civilization in moving raw materials from the center of Asia to Mesopotamia through the Persian Gulf can be found throughout the route. Several Harappan-related sites have been found in Southern Baluchistan and in Afghanistan: these were apparently trading colonies near major lapis lazuli, copper, and tin sources. A recent archaeological literature has used isotopic data from human tooth enamel in Harappan cemetery burials to document an exceptional mobility of Harappan people, with mortuary populations composed almost exclusively of first generation immigrants coming from

resource-rich hinterlands (Kenoyer, Price and Burton, 2013; Valentine et al., 2015). Moreover, a series of archaeological findings point towards the presence of Harappan colonies or trade posts throughout the Persian Gulf. In Oman, archaeologists found a series of metal tools of clear Indus origin, several Indus trade tools used to normalize exchanges (e.g., the Indus-type stamp seals and cubical weights) and several Indus-type artifacts made in Oman by Indus or Indus-trained craftspeople using local raw materials. Also, Indus pottery is steadily being recognized at sites in Oman and the Persian Gulf, while there is some evidence of Indus products that were imitated in the Arabian coast (Edens, 1993, p.354).

Mesopotamia was likely the final destination of the raw materials that were transiting through the Indus Valley. As discussed in the previous subsection, although the tin sources in Mesopotamia are still not fully understood, several scholars have suggested that the Harappan civilization provided a major source. The supply of tin by this sea route is suggested, for instance, in a passage in one of the texts of Gudea, a priest-king reigning in Southern Mesopotamia, who describes the trove of objects reserved for the god and placed in the temple: *"Along with copper, tin, slabs of lapis lazuli, shining metal (and) spotless Meluhha cornelian"*. Another text describes the crossing of Meluhha: *"He crossed to the Kur Meluhha, Enki, the King of the Abzu, decrees its fate: [..] Your silver will be gold. Your copper will be bronze-tin"*.

People of Meluhha are described as traders in the Sumerian texts and there are frequent references to their ships. Harappan-style artifacts, including seals, beads, and shell objects, have been recovered from sites in Mesopotamia dating from 2550 BC (Chakrabarti, 1982; Gensheimer, 1984; Kenoyer, 2008). Conversely, there is no archaeological evidence of Mesopotamian goods in Indus cities. This has been interpreted as a sign that either imports from Mesopotamia were perishable goods, or that the Indus-Mesopotamia trade was mainly indirect, via Dilmun and Magan.

7.3 Assur in the Old Assyrian period (1950-1750 BC)

The Old Assyrian commercial network (1950-1750 BC) stands out as a remarkable example of the emergence of a state that promoted long-distance commerce as its primary political and economic objective and relied on taxing transit traders within a thriving long-distance trade ecosystem. Our understanding of the Assyrian trade primarily comes from a unique collection of some 23,500 merchant records inscribed on clay tablets, excavated in the city of Kanesh. These records stand virtually alone as evidence for the organization of overland trade in the Bronze Age: they are therefore critical for a comprehensive understanding of the relationship between geography, trade, and the rise and organization of a Bronze Age state.

The epicenter of this vast trade network was Assur, a city erected on a sandstone cliff by the Tigris River. The city was surrounded by relatively unproductive farmland. However, its position at the confluence of the Tigris and its two largest tributaries—the Great Zab and the

Little Zab, provided a natural bridge linking Anatolia to Sumer and Iran. One of the very first rulers of Assur, Ilushuma, left behind this inscription: *"Ilushuma, vice-regent of Ashur, built the temple for the goddess Ishtar, his mistress, for his life. A new wall [..] I constructed and subdivided for my city house-plots. The god Ashur opened for me two springs in Mount Ebih and I made bricks for the wall by the two springs. [..] The freedom of the Akkadians and their children I established. I purified their copper. I established their freedom from the border of the marshes and Ur and Nippur, Awal and Kismar, Der of the god lshtaran, as far as the City (i.e., Assur)."* This early inscription links the rise of the city with trade in metals. Specifically, the first part of the inscription alludes to the city's foundation, while the final sentence delineates what seems to be three trade routes leading to Assur from the south: one from Ur, the copper entry point from the Gulf, via Nippur; one through the Tigris from Awal and Kismar in the Hamrin region; and one from Elam, via Der, east of the Tigris, passing by Susa (Larsen, 1976). The inscription explicitly mentions copper and omits tin, possibly due to the text's early date (Barjamovic, 2008). The central role of the metal trade in the city's rise is echoed in the only inscription referring to Ilhusuma's successor, Erishum I, which states that Erishum made tax-exempt trade in copper, tin, and barley, transiting the city.

In 1950-1750 BC, Assur controlled the trade corridor between Assur and Anatolia, and a commercial circuit within central Anatolia. These trade routes likely formed part of a chain of interlocking commercial networks that most likely was ultimately connecting the Chinese frontier with the Balkans (Barjamovic, 2008). Assur and Kanesh functioned as the main markets for Assyrian traders. Assur was the endpoint of "the caravan of the Lower Country," which transported the tin, mined in Central Asia, from the city of Susa in Southern Mesopotamia. Assyrian traders would then purchase this tin (along with textiles) in Assur, transport it to Kanesh—the city where all imports coming to Anatolia were cleared—and then transport it to other Anatolian settlements. Kanesh also served as a central node in the Anatolian copper trade, with Assyrian traders connecting northern Anatolia's copper-rich areas with the West's urban centers.

The scale of the metal trade was immense. Recent estimates (Stratford, 2010; Barjamovic, 2018) suggest that roughly 1500 donkeys, carrying around 15 tons of tin and 32,000 textiles annually, traveled from Assur to Kanesh. To provide a sense of the scale, 15 tons of tin could be exchanged in Kanesh for an average of 2 tons of silver (although prices would fluctuate considerably), which was enough to cover the annual cost of living for two to four thousand individuals in Kanesh (Dercksen, 2014). Detailed accounts also point towards significant volumes of copper and textile traded by Assyrian merchants across Anatolian settlements. In one instance, a single transaction involved 23 tons of copper and 15 tons of wool. In general, references to the transport of copper by the ton are not rare (Barjamovic, 2011).

The Assyrian texts depict a flourishing market economy based on free enterprise and private initiative, with profit-oriented and risk-taking merchants supported by sophisticated financial

contracts and a well-functioning judicial system. Assyrian merchants established trade outposts or "ports" among the small city-states of Anatolia. These trading posts had their own legal and financial institutions, mirroring those of Assur.

Trade activities were regulated by taxes levied at various stages within the metal trade network. For instance, consider the tin trade (which was the most significant in terms of value). Upon arrival in Assur, the tin destined for sale in Anatolia was wrapped in textiles, and the package was put under sealing, hence the name "sealed tin". The "sealed tin" was distinguished from the "hand-tin", brought to pay the taxes along the route. The "sealed tin" was then subject to an export tax when leaving Assur (wasitum: 1/120 over the value of all merchandise and donkeys), a transit tax on the route between Assur and Kanesh (datum: 6-10 percent), an entry tax (nishatum: 3 percent) in Kanesh, an export tax from Kanesh (sadduatum: 6 percent) and finally was subject to a series of toll taxes to local rulers when transiting through the Anatolian city-states.

Traders often attempted to evade these taxes by using a series of smuggling routes. Despite the risk of punitive measures such as imprisonment and fines, when tin prices fell in Kanesh, merchants were willing to take the chance. Assyrian texts reveal candid discussions among traders regarding smuggling routes, their potential profits, and associated risks.

Guards and guard posts located at bridges or along roads traveled by the Assyrians are also a recurring theme in the records (Barjamovic, 2011). Their number and distribution imply that barracks or forts must have been a common sight in the Anatolian landscape. These posts were likely both patrolling the countryside, discouraging smugglers and protecting traders, and maintaining roads or mountain passes clear and in good conditions.

7.4 The city of Mari in the Mari Age (1810-1760 BC)

Mari was an ancient Semitic city-state in modern-day Syria. It was an important political power already starting from 2600 BC. Our primary understanding of this society is derived from nearly 25,000 cuneiform tablets excavated in Mari starting from the 1930s and spanning the years between 1810-1760 BC (the Mari Age). Nevertheless, glimpses into the city's political and economic landscape also emerge from select inscriptions in the city dating from 2500-2350 BC (Charpin, 1987), as well as the Ebla archives (dating approximately 2500-2200 BC).

Mari was strategically located on the Euphrates, just downstream from the confluence with the Khabur River. One of the factors in Mari's prominence was that, because of its unique position along a series of crucial trade passages, it played a major role as an entrepot in international trade (Kuhrt, 1995, p. 101, and Kristiansen and Larson, 2005, p. 93). The archives suggest that the most relevant commodity that was traded was tin. In particular, a series of tablets deciphered by Dossin (1970) suggests that tin was transported east to west,

using Mari as a nodal point. Tin came from unspecified sources in the east, transiting through Babylon and Susa. Once arrived in Mari, it would then be transshipped to various sites in Syria and Palestine and, through the port of Ugarit, even across the Mediterranean Sea to Crete (Morris, 1992, p. 102)[40]. Over time, Mari emerged as the primary source of tin for the Western regions (Muhly, 1995, p. 1509). The value put on the tin, and Mari's central role in its distribution, is illustrated in a letter (part of Mari's archive) from the king of Qatna, a city located 400 km west of Mari, addressed to the King of Ekallate, a city located to the east of Mari: *"This matter is unspeakable, yet I must speak and relieve my feelings: you are a great king; you asked me for two horses, and I had them sent to you. And now you sent me (only) 20 minas (c. 10 kilos) of tin. Is it not the case that, without any quibbling and in full, you got (what you wanted) from me? And you dare to send me this paltry amount of tin! If you had sent nothing at all, by the god of my fathers, I could not have been so angry!"*

Given Mari's control of crucial commercial routes, royal income derived from trading ventures must have been considerable. The Mari texts show that royal journeys, as well as being an occasion to visit other kings, were accompanied by trade caravans (Durand, 1983, p. 314). While the palace was actively involved in long-distance commerce, often exerting a dominant influence, it was not the sole player. A thriving network of private traders also existed, representing a substantial portion of Mari's economy. For example, the archives highlight the critical role of one Elamite trader, Kuyaya, in the tin trade industry. A local Mari merchant named Ishkhi-Dagan, who made purchases of tin ingots, is similarly mentioned. More generally, there is evidence for private commercial ventures and an extensive private commercial network.

How taxation worked is not completely certain. However, in the words of Amelie Kuhrt (1995): *"state income was certainly derived from revenues levied on the transit trade, crossing-dues, tolls, boat taxes, and dues demanded in return for land grants."* Tax returns must have been substantial, as indicated by the monumental Royal Palace of Mari, one of the wonders of the 18th century BC, and the monumental irrigation works that were undertaken during the Mari Age.

7.5 The Bronze Age Aegean

The Bronze Age Aegean in the eastern Mediterranean encompassed several powerful entities: the Minoans in Crete; the Mycenaeans in mainland Greece, and the Cypriots in Cyprus.

During the third millennium BC, the Minoans were already at the center of the Aegean trade network, with close contact with the Cyclades. This is testified by imports from these

[40] An interesting tablet, which dates back to the eighteenth century BC is set up as a balanced account, listing the tin received and shipped in Mary. It describes the tin received from the kings of Babylon (Hammurabi) and Susa (Shephard), stocked in Mari, and then shipped to individuals residing in Ugarit and Caphtorite, a town presumably located in Crete.

islands, trade in raw materials (e.g., obsidian, copper, lead, silver), the local production of material culture in Cycladic styles or technologies, and a relocation of Cycladic groups along the northern coast of Crete (Renfrew, 1964; Warren, 1984; Karantzali, 1996; Day, Wilson and Kiriatzi, 1998; Dimopoulou-Rethemniotaki, Wilson and Day, 2007). It is during the Middle Minoan period (1900-1800 BC), however, that the trade network of the Minoans starts expanding above the Cyclades: Minoan products and cultural influences starts to be found in mainland Greece, Asia Minor, the entire Mediterranean coast of the Middle East, and even as far as Egypt. At the same time, the Minoans are becoming the most powerful European civilization. Several hallmarks testify social development and economic growth. A state emerged together with writing, monumental burials, roads, and other public infrastructures. Towns such as Knossos, Malia, Gournia, and Plaikastro are often described as the first urban settlements of Bronze Age Europe. These towns were centers of craft production (textile, pottery, and metalworking) and long-distance trade. They developed around royal "palaces", monumental buildings that, in some cases, had true Cyclopean size. These buildings were at the center of an economic system, which has often been referred to as "palace economy", in which a substantial share of wealth was flowing under the control of a centralized administration, centered in the palace. The palaces gathered up, manufactured, traded, and redistributed products and services needed in Crete. They were at the heart of an extensive network of intra-regional and interregional maritime trade of agricultural products in exchange for obsidian and metals (copper and tin). A long-standing fascinating hypothesis in the historical and archaeological literature is that the centrality of Crete in the metal trade network in the Mediterranean might go a long way in explaining the rise of the palaces and the Minoan civilization. The Minoan civilization has often been referred to as the first example in history of a thalassocracy[41], a polity that derives its power from its naval/commercial supremacy on the seas. Already in the fifth century BC, the Greek historian Thucydides wrote: *"Minos is the first to whom tradition ascribes the possession of a navy. He made himself master of a great part of what is now termed the Hellenic Sea; he conquered the Cyclades, and was the first colonizer of most of them, expelling the Carians and appointing his own sons to govern in them. Lastly, it was he who, from a natural desire to protect his growing revenues, sought, as far as he was able, to clear the sea of pirates."* More recently, Gordon Childe (1958) has emphasized the absolute centrality of the Minoans in the Mediterranean trade: *"In the Early Bronze Age peninsula Italy, central Europe, and the west Baltic coastlands, and the British Isles were united by a single system for the distribution of metalware, rooted in the Aegean market."*

Minoan vessels were the primary means of transportation of copper ingots in the Mediterranean (Muhly, 1985). In a shipwreck near present-day Israel, numerous tin ingots, with Minoan seals, have been found: trace-element analysis points towards Cornwall, present-day

[41] Thalassokrateo means "to be master of the sea"

England, as the most likely provenance of the tin (Berger et al., 2019). This finding puts the Minoans at the center of a tin trade route connecting western and northern Europe with the Syrian civilizations.

The Mycenaean civilization appeared later in history, in the middle Bronze Age, from approximately 1750 to 1050 BC. As for the Minoans, the center of the Mycenaean economy was the palace. The production of manufactures, the internal circulation, and the long-distance trade were conducted mainly under their control. Several tables found in the palace in Pylos demonstrate a very tight palatial control of the metal industry. Bronze smiths were distributed throughout the kingdom. Each smith was allocated raw ore and other materials from the palace and assigned a task, and then was expected to deliver the final product to the palace. Chadwick (1994, p. 141) argues that the total number of smiths in the Pylian kingdom was nearly 400 and he estimates that the production would likely exceed the local demand. This fact, together with the absence of local copper and especially tin deposits, made Pylos a major center of exchange. It has been argued that long-distance trade became increasingly important in the region as the quality of the soil for growing cereals (which was already poor) progressively declined as a result of continuous intensive cultivation (Ascherson, 2011). Starting from 1550 BC, the Mycenaeans established a wide network of colonies in coastal Anatolia, in southern Italy, and western Sicily, as well as in the Black Sea, Spain, and Southern France. These colonies helped to facilitate international trade with the Mycenaean states, by providing military protection and a uniform set of institutions and customs along the main Mediterranean trade routes. Long-distance trade promoted the rise of a political and administrative palatial elite that directly participated in trade voyages and would often engage in wars to crush their trade rivals. In the Odyssey Book, Menelaus, the legendary Spartan wanax (king), describes the source of his wealth and power in the following way: *"But when it comes to men, I feel that few or none can rival me in wealth, for it took me seven years and great hardship to amass this fortune and bring it home in my ships. My travels took me to Cyprus, to Phoenicia, and to Egypt. Ethiopians, Sidonians, Erembians, I visited them all; and I saw Libya too.."* (The Odyssey, Book 4, 75-85).

While there is little doubt that interregional trade in the Mediterranean was driven by bronze-making metals, it is also clear that it enabled the exchange of luxury, or less utilitarian, goods, items that were enabling powerful statements. This is particularly evident for Myceneans, where eastern regions made the strongest contribution, as the sophisticated states of Egypt, the Levant, Mesopotamia, and Anatolia provided a wealth of precious items that functioned as technological and artistic models for the development of local arts and society (Burns, 2010).

Another influential Aegean civilization rose in Cyprus. Starting from 1650 BC, the island experienced a rapid change from a somewhat isolated, village-oriented culture to an international urban-centered and highly complex society. It is generally agreed that the first urban

developments and the gradual movement of population from rural hinterland to coastal towns were not merely an internal socioeconomic process, but rather the outcome of overseas demand for Cypriot copper (Knapp, 2013; Negbi, 2005). The development of metallurgy on Cyprus was driven by the local copper mines and the need to meet the increasing demand for copper in the Mediterranean basin. Eventually, the intensified production and trade of copper catapulted Cyprus into the role of the most important purveyor of this metal in the Mediterranean region, which lasted until the Roman Empire (the name Cyprus is directly related to the Latin word for copper, cuprum). A large number of documents of the second millennium Egyptian, Syrian, Babylonian, Anatolian, and Mycenaean mention exchanges with Cyprus (Alashiya) and gifts of coppers.

7.6 The Bronze Age in China and the Erlitou period (1900-1500 BC)

Bronze metallurgy in China originated in what is referred to as the Erlitou period and it probably developed inside China separately from outside influence (Liu, 2005). The site of Erlitou is the largest among all its contemporary sites in China; several scholars have argued that it was the capital of the first state in China (Liu, Chen et al., 2003; Liu and Chen, 2012; Liu et al., 2004) [42].

Erlitou was nestled in an alluvial basin, positioned on the boundary between the Chinese lowlands and highlands, encircled by mountain ranges. Despite these natural barriers, the basin maintained effective connections to regions in all directions through an intricate network of rivers. Specifically, Erlitou was situated at the point in which two major rivers, the Yi and Luo, converged in a short canal, the Yiluo. The Yiluo, within a span of less than 30 kilometers, intersected with several smaller rivers, eventually discharging into the Yellow River. This interconnected river system, combined with its prime location, sandwiched between mountains and plains, made of Erlitou an important road knot connecting the mineral-rich mountains with the fertile lowlands.

In the last four decades, more than 200 sites containing Erlitou material assemblages have been found over a very broad region from the middle Yellow River to the middle Yangzy River regions. The sites are distributed along several river systems and the pattern of settlement distribution is indicative of the emergence of a highly integrated and centralized socio-political system (Liu, 2005, p.226). The line expansion of this first state suggests a series of attempts to achieve political domination of metal-rich peripheries. One notable example is Panlongcheng, a site located at the intersection between the Han and the Yangzi River, and in close proximity to both copper and tin deposits. There is evidence that copper was melted at the mining sites, while the elite in Panlongcheng was likely playing a major role in forwarding copper ingots to the primary center at Erlitou (Liu, Chen et al., 2003). There is also evidence of limited

[42] Some scholars believe Erlitou to be the capital of the mythical Xia Dynasty, China's first dynasty, although this is controversial (Wu et al., 2016).

bronze-making dating from the Erlitou period. Another example of an outpost to control metal resources, set up by the Erlitou state, is the site of Donglongshan. Donglongshan is located on the north bank of the Dan River with close proximity to copper resources in Mt. Hongyan. Few pieces of metal slag were found at the site, suggesting that bronze metallurgy was carried out there (Yang, 2000).

The formation of the Erlitou state involved rapid territorial expansion by colonizing the surrounding regions, with the quest for bronze alloys as the main territorial driver. In the words of Li Liu (2005): *"The Erlitou state formed an inter-regional network focused on the production and distribution of prestige goods, especially bronze vessels. This network incorporated two interdependent sectors, core and periphery. The dominant core controlled the production of prestige items (bronze products, etc.), and the subordinate periphery provided raw material resources (e.g., metal ingots) [..] The Erlitou elite in the core achieved domination through military force by establishing outposts in the periphery to ensure the flow of material and information."*

8 Conclusion

The prevailing literature attributes the emergence of the Urban Revolution to farming and sedentism. Although we do not deny that both might represent necessary conditions, we contend they are sufficient. The regions where the Urban Revolution started were not necessarily the most productive. Moreover, the invention of farming preceded by more than five thousand years the explosion of cities, states, and inequality that can be observed from the fourth millennium BC.

We provide first empirical evidence that the discovery of bronze and the ensuing long-distance metal trade played an important role in explaining this phenomenon. Consistent with the qualitative archaeological literature, we document that regions located along trade corridors connecting copper and tin mines to fertile lands were more likely to experience the Urban Revolution. We conjecture that transit bottlenecks allowed a tax-levying elite to emerge and to be sustained. We formally test this appropriability theory and provide several case studies in support.

A clear caveat of this study is that it excludes the New World. We leave the investigation of the link between trade and the Urban Revolution in the Americas for future research.

References

Acemoglu, Daron, Simon Johnson, and James A. Robinson. 2002. "Reversal of Fortune: Geography and Institutions in the Making of the Modern World Income Distribution." *The Quarterly Journal of Economics* 117 (4): 1231–1294.

Adamson, Jeremy. 2021. "Trade and the rise of ancient Greek city-states."

Allen, Robert C., Mattia C. Bertazzini, and Leander Heldring. 2022. "The Economic Origins of Government."

Ascherson, Neal. 2011. *Black Sea: The Birthplace of Civilisation and Barbarism.* London: The Folio Society.

Ashraf, Quamrul, and Oded Galor. 2011. "Dynamics and Stagnation in the Malthusian Epoch." *American Economic Review* 101 (5): 2003–41.

Bagnall, Roger. 2022. "Pleiades: A Gazetteer of Past Places." pleiades.stoa.org.

Bahn, Paul G. 2000. *The Atlas of World Archaeology.* Checkmark Books.

Bakker, Jan David, Stephan Maurer, Jörn-Steffen Pischke, and Ferdinand Rauch. 2021. "Of Mice and Merchants: Trade and Growth in the Iron Age." *Review of Economics and Statistics* 103 (4): 652–665.

Barjamovic, Gojko. 2008. "The geography of trade. Assyrian colonies in Anatolia c. 1975-1725 BC and the study of early interregional networks of exchange." *Anatolia and the Jazira during the Old Assyrian period* 87: 100.

Barjamovic, Gojko. 2011. *A historical geography of Anatolia in the Old Assyrian colony period.* Vol. 38. Museum Tusculanum Press.

Barjamovic, Gojko. 2018. "Interlocking commercial networks and the infrastructure of trade in Western Asia during the Bronze Age."

Barjamovic, Gojko, Thomas Chaney, Kerem Coşar, and Ali Hortaçsu. 2019. "Trade, Merchants, and the Lost Cities of the Bronze Age." *The Quarterly Journal of Economics* 134 (3): 1455–1503.

Begemann, Fabian, Andreas Hauptmann, Sigrid Schmitt-Strecker, and Gerd Weisgerber. 2010. "Lead isotope and chemical signature of copper from Oman and its occurrence in Mesopotamia and sites on the Arabian Gulf coast." *Arabian Archaeology and Epigraphy* 21 (2): 135–169.

Begemann, Fabian, and Sigrid Schmitt-Strecker. 2008. "Bleiisotopie und die Provenienz von Metallen." In *Anatolian Metal IV*, edited by Yalcin, 125–134. Bochum: Der Anschnitt.

Bentzen, Jeanet Sinding, Nicolai Kaarsen, and Asger Moll Wingender. 2017. "Irrigation and autocracy." *Journal of the European Economic Association* 15 (1): 1–53.

Berger, Daniel, et al. 2019. "Isotope systematics and chemical composition of tin ingots

from Mochlos (Crete) and other Late Bronze Age sites in the eastern Mediterranean Sea: An ultimate key to tin provenance?" *PloS one* 14 (6): e0218326.

Bleaney, Michael, and Arcangelo Dimico. 2011. "How different are the correlates of onset and continuation of civil wars?" *Journal of Peace Research* 48 (2): 145–155.

Borcan, Oana, Ola Olsson, and Louis Putterman. 2018. "State history and economic development: evidence from six millennia." *Journal of Economic Growth* 23 (1): 1–40.

Burns, Bryan E. 2010. *Mycenaean Greece, Mediterranean commerce, and the formation of identity.* Cambridge: Cambridge University Press.

Carneiro, R L. 1970. "A Theory of the Origin of the State: Traditional theories of state origins are considered and rejected in favor of a new ecological hypothesis." *Science* 169 (3947): 733–738.

Chadwick, John. 1994. *The Mycenaean World, 8th edition.* Cambridge University Press.

Chakrabarti, Dilip K. 1982. "Long-barrel cylinder'beads and the issue of Pre-Sargonic contact between the Harappan civilization and Mesopotamia." *Harappan Civilization: A Contemporary Perspective (ed. GL Possehl). New Delhi: Oxford & IBH Publishing* 265–70.

Chanda, Areendam, C. Justin Cook, and Louis Putterman. 2014. "Persistence of Fortune: Accounting for Population Movements, There Was No Post-Columbian Reversal." *American Economic Journal: Macroeconomics* 6 (3): 1–28.

Chandler, Tertius. 1987. *Four Thousand Years of Urban Growth: An Historical Census.* New York: Edwin Mellen.

Charpin, D. 1987. "Tablettes presargoniques de Marie." *Mari: annales de recherches interdisciplinaires* 5: 65–127.

Childe, Gordon. 1930. *The Bronze Age.* Cambridge University Press.

Childe, Vere Gordon. 1958. *The prehistory of European society.* Pelican London.

Childe, V. Gordon. 1950. "The Urban Revolution." *The Town Planning Review* 21 (1): 3–17.

Cleuziou, Serge. 1982. "Early Tin in the Near East." *Expedition Magazine* 25 (1).

Comin, Diego, William Easterly, and Erick Gong. 2010. "Was the Wealth of Nations Determined in 1000 BC?" *American Economic Journal: Macroeconomics* 2 (3): 65–97.

Conley, T. G. 1999. "GMM estimation with cross sectional dependence." *Journal of Econometrics* 92 (1): 1–45.

Cunliffe, Barry. 2011. *Europe Between the Oceans, 9000 BC-AD 1000.* Yale University Press.

Dal Bó, Ernesto, Pablo Hernández-Lagos, and Sebastián Mazzuca. 2022. "The paradox of civilization: Preinstitutional sources of security and prosperity." *American Political Science Review* 116 (1): 213–230.

Davis, Donald R., and David E. Weinstein. 2002. "Bones, Bombs, and Break Points: The Geography of Economic Activity." *American Economic Review* 92 (5): 1269–1289.

Day, Peter M, David E Wilson, and Evangelia Kiriatzi. 1998. "Pots, Labels, and People: Burying Ethnicity in the Cemetery at Aghia Photia, Siteias." In *Cemetery and Society*, 133–149.

Dercksen, J. 1999. *Trade and Finance in Ancient Mesopotamia. MOS Studies.* Istanbul: Nederlands Instituut voor het Nabije Oosten.

Dercksen, Jan G. 2014. "The Old Assyrian trade and its participants." *Documentary Sources in Ancient Near Eastern and Greco-Roman Economic History: Methodology and Practice* 59–112.

Diamond, Jared M. 1998. *Guns, Germs, and Steel: the Fates of Human Societies.* New York: W. W. Norton & Co.

Dijkstra, Edsger W. 1959. "A Note on Two Problems in Connexion with Graphs." *Numerische Mathematik* 1 (1): 269–271.

Dimopoulou-Rethemniotaki, Nota, David E Wilson, and Peter M Day. 2007. "The Earlier Prepalatial Settlement of Poros-Katsambas: Craft Production and Exchange at the Harbour Town of Knossos."

Donaldson, Dave. 2018. "Railroads of the Raj: Estimating the Impact of Transportation Infrastructure." *American Economic Review* 108 (4–5): 899–934.

Dossin, Georges. 1970. "La route de l'étain en Mésopotamie au temps de Zimri-Lim." *Revue d'Assyriologie* 64: 97–106.

Durand, Jean-Marie. 1983. "Archives royales de Mari/21 Textes administratifs des salles 134 et 160 du Palais de Mari/transcrits, traduits et comm. par Jean-Marie Durand." *Archives royales de Mari.*

Earle, Timothy. 2002. *Bronze Age Economics: The Beginnings of Political Economies.* Cambridge Westview Press.

Earle, Timothy. 2013. "The 3M: materiality, materialism and materialization." In *Counterpoint: essays in archaeology and heritage studies in honour of Professor Kristian Kristiansen*, *BAR International Series*, edited by Sophie Bergerbrant and Serena Sabatini, 353–360. Oxford: Oxbow.

Earle, Timothy, and Matthew Spriggs. 2015. "Political economy in prehistory: a Marxist approach to Pacific sequences." *Current Anthropology* 56 (4): 515–544.

Earle, Timothy, Johan Ling, Claes Uhnér, Zofia Stos-Gale, and Lene Melheim. 2015. "The Political Economy and Metal Trade in Bronze Age Europe: Understanding Regional Variability in Terms of Comparative Advantages and Articulations." *European Journal of Archaeology* 18 (4): 633–657.

Edens, Christopher. 1993. "Indus-Arabian interaction during the Bronze Age: a review of

evidence." In *Harappan Civilization: a recent perspective*, Second revised edition, edited by Gregory L. Possehl, 335–363. New Delhi.

Engels, Friedrich. 1942. *The origin of the Family.* Current Book Distributors.

Ertan, Arhan, Martin Fiszbein, and Louis Putterman. 2016. "Who was colonized and when? A cross-country analysis of determinants." *European Economic Review* 83: 165–184.

FAO/IIASA. 2011. "Global Agro-ecological Zones (GAEZ v3.0)." FAO Rome and IIASA, Laxenburg, Austria.

Foster, Benjamin R. 1997. "Akkadians." In *The Oxford Encyclopedia of Archaeology in the Near East*, Vol. 1, edited by Eric Meyers, 49–54. Oxford: Oxford University Press.

Galor, Oded. 2011. *Unified growth theory.* Princeton University Press.

Galor, Oded. 2022. *The journey of humanity: The origins of wealth and inequality.* Penguin.

Galor, Oded, and Ömer Özak. 2016. "The Agricultural Origins of Time Preference." *American Economic Review* 106 (10): 3064–3103.

Gensheimer, Thomas R. 1984. "The role of shell in Mesopotamia: evidence for trade exchange with Oman and the Indus valley." *Paléorient* 65–73.

Giardino, Claudio. 2019. *Magan - the Land of Copper: Prehistoric Metallurgy of Oman. Archaeopress Archaeology.* Archaeopress Archaeology.

Green, Adam S, and Cameron A Petrie. 2018. "Landscapes of urbanization and de-urbanization: A large-scale Approach to investigating the indus civilization's settlement distributions in Northwest India." *Journal of Field Archaeology* 43 (4): 284–299.

Hahnekamp, Christine. 2011. "Vergleichende Untersuchung zum Fundkontext bronze- und urnenfelderzeitlicher Schwerter in Ostfrankreich und Süddeutschland." *Diplomarbeit, Universität Wien.*

Henderson, J Vernon, Tim Squires, Adam Storeygard, and David Weil. 2018. "The Global Distribution of Economic Activity: Nature, History, and the Role of Trade1." *The Quarterly Journal of Economics* 133 (1): 357–406.

Hibbs, Douglas A., and Ola Olsson. 2004. "Geography, biogeography, and why some countries are rich and others are poor." *Proceedings of the National Academy of Sciences* 101 (10): 3715–3720.

Jansen, Michael. 2002. "Settlement networks of the Indus Civilization." *Indian Archaeology in Retrospect* 2: 105–128.

Karantzali, E. 1996. *Le Bronze Ancien dans les Cyclades et en Crète: Les Relations Entre les Deux Regions—Influence de la Grèce Continentale. BAR-IS.* Oxford: Archaeopress.

Karger, Dirk Niklaus, Michael P. Nobis, Signe Normand, Catherine H. Graham, and Niklaus E. Zimmermann. 2021. "CHELSA-TraCE21k v1.0. Downscaled transient temperature and precipitation data since the last glacial maximum." *Climate of the Past*

Discussions 2021: 1–27.

Kenoyer, J Mark, T Douglas Price, and James H Burton. 2013. "A new approach to tracking connections between the Indus Valley and Mesopotamia: initial results of strontium isotope analyses from Harappa and Ur." *Journal of Archaeological Science* 40 (5): 2286–2297.

Kenoyer, Jonathan Mark. 2008. "Indus and Mesopotamian trade networks: New insights from shell and carnelian artifacts." *Intercultural Relations between South and Southwest Asia: Studies in Commemoration of ECL During Caspers (1934–1996), E. Olijdam, RH Spoor, Eds.(Archaeopress, 2008)* 19–28.

Kiszewski, A., A. Mellinger, A. Spielman, P. Malaney, S. E. Sachs, and J. Sachs. 2004. "A global index representing the stability of malaria transmission." *American Journal of Tropical Medicine and Hygiene* 70 (5): 486–498.

Klein Goldewijk, Kees, Arthur Beusen, and Peter Janssen. 2010. "Long-term dynamic modeling of global population and built-up area in a spatially explicit way: HYDE 3.1." *The Holocene* 20 (4): 565–573.

Kristiansen, K., and T. Earle. 2015. "Neolithic versus Bronze Age social formations: a political economy approach." In *Paradigm Found: Archaeological Theory: Present, Past and Future. Essays in Honour of Evzen Neustupny*, Oxbow Books.

Kristiansen, Kristian, and Paulina Suchowska-Ducke. 2015. "Connected Histories: The Dynamics of Bronze Age Interaction and Trade 1500–1100 BC." *Proceedings of the Prehistoric Society* 81: 361–392.

Kristiansen, Kristian, and Thomas Larson. 2005. *The Rise of Bronze Age Society: Travels, Transmissions and Transformations.* Cambridge University Press.

Kuhrt, A. 1995. *The ancient near east, c. 3000-330 BC.* Vol. 2. Taylor & Francis US.

Lambert, M. 1953. "Textes commerciaux de Lagash." *Revue d'Assyriologie* 47: 57–69, 105–20.

Larsen, Mogens Trolle. 1976. *The old Assyrian city-state and its colonies.* Vol. 4. Akademisk Forlag.

Leemans, W. F. 1975. "Handel." *Reallexikon der Assyriologie* 4: 76–90.

Lieth, Helmut. 1975. "Modeling the Primary Productivity of the World." *Primary Productivity of the Biosphere*, edited by Helmut Lieth and Robert H. Whittaker, 237–263. Berlin, Heidelberg: Springer Berlin Heidelberg.

Liu, Li. 2005. *The Chinese Neolithic: trajectories to early states.* Cambridge University Press.

Liu, Li, and Xingcan Chen. 2012. *The archaeology of China: from the late Paleolithic to the early Bronze Age.* Cambridge University Press.

Liu, Li, Xingcan Chen, Yun Kuen Lee, Henry Wright, and Arlene Rosen. 2004. "Settlement patterns and development of social complexity in the Yiluo region, North

China." *Journal of Field Archaeology* 29 (1-2): 75–100.

Liu, Li, Xingcan Chen, et al. 2003. "State formation in early China."

Maloney, William F., and Felipe Valencia Caicedo. 2016. "The Persistence of (Subnational) Fortune." *The Economic Journal* 126 (598): 2363–2401.

Matranga, Andrea, and Luigi Pascali. 2021. "Chapter 5 - The use of archaeological data in economics." In *The Handbook of Historical Economics*, edited by Alberto Bisin and Giovanni Federico, 125–145. Academic Press.

Mayoral, Laura, and Ola Olsson. 2020. "Pharaoh's Cage: Environmental Circumscription and Appropriability in Early State Development."

Mayshar, Joram, Omer Moav, and Luigi Pascali. 2022. "The Origin of the State: Land Productivity or Appropriability?" *Journal of Political Economy* 130 (4): 1091–1144.

McIntosh, Jane R. 2007. *The ancient Indus valley: new perspectives.* Bloomsbury Publishing USA.

Meller, Harald, and Kai Michel. 2020. *El disco celeste de Nebra: la clave de una civilización extinta en el corazón de Europa.* Antoni Bosch editor.

Modelski, George. 2003. *World Cities: -3000 to 2000.* Washington, DC:: FAROS.

Morris, S. P. 1992. *Daidalos and the Origins of Greek Civilization.* Princeton: Princeton University Press.

Morr, Z., and F. Cattin. 2013. "Copper Quality and Provenance in Middle Bronze Age I Byblos and Tell Arqa (Lebanon)." *Journal of Archaeological Science* 40: 4291–4305.

Muhly, James D. 1985. "Sources of Tin and the Beginnings of Bronze Metallurgy." *American Journal of Archaeology* 89 (2): 275–291.

Muhly, J. D. 1973. *Copper and Tin.* Hamden, CT: The Connecticut Academy of Arts and Sciences.

Muhly, J. D. 1995. "Mining and Metalwork in Ancient Western Asia." 1501–1521. New York: Hendrickson Publishers.

Murr, Lawrence E. 2015. "A Brief History of Metals." *Handbook of Materials Structures, Properties, Processing and Performance*, 3–9. Cham: Springer International Publishing.

Nessel, Bianka, Daniel Neumann, and Martin Bartelheim, ed. 2018. *Bronzezeitlicher Transport - Akteure, Mittel und Wege.* Vol. 8 of *RessourcenKulturenBand - Editor of Series: Martin Bartelheim and Thomas Scholten.* Tübingem University Press.

NGA. 2019. *World Port Index.* 27th edition. Springfield, Virginia: National Geospatial-Intelligence Agency.

Nunn, Nathan, and Diego Puga. 2012. "Ruggedness: The Blessing of Bad Geography in Africa." *The Review of Economics and Statistics* 94 (1): 20–36.

Olson, David M, Eric Dinerstein, Eric Wikramanayake, [...], Wesley Wettengel,

Prashant Hedao, and Kenneth Kassem. 2001. "Terrestrial Ecoregions of the World: A New Map of Life on Earth: A new global map of terrestrial ecoregions provides an innovative tool for conserving biodiversity." *BioScience* 51 (11): 933–938.

Olson, Mancur. 1993. "Dictatorship, democracy, and development." *American political science review* 87 (3): 567–576.

Olsson, Ola, and Christopher Paik. 2020. "A Western Reversal Since the Neolithic? The Long-Run Impact of Early Agriculture." *The Journal of Economic History* 80 (1): 100–135.

Palmer, Leonard R. 1962. *Mycenaeans and Minoans: Aegean Prehistory in the Light of the Linear B Tablets.* New York: Alfred A. Knopf.

Petersen, Michael Bang, and Svend-Erik Skaaning. 2010. "Ultimate Causes of State Formation: The Significance of Biogeography, Diffusion, and Neolithic Revolutions / Ultimative Ursachen für die Staatsbildung: Die Signifikanz von Biogeographie, Diffusion und Neolithische Revolutionen." *Historical Social Research / Historische Sozialforschung* 35 (3 (133)): 200–226.

Pétrequin, Pierre, Serge Cassen, Michel Errera, L. Klassen, Alison Sheridan, and Anne Marie Pétrequin. 2012. *Jade: Grandes haches alpines du Néolithique européen, Ve et IVe millénaires av. J.-C.* Centre de Recherche Archéologique de la Vallée de l'Ain.

Polanyi, Karl, Harry Pearson, and C. M. Ahrensburg. 1957. *Trade and Market in the Early Empires.* Glencoe: Free Press.

Possehl, G. L. 1990. *Revolution in the Urban Revolution: The emergence of Indus urbanism.*

Prentice, Robert. 2010. *The Exchange of Goods and Services in Pre-Sargonic Lagash. Alter Orient und Altes Testament.* Münster: Ugarit-Verlag.

Putterman, Louis, and David N. Weil. 2010. "Post-1500 Population Flows and The Long-Run Determinants of Economic Growth and Inequality*." *The Quarterly Journal of Economics* 125 (4): 1627–1682.

Rahmstorf, Lorenz. 2010. "Die Nutzung von Booten und Schiffen in der bronzezeitlichen Ägäis und die Fernkontakte der Frühbronzezeit." *Der Griff nach den Sternen Internationales Symposium in Halle (Saale) 16.-21. Februar 2005.* Landesamt für Denkmalpflege u. Archäologie Sachsen-Anhalt.

Ramankutty, Navin, Jonathan A. Foley, John Norman, and Kevin McSweeney. 2002. "The global distribution of cultivable lands: current patterns and sensitivity to possible climate change." *Global Ecology and Biogeography* 11 (5): 377–392.

Ramsay, William Mitchell. 1890. *The historical geography of Asia Minor.* Vol. 4. John Murray.

Ratnagar, Shereen. 1981. *Encounters, The Westerly Trade of the Harappa Civilization.* Delhi: Oxford University Press.

Reba, Meredith, Femke Reitsma, and Karen C. Seto. 2016. "Spatializing 6,000 years

of global urbanization from 3700 BC to AD 2000." *Scientific Data* 3 (1): 160034.

Renfrew, Colin. 1964. "Crete and the Cyclades before Rhadamanthus." *Kritika Chronika* 18: 107–141.

Renfrew, Colin, and Paul Bahn. 2016. *Archaeology: Theories, Methods and Practice, 11ed.* Thames & Hudson.

Riley, Shawn, Stephen Degloria, and S.D. Elliot. 1999. "A Terrain Ruggedness Index that Quantifies Topographic Heterogeneity." *Internation Journal of Science* 5: 23–27.

Sanders, William T. 1968. "Hydraulic Agriculture, Economic Symbiosis, and the Evolution of States in Central Mexico." In *Anthropological Archeology in the Americas*, edited by Betty J Meggers. Washington, DC: Anthropological Society of Washington.

Schauer, Peter. 1971. *Die Schwerter in Süddeutschland, Österreich und der Schweiz I: Griffplatten-, Griffangel- und Griffzungenschwerter.* Vol. 2 of *Prähistorische Bronzefunde IV*. München: Beck.

Schauer, Peter, Andrew Bevan, Stephen Shennan, Kevan Edinborough, Tim Kerig, and Mike Parker Pearson. 2020. "British Neolithic Axehead Distributions and Their Implications." *Journal of Archaeological Method and Theory* 27: 836–859.

Schönholzer, David, and Pieter François. 2023. "The Origin of the Incentive Compatible State: Environmental Circumscription."

Smith, Adam. 1978. *Lectures on jurisprudence.* Vol. 5. VM eBooks.

Stratford, Edward Paul. 2010. *Agents, archives, and risk: A micronarrative account of Old Assyrian trade through Šalim-ahum's activities in 1890 BC.* The University of Chicago.

Testart, Alain, Richard G Forbis, Brian Hayden, Tim Ingold, Stephen M Perlman, David L Pokotylo, Peter Rowley-Conwy, and David E Stuart. 1982. "The significance of food storage among hunter-gatherers: Residence patterns, population densities, and social inequalities [and comments and reply]." *Current anthropology* 23 (5): 523–537.

Uckelmann, Marion. 2013. "The Oxford Handbook of the European Bronze Age." edited by Harry Fokkens and Anthony Harding, Chapter Land Transport in the Bronze Age. Oxford University Press.

U.S. Geological Survey. 2011. "Mineral Resources Data System."

Valentine, Benjamin, George D Kamenov, Jonathan Mark Kenoyer, Vasant Shinde, Veena Mushrif-Tripathy, Erik Otarola-Castillo, and John Krigbaum. 2015. "Evidence for patterns of selective urban migration in the Greater Indus Valley (2600-1900 BC): a lead and strontium isotope mortuary analysis." *PLoS One* 10 (4): e0123103.

Vogt, Burkhard. 1996. "Indian Ocean In Antiquity." Chapter Bronze Age maritime trade in the Indian Ocean: Harappan traits on the Oman peninsula. Routledge.

Vörösmarty, C. J., B. M. Fekete, M. Meybeck, and R. B. Lammers. 2000. "Global

System of Rivers: Its Role in Organizing Continental Land Mass and Defining Land-to-ocean Linkages." *Global Biogeochemical Cycles* 14 (2): 599–621.

Wang, Yunchuan, Shasha Wang, and Yong Deng. 2019. "A modified efficiency centrality to identify influential nodes in weighted networks." *Pramana* 92.

Warren, Peter. 1984. "Early Minoan—Early Cycladic Chronological Correlations." In *Prehistoric Cyclades*, 55–62.

Weisgerber, G. 1981. "Makan and Mel- uhha — Third Millennium BC Copper Production in Oman and the Evidence of Contact with the Indus Valley." In *South Asian Archaeology 1981*, edited by Bridget Allchin, 196–201. Cambridge: Cambridge University Press.

Weisgerber, G. 1983. "Copper Production during the Third Millennium BC in Oman and the Question of Makan." *Journal of Oman Studies* 6 (2): 269–276.

Wittfogel, K.A. 1957. *Oriental Despotism: A Comparative Study of Total Power. Oriental Despotism: A Comparative Study of Total Power*. Yale University Press.

Wright, Rita P. 2010. *The ancient Indus: Urbanism, economy, and society.* Cambridge University Press Cambridge.

Wu, Qinglong, Zhijun Zhao, Li Liu, Darryl E Granger, Hui Wang, David J Cohen, Xiaohong Wu, Maolin Ye, Ofer Bar-Yosef, Bin Lu, et al. 2016. "Outburst flood at 1920 BCE supports historicity of China's Great Flood and the Xia dynasty." *science* 353 (6299): 579–582.

Yang, Yachang. 2000. "Shaanxi Xia shiqi kaogu de xin jinzhan (New progress of the Xia archaeology in Shaanxi)." *Gudai Wenming Yanjiu Tongxun* 5: 34–6.

Yener, K. Asli. 2021. *Göltepe Excavations Tin Production at an Early Bronze Age Mining Town in the Central Taurus Mountains Turkey.* INSTAP Academic Press.

Yener, K. Asli, and Pamela B Vandiver. 1993. "Tin Processing at Goltepe, an Early Bronze Age site in Anatolia." *American Journal of Archaeology* 97: 207–238.

Appendices

A Additional Tables

Table A.1: Summary statistics of key variables

Variable	Mean	Std. Dev.	Min.	Max.	Obs.
	A. Cross-sectional dataset (Section 5.1)				
Any City by 1300 BC (×100)	0.419	6.462	0	100	10970
# Cities	0.006	0.113	0	7	10970
Transit Index	174.484	1002.721	0	27409.867	10970
IV Transit trade	231.287	657.171	0	18140.967	10970
Blockage cost	12.041	169.785	0	11854.721	10970
Proximity mines	25.995	32.657	0.007	1515.855	10970
Proximity croplands	198.039	110.086	0.172	837.821	10970
Sea	0.261	0.439	0	1	10970
River	0.159	0.365	0	1	10970
Mountains	0.025	0.157	0	1	10970
Centrality	6465.834	308265.612	0	21797914.336	10970
	B. Panel dataset archaeological sites (Section 5.2)				
Any Site (×100)[a]	4.923	21.634	0	100	21940
# Sites[a]	0.120	0.929	0	43	21940
Any Settlement (×100)[a]	0.670	8.158	0	100	21940
# Settlements[a]	0.011	0.187	0	16	21940
Any Site (×100)[b]	1.964	13.878	0	100	21940
# Sites[b]	0.052	0.729	0	51	21940
Any Settlement (×100)[b]	1.541	12.316	0	100	21940
# Settlements[b]	0.033	0.394	0	19	21940
Transit Index	87.242	714.362	0	27409.867	21940
IV Transit trade	115.644	478.854	0	18140.967	21940
Blockage cost	6.020	120.204	0	11854.721	21940
	C. China (Section 5.3)				
Any Criterion (×100)	17.914	38.356	0	100	2138
#Criteria	1.355	7.546	0	223	2138
Principal component	0	1.975	-0.781	7.871	2138
Transit Index	184.980	1056.716	0	16983.271	2138
IV Transit trade	75.788	195.874	0	3597.915	2138
Blockage cost	12.401	130.400	0	3052.938	2138
	D. Europe (Section 5.4)				
Any elite burial (×100)	23.032	42.121	0	100	1194
Number of elite burials	1.936	6.750	0	88	1194
Transit Index	1106.531	3264.228	0	42013.668	1194
Blockage cost	10433.042	10326.131	0	28032.111	1194

Notes: [a]data from Bahn (2000); [b]data from Pleiades.

Table A.2: Transit trade and Bronze Age cities. Robustness check controlling for differences in land fertility

	Any City by 1300 BC (×100)			
	2SLS (1)	2SLS (2)	2SLS (3)	2SLS (4)
	Panel A: Second stage			
Transit index	0.313	0.488	0.545	0.629
	(0.122)**	(0.146)***	(0.182)***	(0.203)***
	[0.162]*	[0.214]**	[0.259]**	[0.291]**
Farming land	0.990	-0.176	-0.053	-0.255
	(0.458)**	(0.079)**	(0.026)**	(0.103)**
	[0.514]*	[0.090]**	[0.035]	[0.138]*
	Panel B: First stage			
IV Transit index	0.671	0.728	0.568	0.545
	(0.045)***	(0.046)***	(0.047)***	(0.049)***
	[0.069]***	[0.070]***	[0.071]***	[0.075]***
Farming land	Share cropland area	NPP	CSI Galor and Özak (2016)	Ramankutty et al (2011)
Continent fixed effects	Yes	Yes	Yes	Yes
Observations	10,970	10,970	10,970	10,970
Mean	0.419	0.419	0.419	0.419
First-stage F-stat (5×5 grids)	220.7	252.9	146.5	125.3
First-stage F-stat (Conley 1000km)	93.59	107.5	63.30	52.49

Notes: Panel A reports cross-sectional 2SLS estimates of equation (4). Panel B reports the corresponding first-stage estimates (equation (5)). The unit of observation is a 1×1 grid-cell k. 'Any city by 1300 BC' equals 100 if a city was present in a grid cell k by 1300 BC and 0 otherwise. 'Transit index' is defined by equation (2), while 'IV Transit index' is defined by equation (3). 'Farming land' is 1) the share of cropland area in the grid cell in 3000 BC (column 1); 2) the Net Primary Production using reconstructed climatic conditions in 3000 BC (column 2); 3) the Caloric Suitability index (Galor and Özak, 2015) (column 3); 4) the fraction of land suitable for agriculture (Ramankutty et al., 2002) (column 4). Standard errors clustered at the level of 5×5 degree grid cells are reported in parentheses. Standard errors computed using the approach of Conley (1999) (cut-off 1000km) are reported in square brackets. * $p < 0.10$, ** $p < 0.05$, *** $p < 0.01$.

Table A.3: Transit trade and Bronze Age cities. Robustness checks

	Any City by 1000 BC (×100)			
	(1)	(2)	(3)	(4)
	Panel A: Second stage			
Transit index	0.499	0.640	0.434	0.560
	(0.155)***	(0.217)***	(0.167)***	(0.242)**
	[0.212]**	[0.294]**	[0.213]**	[0.306]*
	Panel B: First stage			
IV Transit index	0.500	0.628	0.406	0.421
	(0.051)***	(0.069)***	(0.040)***	(0.054)***
	[0.076]***	[0.105]***	[0.059]***	[0.070]***
Geography controls	Yes	Yes	Yes	Yes
Continent fixed effects	Yes	Yes	Yes	Yes
Observations	10,040	10,970	10,970	10,970
Mean dependent variable	0.289	0.419	0.419	0.419
First-stage F-statistic (5×5 grids)	97.33	81.96	101.1	60.94
First-stage F-statistic (Conley 1000km)	42.72	35.07	46.60	35.83
Robustness check	Drop extent $\boldsymbol{\alpha_{BA}}$	IV using $\boldsymbol{\alpha_{SA}}$	Controls Henderson et al. (2018)	Metal transit

Notes: Panel A of this table reports second-stage estimates of the cross-sectional 2SLS model (4). Panel B reports the corresponding first-stage estimates (equation ((5)). The unit of observation is a 1×1 grid-cell k. 'Any city by 1300 BC' equals 100 if a city was present in a grid cell k by 1300 BC and 0 otherwise. 'Transit index' is defined by equation (2), while 'IV Transit index' is defined by equation (3). Column (1) restricts the spatial extent of the analysis to grid cells not used in the estimation of the relative transport costs across different transportation modes during the Bronze Age. In column (2), the instrumental variable is constructed using the relative transport costs estimated for the Stone Age rather than the Bronze Age. Column (3) extends the set of controls by the characteristics used in Henderson et al. (2018): average temperature, precipitation, (absolute) latitude, distance to the coastline, length of the growing season, ruggedness, Kiszewski et al. (2004)'s malaria index, 14 biome indicators, and natural harbors. Column (4) controls for the transit index in gold, lead, and silver. Standard errors clustered at the level of 5×5 degree grid cells are reported in parentheses. Standard errors computed using the approach of Conley (1999) (cut-off 1000km) are reported in square brackets. * $p < 0.10$, ** $p < 0.05$, *** $p < 0.01$.

Table A.4: Transit trade and Bronze Age cities. Robustness check using HYDE 3.1 data on urban population

	IHS urban population 2000 BC						
	(1)	(2)	(3)	(4)	(5)	(6)	(7)
	OLS	**Panel A: Second stage**					
Transit index	0.119 (0.015)*** [0.024]***	0.098 (0.022)*** [0.032]***	0.070 (0.026)*** [0.037]*	0.077 (0.024)*** [0.034]**	0.104 (0.026)*** [0.033]***	0.090 (0.023)*** [0.032]***	0.071 (0.031)** [0.038]*
Proximity mines			0.080 (0.019)*** [0.031]***				0.200 (0.091)** [0.134]
Proximity croplands				0.079 (0.019)*** [0.032]**			-0.157 (0.102) [0.155]
Sea					0.320 (0.062)*** [0.095]***		0.300 (0.063)*** [0.093]***
River					0.032 (0.073) [0.077]		0.041 (0.075) [0.077]
Mountains					-0.081 (0.058) [0.064]		0.065 (0.078) [0.098]
Centrality						-0.014 (0.006)** [0.007]**	-0.005 (0.005) [0.006]
		Panel B: First stage					
IV Transit index		0.714 (0.047)*** [0.073]***	0.616 (0.045)*** [0.069]***	0.648 (0.046)*** [0.070]***	0.623 (0.049)*** [0.074]***	0.689 (0.048)*** [0.074]***	0.518 (0.048)*** [0.072]***
Continent fixed effects	Yes	Yes	Yes	Yes	Yes	Yes	
Area grid cell	Yes	Yes	Yes	Yes	Yes	Yes	Yes
Observations	10,970	10,970	10,970	10,970	10,970	10,970	10,970
Mean dependent variable	0.195	0.195	0.195	0.195	0.195	0.195	0.195
First-stage F-stat (5×5 grids)		228.2	186.1	198.8	159	205.9	115.6
First-stage F-stat (Conley 1000km)		94.31	79.31	84.67	70.40	86.39	51.60

Notes: Panel A of this table reports cross-sectional OLS and 2SLS estimates of equation (4). Panel B reports the corresponding first-stage estimates (equation (5)). The unit of observation is a 1×1 grid-cell k. 'IHS urban population 2000 BC' is the IHS of the total number of urban inhabitants in 2000 BC (source: HYDE 3.1). 'Transit index' is defined by equation (2), while 'IV Transit index' is defined by equation (3). Footnotes 31, 32, and 34 describe the construction of the controls: 'Proximity mines,' 'Proximity croplands,' and 'Centrality.' 'Sea' identifies coastline cells. 'River' identifies cells intersected by a river. 'Mountains' identifies cells with mean elevation above 15,000 feet (4,500 meters). Standard errors clustered at the level of 5×5 degree grid cells are reported in parentheses. Standard errors computed using the approach of Conley (1999) (cut-off 1000km) are reported in square brackets. * $p < 0.10$, ** $p < 0.05$, *** $p < 0.01$.

Table A.5: Transit trade and Bronze Age cities. Disentangling the transit index.

	Any City by 1300 BC							
	(1)	(2)	(3)	(4)	(5)	(6)	(7)	(8)
	Panel A: OLS							
Transit index (Transport Costs)	0.407 (0.093)*** [0.145]***				0.398 (0.089)*** [0.138]***	0.424 (0.100)*** [0.156]***	0.315 (0.077)*** [0.121]***	0.328 (0.083)*** [0.131]**
Paths to Cropland		-0.294 (0.090)*** [0.136]**			-0.044 (0.046) [0.058]			0.006 (0.045) [0.057]
Paths to Mines			0.234 (0.066)*** [0.098]**			-0.056 (0.055) [0.083]		-0.035 (0.054) [0.081]
Transit Index (Distance)				0.290 (0.068)*** [0.102]***			0.127 (0.036)*** [0.046]***	0.125 (0.035)*** [0.044]***
	Panel B: Reduced Form							
IV Transit index (Transport Costs)	0.209 (0.080)*** [0.113]*				0.208 (0.080)*** [0.113]*	0.336 (0.115)*** [0.174]*	0.191 (0.083)** [0.104]*	0.356 (0.128)*** [0.180]**
Paths to NPP		-0.517 (0.301)* [0.297]*			-0.168 (0.480) [0.383]			0.472 (0.650) [0.622]
Paths to Deposits			0.010 (0.057) [0.069]			-0.243 (0.095)** [0.144]*		-0.252 (0.099)** [0.148]*
IV Transit Index (Distance)				0.146 (0.065)** [0.093]			0.029 (0.058) [0.063]	-0.025 (0.059) [0.059]
Geography controls	Yes	Yes	Yes	Yes	Yes	Yes	Yes	Yes
Observations	10,970	10,970	10,970	10,970	10,970	10,970	10,970	10,970
Mean dependent variable	0.419	0.419	0.419	0.419	0.419	0.419	0.419	0.419

Notes: This table reports cross-sectional OLS estimates of equation (4) and cross-sectional reduced-form estimates. The unit of observation is a 1×1 grid-cell k. 'Any city by 1300 BC' equals 100 if a city was present in a grid cell k by 1300 BC and 0 otherwise. 'Transit index' is defined by equation (2), while 'IV Transit index' is defined by equation (3). 'Paths to Cropland' counts the least-cost paths intersecting the cell while connecting every grid cell in the Old World to the nearest farmland. 'Paths to Mines' counts the least-cost paths intersecting the cell while connecting every grid cell in the Old World to the nearest copper and tin mine. 'Paths to NPP counts the least-cost paths intersecting the cell while connecting every grid cell in the Old World to the nearest cell with positive estimated net primary production. 'Paths to Deposits' counts the least-cost paths intersecting the cell while connecting every grid cell in the Old World to the nearest copper and tin deposits. Geography controls include proximity to mines, proximity to croplands, sea dummy, river dummy, mountains dummy, and centrality. Standard errors clustered at the level of 5×5 degree grid cells are reported in parentheses. Standard errors computed using the approach of Conley (1999) (cut-off 1000km) are reported in square brackets. * $p < 0.10$, ** $p < 0.05$, *** $p < 0.01$.

Table A.6: Transit trade and archaeological sites: Robustness checks

	Any Site (×100)			
	(1)	(2)	(3)	(4)
	Panel A: Second stage Bahn (2000) archaeological sites			
Transit index×Bronze Age	1.820	1.500	1.957	2.648
	(0.600)***	(0.773)*	(0.765)**	(0.882)***
	[0.601]***	[0.724]**	[0.651]***	[0.714]***
	Panel B: Second stage Pleiades Gazetteer (Bagnall, 2022)			
Transit index×Bronze Age	0.630	0.844	0.390	0.775
	(0.208)***	(0.249)***	(0.332)	(0.410)*
	[0.178]***	[0.220]***	[0.283]	[0.339]**
	Panel C: First stage			
IV Transit index×Bronze Age	0.422	0.647	0.377	0.422
	(0.041)***	(0.068)***	(0.035)***	(0.054)***
	[0.044]***	[0.073]***	[0.036]***	[0.050]***
Geography controls×Bronze Age	Yes	Yes	Yes	Yes
Grid cell fixed effects	Yes	Yes	Yes	Yes
Continent×Bronze Age	Yes	Yes	Yes	Yes
Observations	20,080	21,940	21,940	21,940
Mean dependent variable Panel A	3.048	4.923	4.923	4.923
Mean dependent variable Panel B	1.001	1.964	1.964	1.964
First-stage F-statistic (5×5 grids)	106.6	91.40	117.9	61.07
First-stage F-statistic (Conley 1000km)	89.57	76.82	109.9	71.21
Check	Drop extent $\boldsymbol{\alpha_{BA}}$	IV using $\boldsymbol{\alpha_{SA}}$	Controls Henderson et al. (2018)	Metal transit

This table reports difference-in-difference 2SLS estimates of equation (6). The unit of observation is a 1×1 grid-cell k in period p (Stone Age or Bronze Age). 'Any Site' equals 100 (rather than 0) for a grid cell k in period p if there is at least one archaeological site in cell k dating from period p. 'Transit index' is defined by equation (2), while 'IV Transit index' is defined by equation (3). Geography controls include proximity to mines, proximity to croplands, sea dummy, river dummy, mountains dummy, and centrality. Panel A uses archaeological data from Bahn (2000), while Panel B uses data from Bagnall (2022). Panel C reports first-stage estimates (equation (7)). Column (1) restricts the spatial extent of the analysis to grid cells not used in the estimation of $\boldsymbol{\alpha_{BA}}$. In column (2), the instrumental variable is constructed using the relative transport costs estimated for the Stone Age rather than the Bronze Age. Column (3) extends the set of controls by the geographical features discussed in Henderson et al. (2018): average temperature, precipitation, (absolute) latitude, distance to the coastline, length of the growing season, ruggedness, Kiszewski et al. (2004)'s malaria index, 14 biome indicators, and natural harbors (interacted with the Bronze-Age dummy). Column (4) controls for the transit index in gold, lead, and silver. Standard errors clustered at the level of 5×5 degree grid cells are reported in parentheses. Standard errors computed using the approach of Conley (1999) (cut-off 1000km) are reported in square brackets. * $p < 0.10$, ** $p < 0.05$, *** $p < 0.01$.

B Additional Figures

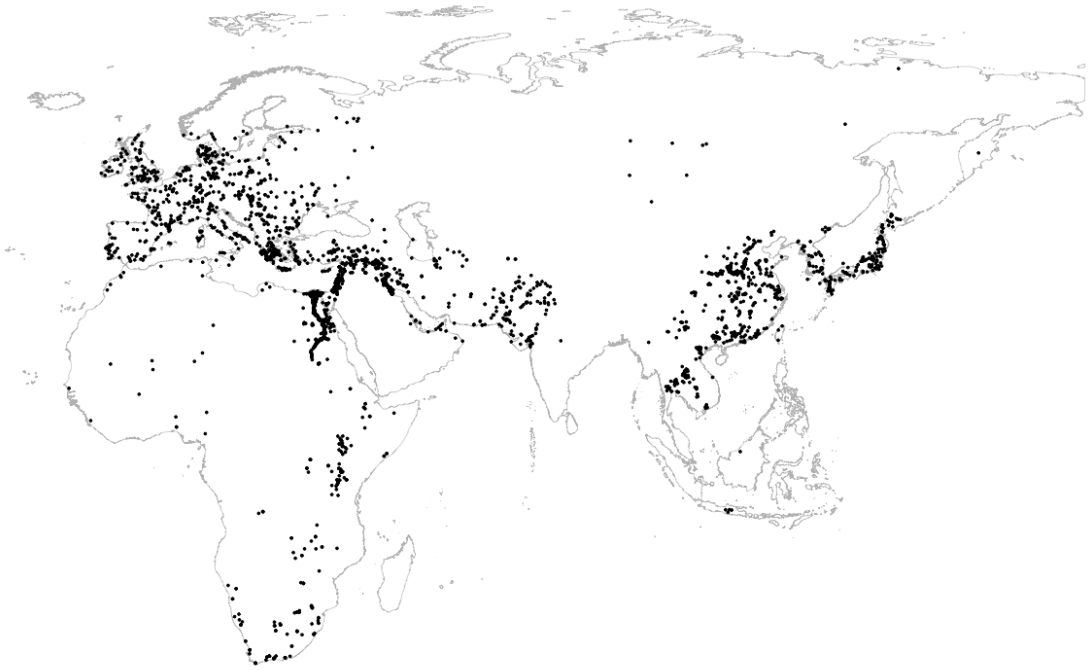

Figure B.1: Sites Bahn (2000)
Figure depicts the location of archaeological sites from Bahn (2000)'s Atlas of World Archaeology used in our analysis.

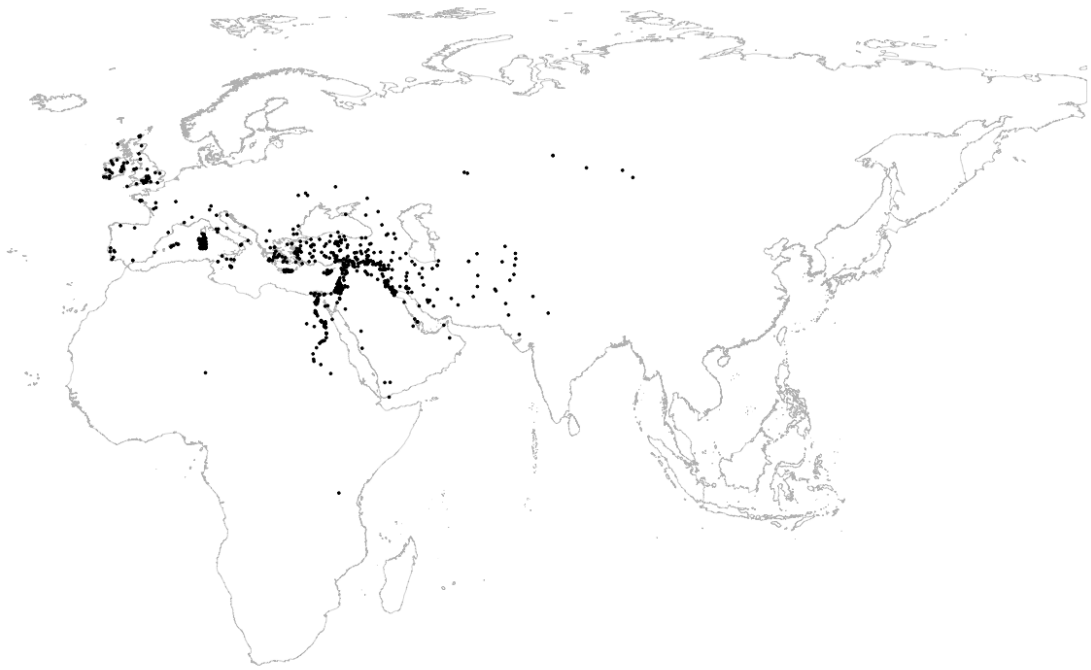

Figure B.2: Sites Pleiades Gazetteer
Figure depicts the location of archaeological sites from the Pleiades Gazetteer Bagnall (2022) used in our analysis.

Figure B.3: Sites Atlas of Chinese Relics
Figure depicts the location of archaeological sites of the Atlas of Chinese relics. Data is unavailable for provinces shaded in grey.

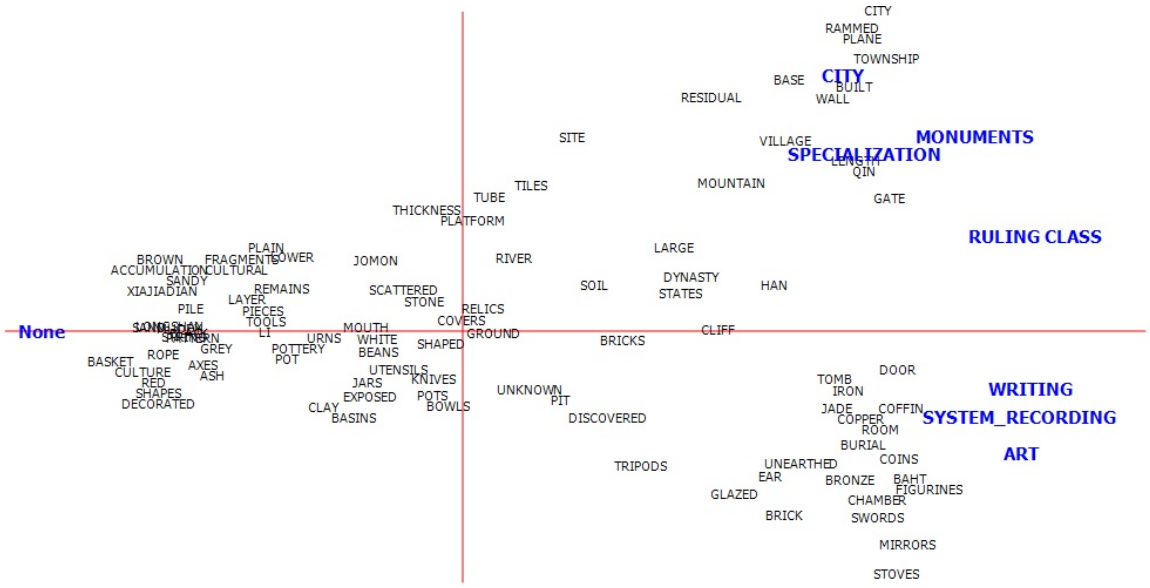

Figure B.4: Correspondence plot
Figure depicts the correspondence plot between the most frequent 100 words in the Atlas of Chinese Relics and the criteria indicative of the rise of the Urban Revolution recognized by the classifier.

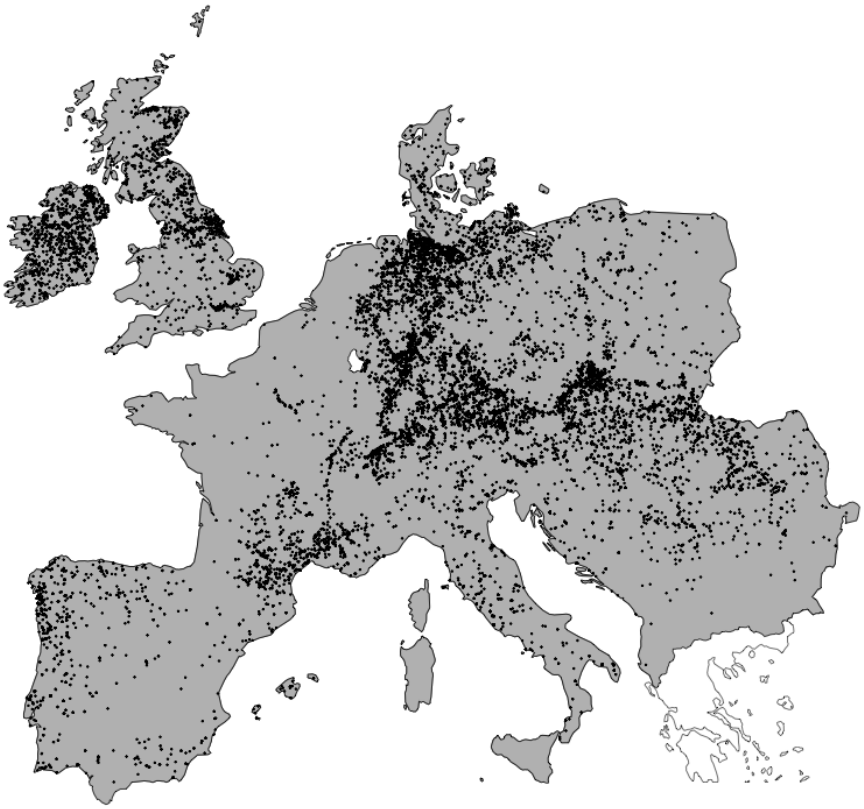

Figure B.5: Bronze weapons
Figure depicts the location of bronze weapon finds as recorded by Prähistorische Bronzefunde (*Abteilung IX* and *Abteilung IV*). Regions shaded in gray are included in our analysis.

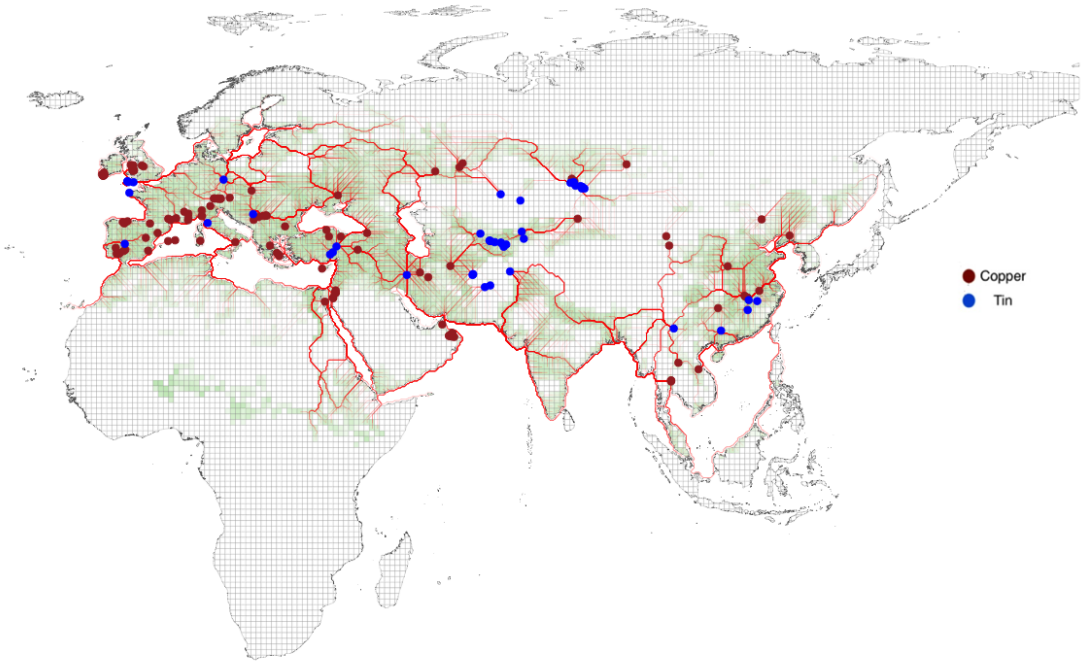

Figure B.6: Least-cost paths to mines
Figure shows least-cost paths between grid cell and mines. Copper mines are symbolized by red dots, tin mines by blue dots. The least-cost paths are drawn in red.

(a)

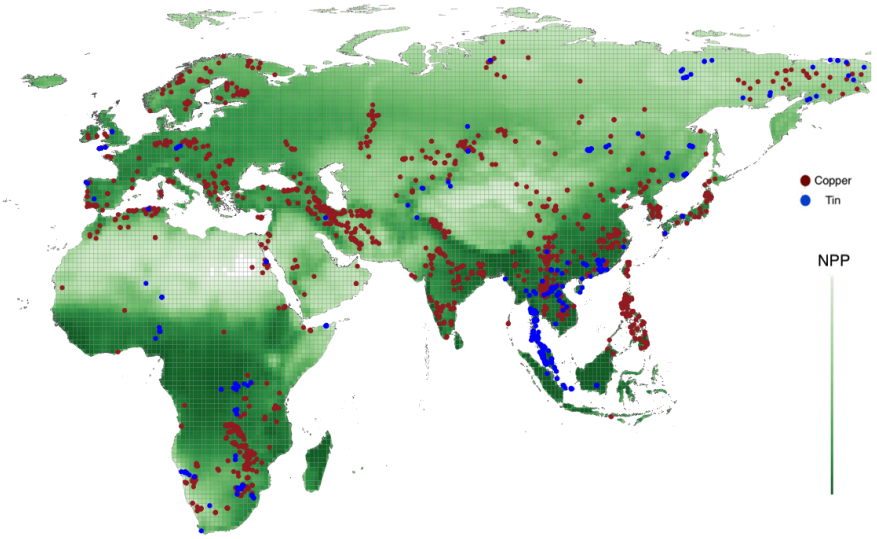

(b)

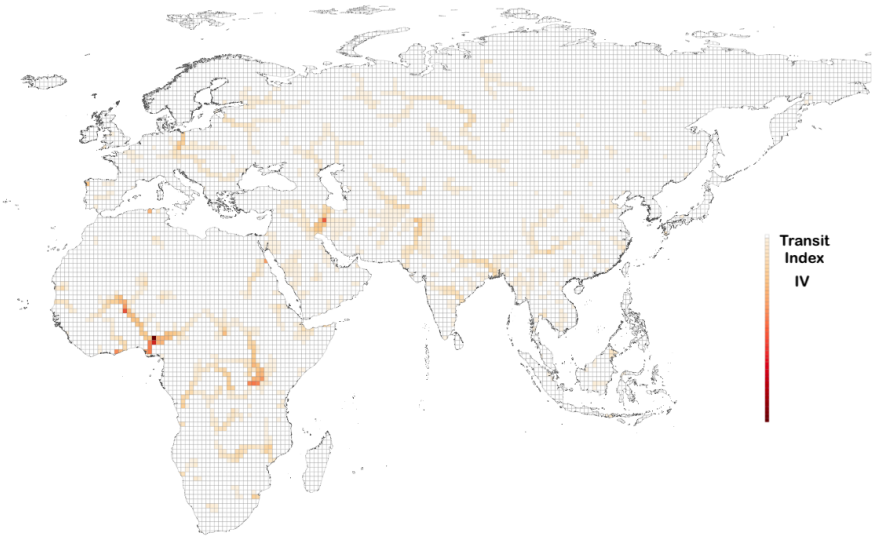

Figure B.7: Deposits, NPP and IV
Panel (a) depicts the spatial distribution copper deposits (brown dots), tin deposits (blue dots), and NPP (green shadings, where darker shadings imply higher values of NPP). Panel (b) visualises the instrumental variable (where continent fixed effects are partialled out).

Panel (a)

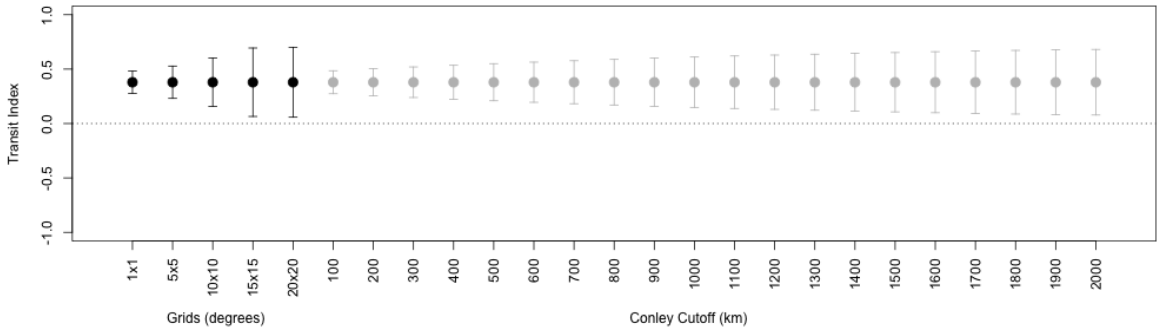

(a) Figure shows the point estimate of Table 1 (column (1)) along with alternative standard error clustering approaches. Standard errors depicted in black are clustered at grid cells of various sizes, while Conley (1999) standard errors are shown in grey using different cutoff levels.

Panel (b)

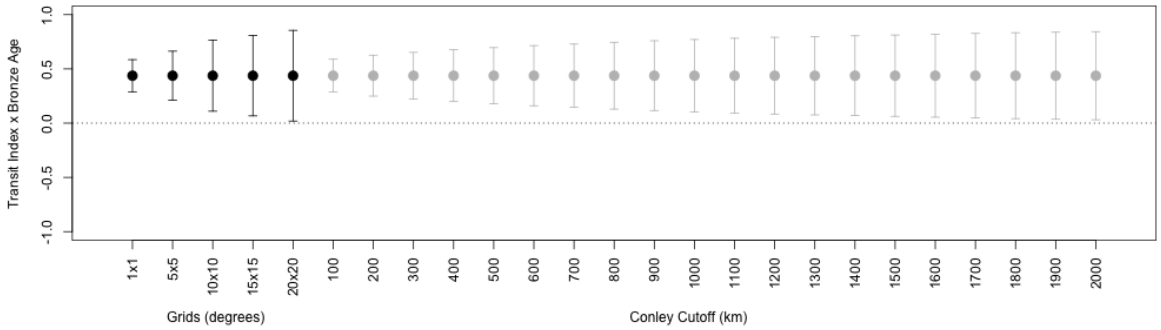

(b) Figure shows the point estimate of Table 1 (column (2)) along with alternative standard error clustering approaches. Standard errors depicted in black are clustered at grid cells of various sizes, while Conley (1999) standard errors are shown in grey using different cutoff levels.

Figure B.8: Alternative standard error clustering approaches cross-sectional data

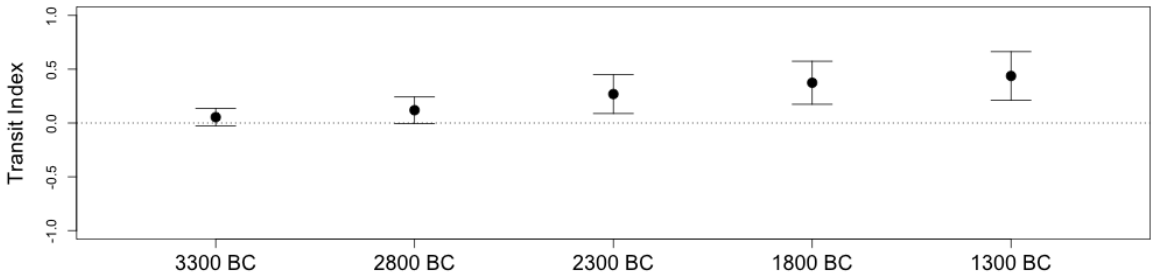

Figure B.9: Cities and transit index over time

Figure depicts 2SLS-cross-sectional IV point estimates and 90% confidence intervals of transit trade. Standard errors are clustered at the level of 5×5 degree grid cells. Dependent variable is a dummy equal to one if a city site was present in a given 1×1 degree grid and period. Variable is multiplied by hundred to facilitate interpretation.

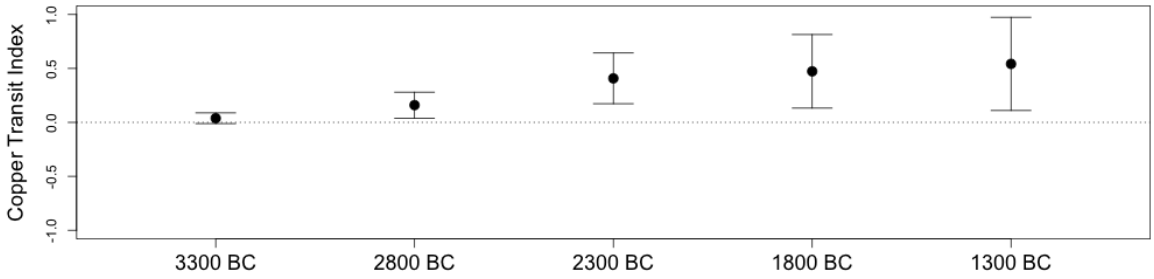

Figure B.10: Cities and copper transit index over time
Figure depicts 2SLS-cross-sectional IV point estimates and 90% confidence intervals of transit trade. Standard errors are clustered at the level of 5×5 degree grid cells. Dependent variable is a dummy equal to one if a city site was present in a given 1×1 degree grid and period. Variable is multiplied by hundred to facilitate interpretation.

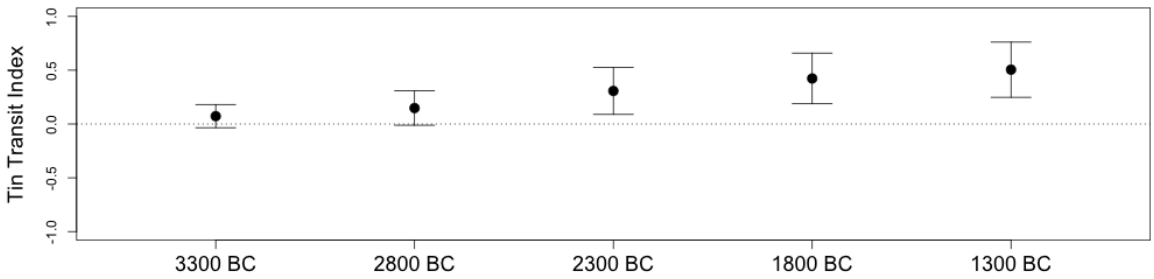

Figure B.11: Cities and tin transit index over time
Figure depicts 2SLS-cross-sectional IV point estimates and 90% confidence intervals of transit trade. Standard errors are clustered at the level of 5×5 degree grid cells. Dependent variable is a dummy equal to one if a city site was present in a given 1×1 degree grid and period. Variable is multiplied by hundred to facilitate interpretation.

Panel (a)

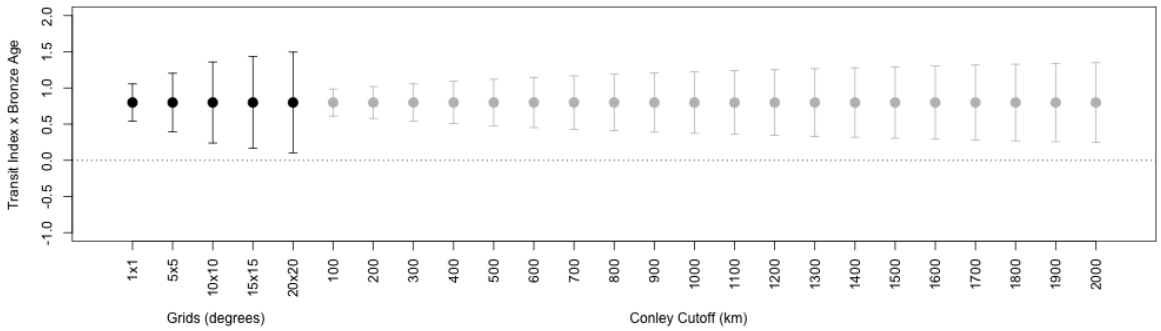

(a) Figure shows the point estimate of Table 2 (Panel A column (1)) along with alternative standard error clustering approaches. Standard errors depicted in black are clustered at grid cells of various sizes, while Conley (1999) standard errors are shown in grey using different cutoff levels.

Panel (b)

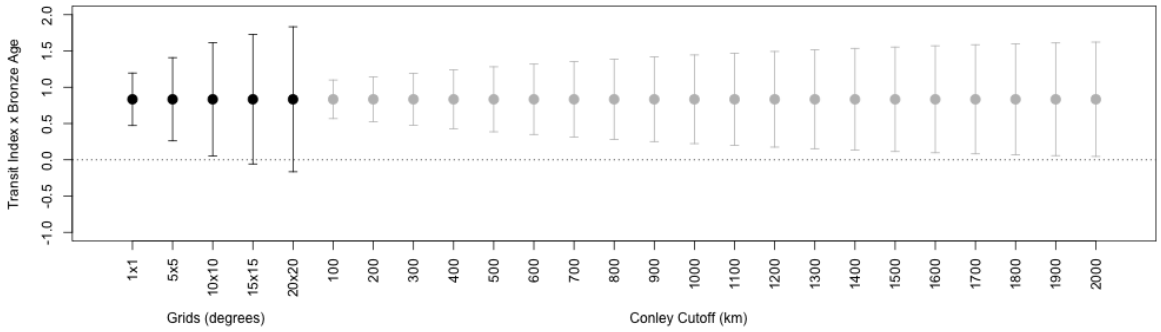

(b) Figure shows the point estimate of Table 2 (Panel A column (6)) along with alternative standard error clustering approaches. Standard errors depicted in black are clustered at grid cells of various sizes, while Conley (1999) standard errors are shown in grey using different cutoff levels.

Panel (c)

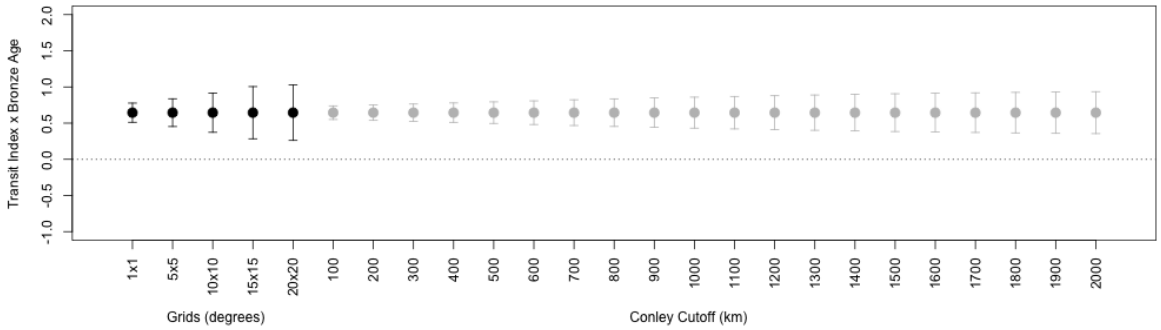

(c) Figure shows the point estimate of Table 2 (Panel B column (1)) along with alternative standard error clustering approaches. Standard errors depicted in black are clustered at grid cells of various sizes, while Conley (1999) standard errors are shown in grey using different cutoff levels.

Panel (d)

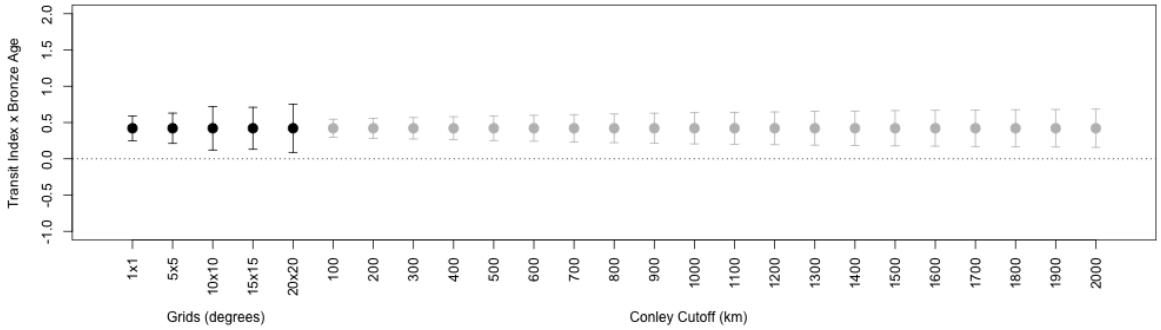

(d) Figure shows the point estimate of Table 2 (Panel B column (6)) along with alternative standard error clustering approaches. Standard errors depicted in black are clustered at grid cells of various sizes, while Conley (1999) standard errors are shown in grey using different cutoff levels.

Figure B.12: Alternative standard error clustering approaches panel data

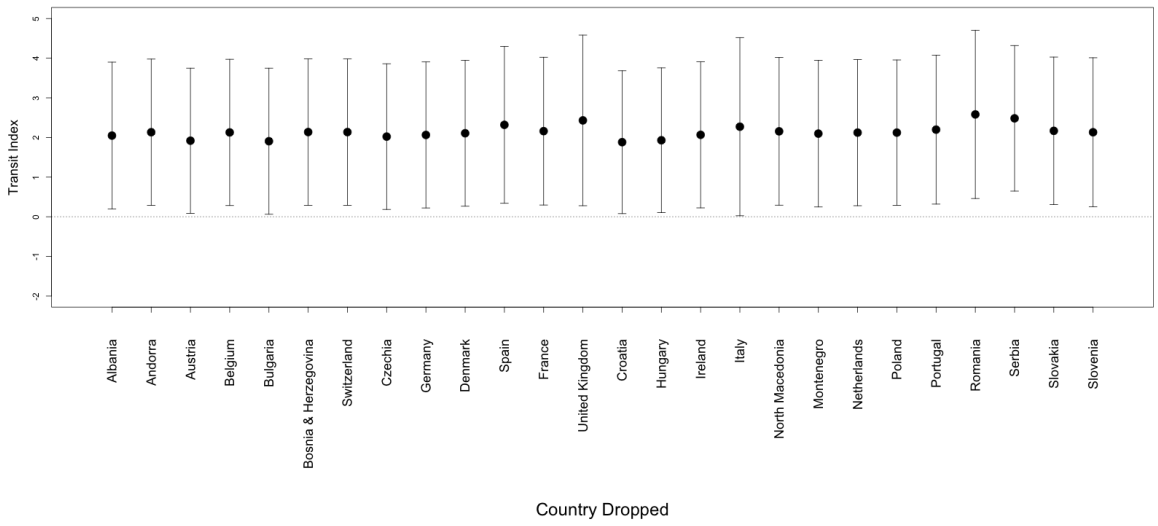

Figure B.13: Dropping one country at a time

Figure depicts point estimates and 90% confidence intervals of the effect of transit trade on the probability that an elite burial is present in a given grid cell and period, where a given country is dropped at a time. Standard errors are clustered at the level of 1×1 degree grid cells. See Sections 3 and 5.4 for details on definition, construction of variables, and regression methodology.

C Europe

This appendix reports details on the information extracted from the *Prähistorische Bronzefunde*. Figure C.1 depicts an illustrative excerpt. Table C.1 lists the references and number of artifacts per book.

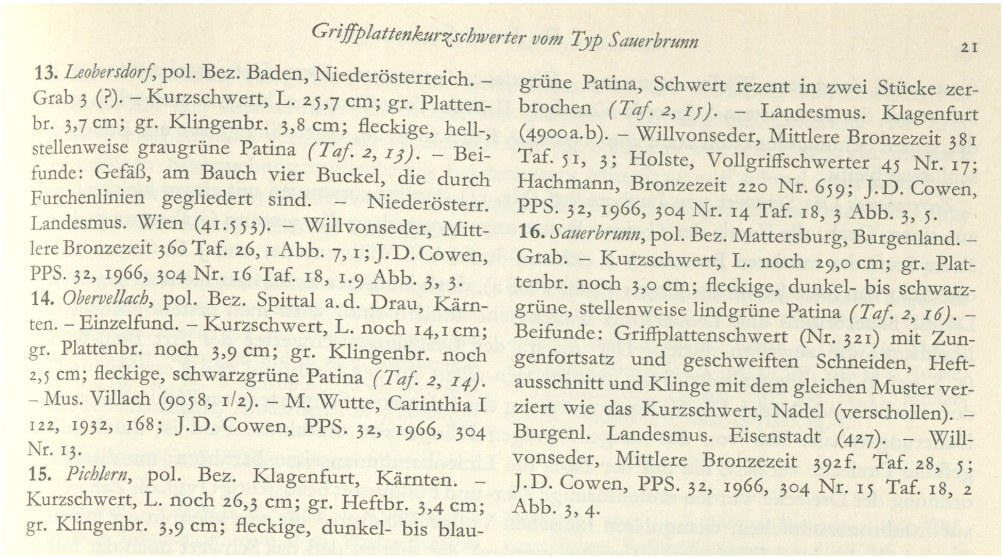

Griffplattenkurzschwerter vom Typ Sauerbrunn 21

13. *Leobersdorf*, pol. Bez. Baden, Niederösterreich. – Grab 3 (?). – Kurzschwert, L. 25,7 cm; gr. Plattenbr. 3,7 cm; gr. Klingenbr. 3,8 cm; fleckige, hell-, stellenweise graugrüne Patina *(Taf. 2, 13)*. – Beifunde: Gefäß, am Bauch vier Buckel, die durch Furchenlinien gegliedert sind. – Niederösterr. Landesmus. Wien (41.553). – Willvonseder, Mittlere Bronzezeit 360 Taf. 26, 1 Abb. 7, 1; J.D. Cowen, PPS. 32, 1966, 304 Nr. 16 Taf. 18, 1.9 Abb. 3, 3.

14. *Obervellach*, pol. Bez. Spittal a.d. Drau, Kärnten. – Einzelfund. – Kurzschwert, L. noch 14,1 cm; gr. Plattenbr. noch 3,9 cm; gr. Klingenbr. noch 2,5 cm; fleckige, schwarzgrüne Patina *(Taf. 2, 14)*. – Mus. Villach (9058, 1/2). – M. Wutte, Carinthia I 122, 1932, 168; J.D. Cowen, PPS. 32, 1966, 304 Nr. 13.

15. *Pichlern*, pol. Bez. Klagenfurt, Kärnten. – Kurzschwert, L. noch 26,3 cm; gr. Heftbr. 3,4 cm; gr. Klingenbr. 3,9 cm; fleckige, dunkel- bis blaugrüne Patina, Schwert rezent in zwei Stücke zerbrochen *(Taf. 2, 15)*. – Landesmus. Klagenfurt (4900a.b). – Willvonseder, Mittlere Bronzezeit 381 Taf. 51, 3; Holste, Vollgriffschwerter 45 Nr. 17; Hachmann, Bronzezeit 220 Nr. 659; J.D. Cowen, PPS. 32, 1966, 304 Nr. 14 Taf. 18, 3 Abb. 3, 5.

16. *Sauerbrunn*, pol. Bez. Mattersburg, Burgenland. – Grab. – Kurzschwert, L. noch 29,0 cm; gr. Plattenbr. noch 3,0 cm; fleckige, dunkel- bis schwarzgrüne, stellenweise lindgrüne Patina *(Taf. 2, 16)*. – Beifunde: Griffplattenschwert (Nr. 321) mit Zungenfortsatz und geschweiften Schneiden, Heftausschnitt und Klinge mit dem gleichen Muster verziert wie das Kurzschwert, Nadel (verschollen). – Burgenl. Landesmus. Eisenstadt (427). – Willvonseder, Mittlere Bronzezeit 392f. Taf. 28, 5; J.D. Cowen, PPS. 32, 1966, 304 Nr. 15 Taf. 18, 2 Abb. 3, 4.

Figure C.1: Entry from the book *Prähistorische Bronzefunde IV, Band 02*: page 21 of Schauer (1971).

Prähistorische Bronzefunde

Abt. IX: Äxte, Beile

Book number	Author	Book title and publication year	# Artifacts
1.	P. Harbison	The Axes of the Early Bronze Age in Ireland (1969)	2028
2.	A. Vulpe	Die Äxte und Beile in Rumänien I (1970)	580
3.	M. Novotná	Die Äxte und Beile in der Slowakei (1970)	866
4.	B.-U. Abels	Die Randleistenbeile in Baden-Württemberg, dem Elsaß, der Franche-Comté und der Schweiz (1972)	659
5	A. Vulpe	Die Äxte und Beile in Rumänien II (1975)	545
6.	L. Monteagudo	Die Beile auf der Iberischen Halbinsel (1977)	2015
7.	P. K. Schmidt and C. B. Burgess	The Axes of Scotland and Northern England (1981)	1803
8.	H. Erkanal	Die Äxte und Beile des 2. Jahrtausends in Zentralanatolien (1977)	203
9.	E. F. Mayer	Die Äxte und Beile in Österreich (1977)	1543
10.	K. Kibbert	Die Äxte und Beile im mittleren Westdeutschland I (1980)	897
11.	M.-B. Chardenoux and J.-C. Courtois	Les haches dans la France Méridionale (1979)	1806
12.	G. L. Carancini	Le asce nell'Italia continentale II (1984)	2521
13.	K. Kibbert	Die Äxte und Beile im mittleren Westdeutschland II (1984)	1000
14.	H. Todorova	Die kupferzeitlichen Äxte und Beile in Bulgarien (1981)	not Bronze Age
15.	P. Patay	Die kupferzeitlichen Meißel, Beile und Äxte in Ungarn (1984)	not Bronze Age
16.	A. Szpunar	Die Beile in Polen I (Flachbeile, Randleistenbeile, Randleistenmeißel) (1987)	616
17.	J. Říhovský	Die Äxte, Beile, Meißel und Hämmer in Mähren (1992)	1383
18.	Z. Žeravica	Äxte und Beile aus Dalmatien und anderen Teilen Kroatiens, Montenegro,Bosnien und Herzegowina (1993)	854
19.	E. Miron	Axes and Adzes from Canaan (1992)	not Europe
20.	K. Pászthory and E. F. Mayer	Die Äxte und Beile in Bayern (1998)	1219
21.	J. Kuśnierz	Die Beile in Polen III (Tüllenbeile) (1998)	892
22.	G. Eogan	The Socketed Axes in Ireland (2000)	2203
23.	F. Laux	Die Äxte und Beile in Niedersachen I (Flach-, Randleisten- und Absatzbeile) (2000)	1109
24.	M. Gedl	Die Beile in Polen IV (Metalläxte, Eisenbeile, Hämmer, Ambosse, Meißel, Pfrieme) (2004)	590
25.	F. Laux	Die Äxte und Beile in Niedersachsen II (2005)	430
26.	M. Michler	Les haches du Chalcolithique et de l'Âge du Bronze en Alsace (2013)	203
27.	D. Antonović	Kupferzeitliche Äxte und Beile in Serbien (2014)	425
		Total	26390

Table C.1: References and number of artifacts per book
Table list the references for database of European bronze artifactsFigure shows Source: page 21 of Schauer (1971).

Prähistorische Bronzefunde

Abt. IV: Schwerter

Book number	Author	Book title and publication year	# Artifacts
1.	V. Bianco Peroni	Die Schwerter in Italien. Le spade nell'Italia continentale (1970).	395
2.	P. Schauer	Die Schwerter in Süddeutschland, Österreich und der Schweiz I .	683
		(Griffplatten-, Griffangel- und Griffzungenschwerter) (1971).	683
3.	H. Reim	Die spätbronzezeitlichen Griffplatten-, Griffdorn- und Griffangelschwerter in Ostfrankreich (1974).	49
4.	P. Novák	Die Schwerter in der Tschechoslowakei I (1975).	204
5.	I. A. Colquhoun and C. B. Burgess	The Swords of Britain (1988).	765
6.	T. Kemenczei	Die Schwerter in Ungarn I (Griffplatten-, Griffangel- und Griffzungenschwerter) (1988).	420
7.	C. B. Burgess and S. Gerloff	The Dirks and Rapiers of Great Britain and Ireland (1981).	1000
8.	T. Bader	Die Schwerter in Rumänien (1991).	472
9.	T. Kemenczei	Die Schwerter in Ungarn II (Vollgriffschwerter) (1991).	550
10.	W. Krämer	Die Vollgriffschwerter in Österreich und der Schweiz (1985).	175
11.	I. v. Quillfeldt	Die Vollgriffschwerter in Süddeutschland (1995).	314
12.	I. Kilian-Dirlmeier	Die Schwerter in Griechenland (außerhalb der Peloponnes), Bulgarien und Albanien (1993).	471
13.	S. Shalev	Swords and Daggers in Late Bronze Age Canaan (2004).	not Europe
14.	A. F. Harding	Die Schwerter im ehemaligen Jugoslawien (1995).	431
15.	H. Wüstemann	Die Schwerter in Ostdeutschland (2004).	802
16.	D. Brandherm	Las Espadas del Bronce Final en la Península Ibérica y Baleares (2007).	242
17.	F. Laux	Die Schwerter in Niedersachsen (2009).	430
18.	M. Novotná	Die Vollgriffschwerter in der Slowakei (2014).	187
19.	J. Winiker	Die bronzezeitlichen Vollgriffschwerter in Böhmen (2015).	119
		Total	7709

D Period-specific per-unit transport costs

To estimate period-specific transport costs we require two main inputs: bilateral trade data and a suitable estimation framework. We describe these two components below.

D.1 Bilateral trade data

Following Flückiger et al. (2022), we reconstruct trade flows by defining the archaeological excavation site of an artifact as the destination and the production site as the origin. A first prerequisite for artifacts to be included in our analysis therefore is that their find site as well as provenance can be identified. A second prerequisite is that the time period can be assigned to the artifacts (i.e., Stone or Bronze Age). To identify suitable data, we systematically scoured the archaeological literature. We identified two existing large-scale databases on trade during the Stone Age that report precise origin and destination of artifacts. Trade data for the Bronze Age represent an extended version of the database compiled in Flückiger et al. (2022). Below, we describe the characteristics of the databases as well as the aggregation process from artifact-level to regional-level trade flows. The origins and destinations of artifacts are depicted in Figure D.1. In the context of our analysis, it is important to note that the overwhelming majority of artifacts contained in our datasets were traded within Europe.

D.1.1 Stone Age trade data[43]

Alpine jade–Neolithic period The Alpine jade database was compiled by more than 50 researchers from several European countries as part of the project "JADE: Social inequalities in Neolithic Europe: the circulation of long axeheads of Alpine jades" (Pétrequin et al., 2012). The data was compiled between 2008 and 2018 and focuses on long axeheads made from jade (mainly extracted in the Alps). In total, the database contains precise information on the find site of 2,173 jade axeheads which can be downloaded at http://jade.univ-fcomte.fr. These axes mainly circulated within Europe during the 5th and 4th millennia BC, but some of the objects moved over long distances from the Alpes to the Atlantic coast and the Black Sea via extensive exchange networks. To identify the provenance of the axeheads, the researchers used visual analysis and spectroradiometry. For 1,355 axeheads, the database includes information on the origin of the artifacts with sufficient precision for the purpose of our analysis. The jade included in our analysis primarily originates from high-altitude quarries at Monte Viso near Turin (973 pieces) and Monte Beigua near Genoa (151 pieces) in the Italian Alps. Some of the finds can also be reliably traced back to the Vosges in France or the Pennine Alps in Switzerland.

British axeheads–Early Neolithic period Schauer et al. (2020) provide an extensive database

[43]Description of the Stone Age trade data is in large parts taken from Flückiger et al. (2022).

on British axeheads that combines information collected in projects overseen by the Implement Petrology Group (IPG), the Neolithic Axehead Archive, and the Irish Stone Axe Project. The database contains precise information on the find site of 5,809 axeheads from the Early Neolithic (4100–3400 BC) discovered across England, Wales and southern Scotland. Provenance of the axeheads is identified via petrological analysis. For our analysis, we exclude axeheads made from flint (1,512 pieces) due to the fact that origins could not be unambiguously determined. We further exclude axeheads for which the source was specified as 'other' (1,766 pieces) which includes jade pieces originating from continental Europe. These restrictions leave us 2,345 artifacts for which the provenance is pinpointed within a radius of less than 50 km in Schauer et al. (2020).

D.1.2 Bronze Age trade data

We compile data on goods traded during the Bronze Age based on an extensive literature search. In total, we identify 36 separate publications (listed in Table D.1) that fulfil the criteria for inclusion in our analysis.[44] This database was partially used in Flückiger et al. (2022), we extend it to include finds beyond Western Europe. A large share of the objects contained in their database are weapons, tools, and jewellery. In total, this database encompasses 3,744 artifacts for which find site and provenance can be determined with sufficient precision. In most cases, the artifacts' provenance was identified based on metal parts, such as copper, silver, tin, or lead, using lead isotope analysis and trace element pattern analysis. In a few cases it was determined by typology of similar instruments. For more details on the methodology behind the data collection process see Online Appendix E in Flückiger et al. (2022).

D.1.3 Aggregation

For the inference of trade costs, we aggregate the information of the individual artifacts to the grid-cell-pair level. In keeping with the spatial unit of analysis of our main analysis, we first identify into which of the 1×1 degree grid cells its origin and destination fall. We then aggregate this information to the grid-cell-pair level giving us the number of finds within cell j that originate from cell i. The resulting trade volume represents the dependent variable used in the regression framework. This framework is described next.

D.2 Estimation framework

To infer period-and mode-specific per-unit distance transport costs we proceed in three steps. First, we divide the world into grid cells of 0.25×0.25 degrees and classify each grid as being

[44] I.e., the goods were traded during the Bronze Age and origin as well as destination can be precisely identified.

Table D.1: References for database of Bronze Age metals exchange

Commodity	# Items	# Destinations	# Origins	Source
Bronze axes	2	2	1	Artioli et al. (2020)
Amber jewelry and ornaments	46	1	1	Beck, Fellows and Adams (1970)
Amber jewelry	70	1	1	Beck, Southard and Adams (1972)
Copper ingots	47	6	1	Begemann et al. (2001)
Bronze weapons	9	8	5	Burgess and O'Connor (2008)
Bronze axes and copper ingots	17	2	3	Canovaro et al. (2019)
Lead utensils	71	12	2	Gale and Stos-Gale (1981)
Lead utensils	40	1	2	Gale, Stos-Gale and Davis (1984)
Copper ingots and lead artifacts	614	7	3	Gale and Stos-Gale (2005)
Copper ingots	79	4	1	Gale (2006)
Copper artifacts	120	1	1	Giumlia-Mair (2005)
Copper artifacts	24	2	1	Hauptmann, Begemann and Schmitt-Strecker (1999)
Copper ingots	8	4	1	Kaiser (2013)
Bronze axes	3	3	2	Klassen, Cassen and Pétrequin (2012)
Copper ingots	4	1	1	Kristiansen and Suchowska-Ducke (2015)
Bronze weapons	53	32	12	Ling et al. (2014)
Bronze swords	108	78	8	Ling et al. (2019)
Copper ingots and ceramic goods	3	3	2	Lo Schiavo (2005)
Tin artifacts	142	63	2	Mason (2020)
Bronze utensils	1227	21	2	Matthäus (2005)
Bronze weapons and jewelry	69	38	10	Melheim et al. (2018)
Bronze weapons	1	1	1	Montero Ruiz, Martínez Navarrete and Galán (2016)
Bronze weapons and copper utensils	13	1	3	Montero Ruiz et al. (2018)
Amber jewelry	1	1	1	Murillo-Barroso and Martinón-Torres (2012)
Amber jewelry	268	5	1	Murillo-Barroso et al. (2018)
Bronze weapons and utensils	19	19	1	Needham and Giardino (2008)
Bronze weapons	383	7	2	Pernicka, Lutz and Stöllner (2016)
Bronze weapons and jewelry	12	1	1	Pernicka et al. (2016)
Copper ingots	8	1	2	Pinarelli (2004)
Bronze axes and copper ingots	27	4	3	Reguera-Galan et al. (2019)
Bronze weapons and jewelry	3	1	3	Reiter et al. (2019)
Copper ingots and ceramic goods	51	8	9	Sabatini and Lo Schiavo (2020)
Silver coins	12	1	1	Stos-Gale and Gale (2009)
Bronze, tin and silver artifacts	99	21	7	Stos-Gale and Gale (2010)
Copper ingots	17	3	1	Stos-Gale (2011)
Bronze weapons	74	3	1	Williams and Le Carlier de Veslud (2019)

(a)

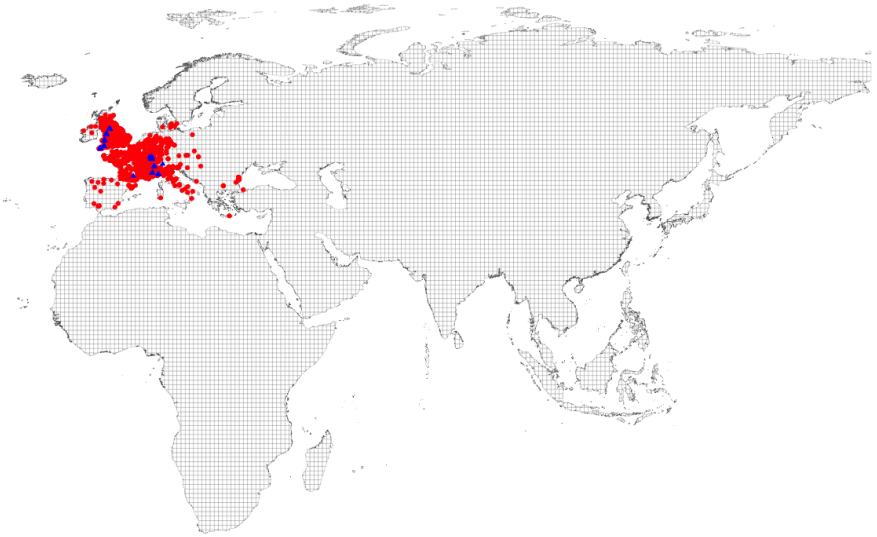

(b)

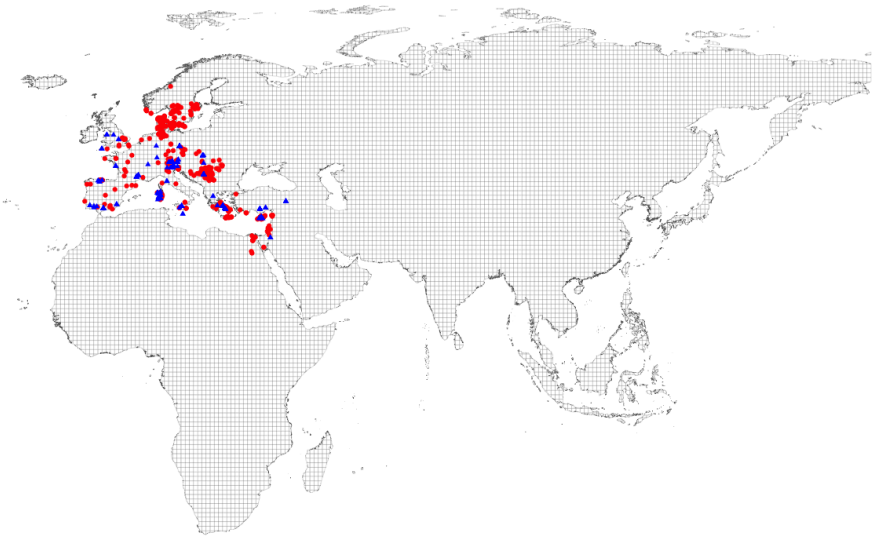

Figure D.1: Origins and Destinations of Artifacts
Panel (a) depicts origins (blue triangles) and destinations (red dots) of artifacts traded during the Stone Age. Panel (b) depicts origins (blue triangles) and destinations (red dots) of artifacts traded during the Bronze Age.

either a sea, river, or land grid.[45] The classification of grids—and equivalently transport modes—is based on spatial data from Natural Earth. As mentioned in the main part, we

[45]The relative coarse size of cells is chosen to account for the fact that coastlines as well as river courses can shift over time.

impose three restrictions: (i) maritime transport is only possible along the coast (below 60° latitude); (ii) riverine transport is only feasible on navigable rivers; and (iii) transport is not possible across high mountain ranges (above 15,000 feet). The resulting transport surface is depicted in Figure D.2.

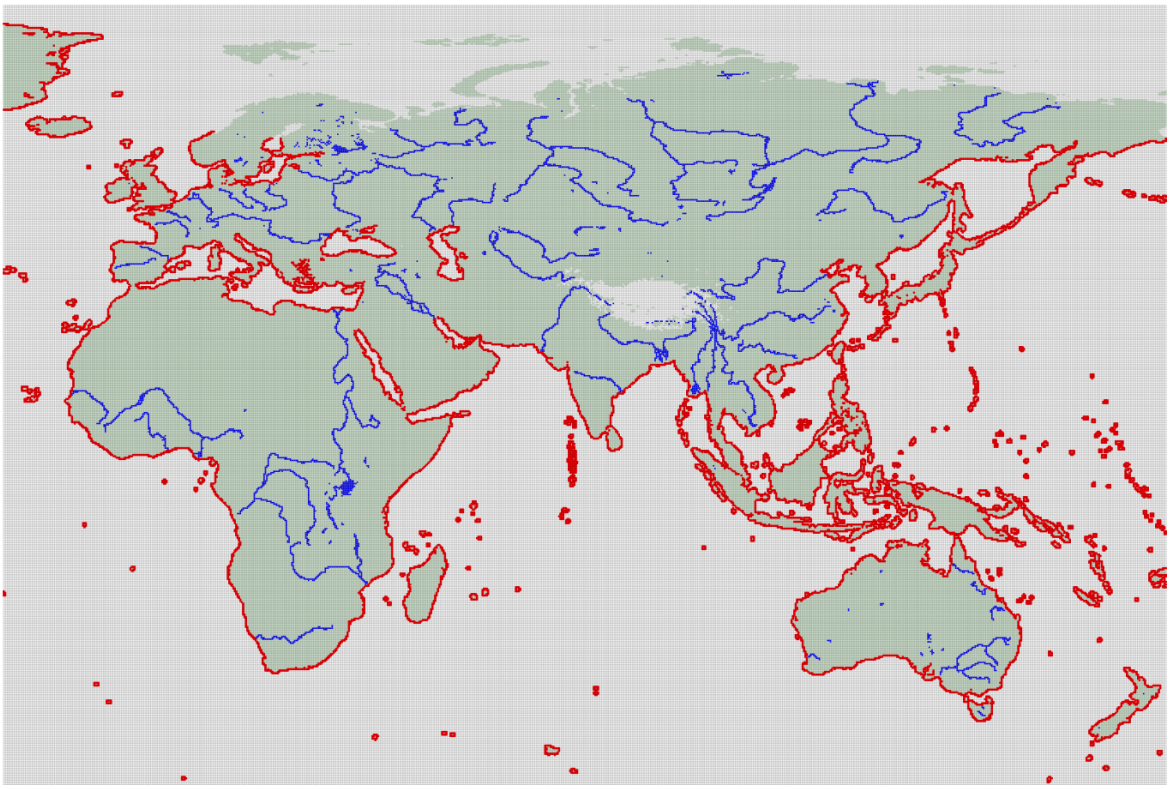

Figure D.2: Transport Cost Surface
Figure depicts transport the cost surface. Coastal sea routes are represented in red and navigable rivers in blue. Areas across which overland transport is possible are depicted in green. Size of an individual raster cell is 0.25×0.25 degree longitude/latitude.

Second, we assign (relative) per-unit-distance transport cost to each shipping mode: $\alpha^{sea}, \alpha^{river}$, and α^{land}. For the transport cost vector $\boldsymbol{\alpha} \equiv \left(1, \alpha^{river}, \alpha^{land}\right)$ we then use Dijkstra (1959)'s algorithm to identify the least-cost path and associated transport cost between any two 1×1 degree grid cells.[46] Throughout, we assume that transshipment between different transport modes is costless.

In the third step, we use the (logarithmized) costs associated with transporting goods along the least-cost path as our main explanatory variable in a standard gravity equation using the Poisson pseudo-maximum likelihood (PPML) estimator:

$$\mathcal{X}^{p}_{mf} = \exp\left(\delta \ln LC_{mf}[\boldsymbol{\alpha}] + \beta_m + \beta_f\right) + \varepsilon_{mf}, \tag{D.1}$$

[46] The geographical centres (centroids) of grid cells are set as origins and destinations.

where $\mathcal{X}^{p}_{mf}$ denotes the number of period-specific artifacts excavated in grid cell f that originate from grid cell m, as described above. The main explanatory variable—$LC_{mf}[\boldsymbol{\alpha}]$—is the cost associated with transport along the least-cost path given the transport cost vector $\boldsymbol{\alpha}$. We account for the full set of origin and destination fixed effects (represented by β_m and β_f, respectively).

Separately for each period (i.e. Stone and Bronze Age), we repeat the three-step procedure described above iterating over all cost combinations $\alpha^{sea} = [1, 20]$, $\alpha^{river} = [1, 50]$, and $\alpha^{land} = [1, 100]$. This implies that we run regression model (D.1) 100,000 times for a given period. Each time we measure model fit using the log-likelihood. Akin to Donaldson (2018) we then define the cost vector that minimises the log-likelihood as our period-specific transport costs ($\boldsymbol{\alpha_P}$). For the Bronze Age, this fit-maximising transport cost vector is given by $\boldsymbol{\alpha_{BA}} = (1, 2, 6)$, where we normalize $\alpha^{sea} = 1$ for ease of interpretation. For the Stone Age, the transport costs are $\boldsymbol{\alpha_{SA}} = (1, 1/14, 2/7)$.

E Theoretical Model

E.1 Prelude

We develop a theoretical model building upon the work of Mayshar, Moav and Pascali (2022) as a foundational framework. Our model introduces the element of interregional metal trade, a fundamental prerequisite for the emergence of the Bronze Age. Within this context, kings play a pivotal role in taxing metal trade, and we show that the optimal tax rate is contingent upon their position within the trade network. This concept leads us to define what we refer to as "blockage costs", representing the maximum tax revenue a king can feasibly collect.

Our model comprises three distinct, crucial categories of economic agents:

(i) Farmers, who utilize cropland and metals to cultivate crops.

(ii) Traders, responsible for transporting metals from mines to farmers. They are subject to taxation and face the risk of bandit raids.

(iii) Foragers, who serve as an alternative resource for bandits and tax collectors.

We analyze two potential states within this framework:

1. Anarchy: In this scenario, a given region is governed by bandits, leading to a lack of centralized authority.

2. Hierarchy: Conversely, under a hierarchical system, kings wield a monopoly on violence to deter banditry and levy taxes on traders as a means to finance their state.

In the following sections, we will provide a detailed description of each agent type and state.

E.2 Farmers

In our economic model, we make the assumption that farmers in region/cell k utilize their cropland, denoted as L_k, and metals, represented as M_k, as perfect complements in the production of crops. This relationship is mathematically expressed as:

$$Y_k = \min \{M_k, L_k\} . \tag{E.1}$$

Consequently, the demand for metals in cell k corresponds to the value of Y_k.

We further assume that crops are sufficiently valuable, implying it is always optimal to produce them, regardless of the prevailing metal prices. Additionally, in our model, we assume that if cell k contains cropland, $L_k = 1$, and if it does not contain cropland, $L_k = 0$.

Consequently, the demand for metals in cell k can be described as follows:

$$M_k = M = \begin{cases} 1 & \text{in cells with cropland,} \\ 0 & \text{in cells without cropland.} \end{cases} \tag{E.2}$$

This formulation delineates the metal demand in two distinct scenarios: one in regions with cropland and the other in regions devoid of cropland.

E.3 Traders

In our economic model, traders play a crucial role in the metal trade process, transporting metals from the mines to specific cells and selling them to farmers. The revenue earned by traders is determined by the quantity of metals they sell, while their costs are influenced by the effort required to transport metals to the farmers.

We make the assumption of perfect competition among traders for each transport route, meaning that metals from each mine to each destination cell are traded under perfect competition conditions. Since we assume uniform production costs across all mines, metal prices at different mines are homogeneous, with trade costs fully determining the prices at the destination cell. Consequently, each destination cell will source its metals from only one mine, specifically the one offering the lowest transportation costs.

Traders navigate along transport routes connecting mines and cells. Given that space is organized into grid cells, the length of these transport routes is measured in terms of the number of grid cells they traverse. Each transport route is associated with route-specific total trade costs, which depend on the sum of transport mode-specific transport costs per cell,[47] denoted as t, along the route and the quantity of metals shipped. Additionally, kings have the authority to levy taxes on traders passing through their cells. In instances where traders pass through cells without a ruling king, they are susceptible to being raided by bandits.

Traders make their route choices based on a least-cost criterion, taking into account both transport costs and taxes. Least cost routes are transport routes with the lowest combined trade costs that connect supply (mines) and demand (grid cells with crop). We denote the least-cost path from mine m to farmers in cell f by $P^{\star}_{mf}$. On a specific route, $P^{\star}_{mf}$, traders may have to pay multiple taxes in addition to pure transport costs, depending on the cells $k \in K$ that the route passes. We denote the total amount of taxes paid for a trader bringing metals from a mine in cell m to a farmer in cell f as T_{mf}.

[47] These cell-specific transport costs are defined by the cheapest available transport mode in k:

$$t_k = \begin{cases} \alpha_{sea} & \text{if} \quad k \in \text{sea grid,} \\ \alpha_{river} & \text{if} \quad k \in \text{river grid,} \\ \alpha_{land} & \text{if} \quad k \in \text{land grid.} \end{cases} \tag{E.3}$$

We now introduce the term *least costs*. These costs encompass the total trade expenses linked to a particular least-cost path and are represented by the notation $LC[t, M, T]$. We assume that traders independently optimize each route, meaning there are no economies of scale gained by serving different routes. Furthermore, there are no capacity constraints regarding the number of routes served.

Given the externally determined costs of metals at the mine ($c_m = c$), the profit function for traders engaged in the sale of metals from mines in cell m to farmers in cell f is defined as follows:

$$\pi^T_{mf} = p_f M - cM - LC_{mf}\left[t_{mf,k}, M, T_{mf,k}\right]. \tag{E.4}$$

The first-order conditions for traders are given by:

$$p_f - c - \frac{\partial LC_{mf}\left[t_{mf,k}, M, T_{mf,k}\right]}{\partial M} \stackrel{!}{=} 0. \tag{E.5}$$

To derive more concrete results, we assume a specific functional form for the least-cost calculations:

$$LC_{mf}\left[t_{mf,k}, M, T_{mf,k}\right] = \min_{P_{mf} \in \mathcal{P}_f} \sum_{k \in K} \left(t^{\rho}_k + \tau^T_{mf,k} + \tau^B_{mf,k}\right) \mathcal{I}_{P_{mf}}[k]\, cM. \tag{E.6}$$

Here, $\mathcal{I}_{P_{mf}}[k]$ is the indicator function:

$$\mathcal{I}_{P_{mf}}[k] = \begin{cases} 1 & \text{if} \quad k \in P_{mf}, \\ 0 & \text{if} \quad k \notin P_{mf}, \end{cases} \tag{E.7}$$

that equals one if the path from m to f, denoted as P_{mf}, passes through cell k, and zero otherwise. Essentially, this indicator function captures all cells belonging to a specific path from m to f. Furthermore, $\mathcal{P}_f$ are all potential paths from all available mines to f. The transport costs in cell k, denoted as t^{ρ}_k, are determined by the most cost-effective transport mode available in that cell. Additionally, traders may be subject to taxes, $T^T_{mf,k}$, imposed by the king governing cell k along the route from m to f. Alternatively, if cell k is not under the rule of a king, traders may pay tolls, $T^B_{mf,k}$, to bandits for metals transported from m to f through that cell.

The total costs of transporting metals from cell m to cell f are calculated as the sum over all cells k that the path $P^{\star}_{mf}$ passes through. In other words, this includes all cells where the indicator function $\mathcal{I}_{P_{mf}}[k]$ for the path P_{mf} is one.

The least-cost path, denoted as $P^{\star}_{mf}(t_{mf,k}, M, T_{mf,k})$, represents the path with the lowest costs, for transporting metals to destination cell f, where m is the mine that serves cell f at the lowest trade costs.

Based on our assumptions, metal transport exclusively occurs on paths of the form $P^{\star}_{mf}$,

meaning that each farming cell f is exclusively supplied by a single mine f.

Metal prices (p_f) can be expressed as follows:

$$p_f = c\left(1 + \sum_{k \in K}\left(t_k^{\rho} + \tau_{mf,k}^{T} + \tau_{mf,k}^{B}\right)\mathcal{I}_{P_{mf}^{\star}}[k]\right). \tag{E.8}$$

As there are potentially different mines that could serve location f, only the one with the lowest marginal costs will actually do so.

Given the assumption of perfect competition, profits for each route mf in equilibrium are zero:

$$\begin{aligned}
\pi_{mf}^{t} &= p_f M - cM - LC_{mf}\left[t_{mf,k}, M, T_{mf,k}\right] \\
&= p_f M - cM \\
&\quad - \sum_{k \in K}\left(t_k^{\rho} + \tau_{mf,k}^{T} + \tau_{mf,k}^{B}\right)\mathcal{I}_{P_{mf}^{\star}}[k]\, cM \\
&= \left(1 + \sum_{k \in K}\left(t_k^{\rho} + \tau_{mf,k}^{T} + \tau_{mf,k}^{B}\right)\mathcal{I}_{P_{mf}^{\star}}[k]\right) cM - cM \\
&\quad - \sum_{k \in K}\left(t_k^{\rho} + \tau_{mf,k}^{T} + \tau_{mf,k}^{B}\right)\mathcal{I}_{P_{mf}^{\star}}[k]\, cM \\
&= 0.
\end{aligned}$$

E.4 Foragers

Foragers are assumed to earn a constant income $s > 0$. Under anarchy, some foragers may turn into bandits. Under hierarchy, i.e., when a king emerges, he hires tax collectors among the foragers. Hence, foraging serves as an outside option for bandits and tax collectors.

E.5 Anarchy

In cells without a king, traders face the risk of bandit raids. $\tau_{mf,k}^{B}$ represents the toll that traders must pay to bandits for transporting metals from location m to f within cell k.

The income earned by a bandit in cell k from trade between cells m and f is determined by the following expression:

$$R_{mf,k}^{B} = \frac{\tau_{mf,k}^{B}\mathcal{I}_{P_{mf}^{\star}}[k]\, cM}{\lambda[\tau_{mf,k}^{B}]}, \tag{E.9}$$

where $\lambda[\tau_{mf,k}^{B}]$ is the measure of bandits as a function of the toll. The function $\lambda[\tau_{mf,k}^{B}]$ is strictly increasing and strictly convex. Bandits are indifferent between staying forager or

becoming a bandit. Therefore, it must be the case that:

$$\frac{\tau^B_{mf,k}\mathcal{I}_{P^\star_{mf}}[k]\,cM}{\lambda[\tau^B_{mf,k}]} = s \Rightarrow$$
$$\tau^B_{mf,k}\mathcal{I}_{P^\star_{mf}}[k]\,cM = s\lambda[\tau^B_{mf,k}].$$

For all cells that are part of at least one least-cost route, $\mathcal{I}_{P^\star_{mf}}[k] = 1$. Hence,

$$\tau^B_{mf,k}cM = s\lambda[\tau^B_{mf,k}]. \tag{E.10}$$

As c, M, and s are identical across cells, we have $\tau^B_{mf,k} = \tau^B$.

E.6 Hierarchy: Kings and Tax Collectors

We assume that kings possess a monopoly on the use of force within a cell. Establishing this monopoly involves incurring a fixed cost, denoted as G, which is greater than zero. This power enables states to deter bandits effectively.

To maintain this monopoly on violence, the king employs a certain number of tax collectors, denoted as λ, at a cost of s per tax collector from the pool of potential foragers. We can think of λ as an expropriation function, and it is assumed to be dependent on the tax rates. We also assume that it is the same function for bandits, making it strictly increasing and strictly convex as well.

Kings, being farsighted, aim to maximize their net revenue while considering the responses of traders and farmers to the tax rate. More precisely, the king in cell k selects a path-specific tax rate, $\tau^T_{mf,k}$, for each path originating from mine m that serves the destination cell f by following the least-cost path $P^\star_{mf}$. This choice aims to maximize the tax profit function within a set of constraints:

$$\max_{\tau^T_{mf,k}\geq 0} R^T_{mf,k} = \tau^T_{mf,k}\mathcal{I}_{P^\star_{mf}}[k]\,cM - s\lambda[\tau^T_{mf,k}], \tag{E.11}$$

$$M = \begin{cases} 1 & \text{in cells with cropland,} \\ 0 & \text{in cells without cropland.} \end{cases} \tag{E.12}$$

E.7 Optimal Taxes and Tax Revenues

Assuming $\mathcal{I}_{P^\star_{mf}}$ is exogenously determined, the first-order condition for $\tau^T_{mf,k}$ is given by:

$$\mathcal{I}_{P^\star_{mf}}[k]\,(cM) = s\frac{\partial\lambda[\tau^T_{mf,k}]}{\partial\tau^T_{mf,k}}. \tag{E.13}$$

The left-hand side term captures the positive direct effect of higher taxes on tax revenues, while the right-hand side term accounts for the cost increase of tax collection caused by the higher tax rate.

Denoting the optimal, path-specific tax rate as $\tau^{T,\star}_{mf,k}$, the total tax revenues of a king in cell k, R^T_k, are given by the sum of $R^{T,\star}_{mf,k}$ for all m in the set of all mines (excluding cell k itself, as we tax transit trade), $\mathcal{M}\backslash\{k\}$, and f in the set of all cells with cropland/farmers (again, excluding cell k), $\mathcal{F}\backslash\{k\}$, i.e.:

$$R^{T,\star}_k = \sum_{m\in\mathcal{M}\backslash\{k\},\, f\in\mathcal{F}\backslash\{k\}} R^{T,\star}_{mf,k} = \sum_{m\in\mathcal{M}\backslash\{k\},\, f\in\mathcal{F}\backslash\{k\}} \left(\tau^{T,\star}_{mf,k}\mathcal{I}_{P^\star_{mf}}[k]\, cM - s\lambda[\tau^{T,\star}_{mf,k}]\right). \quad \text{(E.14)}$$

Several things are noteworthy from Equations (E.13) and (E.14):

1. If the optimal least-cost path from m to f does not go through cell k, i.e., $\mathcal{I}_{P^\star_{mf}}[k] = 0$, then there is also no tax to be collected.

2. The more central cell k is in the network, the more trade flows will go through cell k, i.e., $\mathcal{I}_{P^\star_{mf}}[k]$ will be equal to one for more trade routes P_{mf}, $m \in \mathcal{M}$, $f \in \mathcal{F}$. This allows more taxes to be collected. Note that assuming that there is a unique least-cost path between each mine and destination, the betweenness centrality for cell k, T_k, is given by (see Newman, 2018, for example):

$$T_k = \sum_{m\in\mathcal{M}\backslash\{k\},\, f\in\mathcal{F}\backslash\{k\}} \mathcal{I}_{P^\star_{mf}}[k].$$

   A higher value of betweenness centrality for cell k indicates that kings in that cell have a broader tax base because a greater amount of metals will pass through their territory.

   Alternatively, we can perceive T_k as a weighted betweenness centrality, where cM serves as the weights. In this case, the more metal passing through a cell, the higher the weight attributed to it.

   We call T_k "transit index" in the main text and use as weights the amount of cropeland at origin a.

In summary, the greater the centrality of a cell, meaning the higher the volume of trade passing through it, the more substantial the resulting net tax revenues. This explains why kings tend to establish their authority in central cells, where numerous least-cost paths converge (i.e., when T_k is large), and where there is a significant amount of metal trade.

E.8 Comparing the Optimality Conditions under Anarchy and Hierarchy

Under anarchy we have:

$$\begin{aligned} \tau^B_{mf,k}\mathcal{I}_{P^\star_{mf}}[k]\,cM &= s\lambda[\tau^B_{mf,k}] \Rightarrow \\ \mathcal{I}_{P^\star_{mf}}[k]\,cM &= s\frac{\lambda[\tau^B_{mf,k}]}{\tau^B_{mf,k}}. \end{aligned} \tag{E.15}$$

Under hierarchy we have:

$$\begin{aligned} \mathcal{I}_{P^\star_{mf}}[k]\,cM &= s\frac{\partial\lambda[\tau^T_{mf,k}]}{\partial\tau^T_{mf,k}} \Rightarrow \\ \mathcal{I}_{P^\star_{mf}}[k]\,cM &= s\frac{\partial\lambda[\tau^T_{mf,k}]}{\partial\tau^T_{mf,k}}. \end{aligned} \tag{E.16}$$

The left-hand sides of Equations (E.15) and (E.16) are identical. $\lambda[\tau^B_{mf,k}]$ is strictly increasing and strictly convex and for $\tau = 0$, $\lambda[\tau = 0] = 0$, i.e, it follows that $\frac{\partial\lambda[\tau]}{\partial\tau} > \frac{\lambda[\tau]}{\tau}$ and as a consequence, we have $\tau^B_{mf,k} > \tau^T_{mf,k}$. Lower optimal taxes under hierarchy have important welfare consequences for agents in the respective cell. Traders are under perfect competition, but have lower costs of transportation. Kings are covering all their costs, otherwise they would not come into power. And bandits always earn a constant income s. Hence, the ruling of a king in a cell k leads to the same welfare or welfare-improvements for all agents directly related to cell k.

E.9 Blockage Costs

Up to this point, we have treated $\mathcal{I}_{P^\star_{mf}}[k] = 1$ as exogenous. However, whether a specific grid cell, say $k = l$, is part of a specific least-cost path depends, of course, on the tax rate set in cell l.

Intuitively (assuming that l is a segment of the least-cost route $P^\star_{mf}$), taxes in cell l cannot continually increase without limit. This is because traders have the ability to avoid high-tax grid cells by selecting alternative routes that bypass cell l. The adaptability of traders in choosing their optimal path places a constraint on the maximum tax rate that a king can impose within a particular grid cell.

For a more formal examination, let's focus on the scenario where, for a given tax rate $\tau^T_{mf,l}$, the least-cost path $P^\star_{mf}$ includes cell l, which is to say that $\mathcal{I}_{P^\star_{mf}}[l] = 1$.

With the assumption that $\tau^B_{mf,k} = \tau^B$ for all $k \in K$, the least-cost path passing through cell k is then expressed as follows:

$$LC_{mf}[t_{mf,k}, M, T_{mf,k}] = \min_{P_{mf}\in\mathcal{P}_f} \sum_{k\in K} \left(t^\rho_k + \tau^T_{mf,k} + \tau^B\right)\mathcal{I}_{P_{mf}}[k]\,cM, \tag{E.17}$$

which gives the least-cost path $P^{\star}_{mf}$, i.e., the path with the minimum costs for destination cell f to obtain metals, defining the optimal mine m.

Next, we explore the potential for increasing taxes in cell l. To assess this, we will calculate the least-cost route to serve cell f when we eliminate cell l from the network, meaning that traders will use an alternative path to avoid cell l:

$$LC^{\setminus\{l\}}_{mf}\left[t_{mf,k}, M, T_{mf,k}\right] = \min_{P_{mf}\in\mathcal{P}_f} \sum_{k\in K\setminus\{l\}} \left(t^{\rho}_{k} + \tau^{T}_{mf,k} + \tau^{B}\right) \mathcal{I}_{P_{mf}}[k]\, cM. \tag{E.18}$$

Thus, $LC^{\setminus\{l\}}_{mf}\left[t_{mf,k}, M, T_{mf,k}\right]$ represents the lowest costs associated with the least-cost path $P^{\star}_{mf}$ for serving cell f when using cell l is not an option.

The disparity between $LC^{\setminus\{l\}}_{mf}\left[t_{mf}, M, T_{mf}\right]$ and $LC_{mf}\left[t_{mf}, M, T_{mf}\right]$ indicates the maximum possible tax increase in cell l before traders become indifferent to switching to an alternative transportation route, bypassing cell l to avoid paying taxes there.

In a similar manner, we can compute the total maximum tax that a king can impose in cell l. To do this, we calculate the sum of the differences between all least-cost paths passing through cell l and their respective second-best routes (without cell l), which traders can use. In essence, we "block" grid cell l for transit trade:

$$\begin{aligned}
B_l &= \sum_{m\in\mathcal{M}\setminus\{l\},\, f\in\mathcal{F}\setminus\{l\}} B_{mf,l} = \sum_{m\in\mathcal{M}\setminus\{l\},\, f\in\mathcal{F}\setminus\{l\}} \left(LC^{\setminus\{l\}}_{mf} - LC_{mf}\right) \\
&= \sum_{m\in\mathcal{M}\setminus\{l\},\, f\in\mathcal{F}\setminus\{l\}} \Bigg(\min_{P_{mf}\in\mathcal{P}_f} \sum_{k\in K\setminus\{l\}} \left(t^{\rho}_{k} + \tau^{T}_{mf,k} + \tau^{B}\right) \mathcal{I}_{P_{mf}}[k]\, cM \\
&\quad - \min_{P_{mf}\in\mathcal{P}_f} \sum_{k\in K} \left(t^{\rho}_{k} + \tau^{T}_{mf,k} + \tau^{B}\right) \mathcal{I}_{P_{mf}}[k]\, cM \Bigg) \\
&= \sum_{m\in\mathcal{M}\setminus\{l\},\, f\in\mathcal{F}\setminus\{l\}} \Bigg(\min_{P_{mf}\in\mathcal{P}_f} \sum_{k\in K\setminus\{l\}} \left(t^{\rho}_{k} + \tau^{T}_{mf,k} + \tau^{B}\right) \mathcal{I}_{P_{mf}}[k] \\
&\quad - \min_{P_{mf}\in\mathcal{P}_f} \sum_{k\in K} \left(t^{\rho}_{k} + \tau^{T}_{mf,k} + \tau^{B}\right) \mathcal{I}_{P_{mf}}[k] \Bigg) cM.
\end{aligned} \tag{E.19}$$

The blockage costs B_l are similar in spirit to the efficiency centrality (see Wang, Du and Deng, 2017) and the modified efficiency centrality (see Wang, Wang and Deng, 2019). They represent the total trade cost increase the network will incur, if grid cell l is removed from the network.

They also determine the maximum amount of taxes that the king can collect on each path P_{mf} while keeping traders indifferent between using this path or bypassing cell l and switching to another path. Thus, if a king in cell l already taxes traders transporting metals from mine m to farmers in cell f by an amount of $\tau^{T}_{mf,l}$, the maximum additional tax amount $\bar{\tau}^{T}_{mf,l}$ that

the king can collect before traders opt to avoid passing through cell l is given by:

$$\bar{\tau}^T_{mf,l} = \max \Bigg\{ \min_{P_{mf} \in \mathcal{P}_f} \sum_{k \in K \setminus \{l\}} \left(t^\rho_k + \tau^T_{mf,k} + \tau^B \right) \mathcal{I}_{P_{mf}}[k] \\ - \min_{P_{mf} \in \mathcal{P}_f} \sum_{k \in K} \left(t^\rho_k + \tau^T_{mf,k} + \tau^B \right) \mathcal{I}_{P_{mf}}[k], 0 \Bigg\}. \tag{E.20}$$

Whenever the optimal tax is above the current level plus the maximum additional amount of the tax, i.e., $\tau^T_{mf,l} + \bar{\tau}^T_{mf,l}$, tax revenues will be zero—since traders would switch to another path. Hence, $\bar{\tau}^T_{mf,l}$ is directly linked to the indicator function:

$$\mathcal{I}_{P^\star_{mf}}[l] = \begin{cases} 1 & \text{if} \quad \tau^{T,\star}_{mf,l} < \tau^T_{mf,l} + \bar{\tau}^T_{mf,l}, \\ 0 & \text{else.} \end{cases} \tag{E.21}$$

Using the definition of $\bar{\tau}^T_{mf,l}$, we can write the blockage costs as follows:

$$B_l = \sum_{m \in \mathcal{M} \setminus \{l\},\, f \in \mathcal{F} \setminus \{l\}} \bar{\tau}^T_{mf,l} cM. \tag{E.22}$$

This shows that blockage costs B_l reflect the maximum additional total tax revenue that a king in cell l can generate, on top of the income already obtained through $\tau^T_{mf,l}$. If we assume that $\tau^T_{mf,l} = 0$ for all m and f, then B_l becomes the total maximum amount of taxes that the king in cell l can collect. However, there is a lower limit on the total tax revenue for a king in cell l to be sustainable, considering the fixed costs G, where G is greater than zero. Therefore, we can establish that B_l must be greater than or equal to $R^{T,\star}_l$ given in Equation (E.14), and this, in turn, must be greater than or equal to G.

F Computing the blockage cost

We compute the blockage cost for a given grid cell l using the following procedure:

1. Block cell l for transit trade.
2. For all paths from mine cells m to farmland cells f identify the least-cost path when cell l is blocked. Denote the costs associated with this path by $LC_{mf}^{\setminus\{l\}}$. To proxy for the volume of trade, the croplands area is used, i.e., the least-costs are based on $Crop_f$ (corresponding to M in our theory).
3. Compute the difference between the transport cost in the restricted and unrestricted case (i.e., when trade through all cells is possible).
   Formally: $B_{mf,l} = LC_{mf}^{\setminus\{l\}} - LC_{mf}$, where $B_{mf,l}$ represents the additional transport costs incurred by cell f when grid l is blocked. The total cost in the unrestricted case is represented by LC_{mf}.
4. Compute the total blockage cost resulting from blocking cell l as the sum of additional transport costs across all optimal paths from mines to farmlands.
   Formally: $B_l = \sum_{m \in \mathcal{M}\setminus\{l\}, f \in \mathcal{F}\setminus\{l\}} B_{mf,l}$, where B_l is the total blockage cost for l.

References

Artioli, Gilberto, Caterina Canovaro, Paolo Nimis, and Ivana Angelini. 2020. "LIA of Prehistoric Metals in the Central Mediterranean Area: A Review." *Archaeometry* 62 (S1): 53–85.

Bagnall, Roger. 2022. "Pleiades: A Gazetteer of Past Places." pleiades.stoa.org.

Bahn, Paul G. 2000. *The Atlas of World Archaeology.* Checkmark Books.

Beck, Curt W., Constance A. Fellows, and Audrey B. Adams. 1970. "Analysis and Provenience of Minoan and Mycenaean Amber, III. Kakovatos." *Greek, Roman, and Byzantine Studies* 11 (1): 5–22.

Beck, Curt W., Gretchen C. Southard, and Audrey B. Adams. 1972. "Analysis and Provenience of Minoan and Mycenaean Amber, IV. Mycenae." *Greek, Roman, and Byzantine Studies* 13 (4): 359–385.

Begemann, Friedrich, Sigrid Schmitt-Strecker, Ernst Pernicka, and Fulvia Lo Schiavo. 2001. "Chemical Composition and Lead Isotopy of Copper and Bronze from Nuragic Sardinia." *European Journal of Archaeology* 4 (1): 43–85.

Burgess, Colin, and Brendan O'Connor. 2008. "Iberia, the Atlantic Bronze Age and the Mediterranean." *Contacto Cultural entre el Mediterráneo y el Atlántico (siglos XII-VIII Ane). La Precolonización a Debate. Serie Arqueológica* 11: 41–58.

Canovaro, Caterina, Ivana Angelini, Gilberto Artioli, Paolo Nimis, and Elisabetta Borgna. 2019. "Metal Flow in the Late Bronze Age across the Friuli-Venezia Giulia Plain (Italy): New Insights on Cervignano and Muscoli Hoards by Chemical and Isotopic Investigations." *Archaeological and Anthropological Sciences* 11 (9): 4829–4846.

Conley, T. G. 1999. "GMM estimation with cross sectional dependence." *Journal of Econometrics* 92 (1): 1–45.

Dijkstra, Edsger W. 1959. "A Note on Two Problems in Connexion with Graphs." *Numerische Mathematik* 1 (1): 269–271.

Donaldson, Dave. 2018. "Railroads of the Raj: Estimating the Impact of Transportation Infrastructure." *American Economic Review* 108 (4–5): 899–934.

Flückiger, Matthias, Erik Hornung, Mario Larch, Markus Ludwig, and Allard Mees. 2022. "Roman Transport Network Connectivity and Economic Integration." *The Review of Economic Studies* 8989 (2): 774–810.

Gale, Noel H. 2006. "Lead Isotope Studies-Sardinia and the Mediterranean: Provenance Studies of Artefacts Found in Sardinia." *Instrumentum* 23: 29–34.

Gale, Noel H., and Zofia A. Stos-Gale. 1981. "Lead and Silver in the Ancient Aegean." *Scientific American* 244 (6): 176–193.

Gale, Noel H., and Zofia A. Stos-Gale. 2005. "Zur Herkunft der Kupferbarren aus dem

Schiffwrack von Uluburun und der Spätbronzezeitliche Metallhandel im Mittelmeerraum." 117–132. Deutsches Bergbau-Museum.

Gale, Noel H., Zofia A. Stos-Gale, and Jack L. Davis. 1984. "The Provenance of Lead Used at Ayia Irini, Keos." *Hesperia: The Journal of the American School of Classical Studies at Athens* 53 (4): 389–406.

Galor, Oded, and Ömer Özak. 2015. "Land Productivity and Economic Development: Caloric Suitability vs. Agricultural Suitability,." Brown University Working Paper.

Galor, Oded, and Ömer Özak. 2016. "The Agricultural Origins of Time Preference." *American Economic Review* 106 (10): 3064–3103.

Giumlia-Mair, Alessandra. 2005. "Handel und Rohstoffgewinnung im Italien der Späten Bronzezeit." 415–430. Deutsches Bergbau-Museum.

Hauptmann, Andreas, Friedrich Begemann, and Sigrid Schmitt-Strecker. 1999. "Copper Objects from Arad: Their Composition and Provenance." *Bulletin of the American Schools of Oriental Research* 314 (1): 1–17.

Henderson, J Vernon, Tim Squires, Adam Storeygard, and David Weil. 2018. "The Global Distribution of Economic Activity: Nature, History, and the Role of Trade1." *The Quarterly Journal of Economics* 133 (1): 357–406.

Kaiser, Alaina. 2013. "Copper Oxhide Ingot Marks: A Database and Comparative Analysis." Master's diss. Cornell University.

Kiszewski, A., A. Mellinger, A. Spielman, P. Malaney, S. E. Sachs, and J. Sachs. 2004. "A global index representing the stability of malaria transmission." *American Journal of Tropical Medicine and Hygiene* 70 (5): 486–498.

Klassen, Lutz, Serge Cassen, and Pierre Pétrequin. 2012. "Alpine Axes and Early Metallurgy." 1280–1309. Centre de Recherche Archéologique de la Vallée de l'Ain.

Kristiansen, Kristian, and Paulina Suchowska-Ducke. 2015. "Connected Histories: The Dynamics of Bronze Age Interaction and Trade 1500–1100 BC." *Proceedings of the Prehistoric Society* 81: 361–392.

Ling, Johan, Eva Hjärthner-Holdar, Lena Grandin, Zofia A. Stos-Gale, Kristian Kristiansen, Anne L. Melheim, Gilberto Artioli, Ivana Angelini, Rüdiger Krause, and Caterina Canovaro. 2019. "Moving Metals IV: Swords, Metal Sources and Trade Networks in Bronze Age Europe." *Journal of Archaeological Science: Reports* 26: 1–34.

Ling, Johan, Zofia A. Stos-Gale, Lena Grandin, Kjell Billström, Eva Hjärthner-Holdar, and Per-Olof Persson. 2014. "Moving Metals II: Provenancing Scandinavian Bronze Age Artefacts by Lead Isotope and Elemental Analyses." *Journal of Archaeological Science* 41: 106–132.

Lo Schiavo, Fulvia. 2005. "Metallhandel im Zentralen Mittelmeer." 399–414. Deutsches

Bergbau-Museum.

Mason, Andrea H. 2020. "Provenance of Tin in the Late Bronze Age Balkans: Preparation of Cassiterite for Sn Isotope Analysis and the Probabilistic and Spatial Analysis of Sn Isotopes." PhD diss. City University of New York.

Matthäus, Hartmut. 2005. "Kulturaustausch, Handel und Seefahrt im Mittelmeerraum während der Späten Bronzezeit." 333–366. Deutsches Bergbau-Museum.

Mayshar, Joram, Omer Moav, and Luigi Pascali. 2022. "The Origin of the State: Land Productivity or Appropriability?" *Journal of Political Economy* 130 (4): 1091–1144.

Melheim, Anne L., Lena Grandin, Per-Olof Persson, Kjell Billström, Zofia A. Stos-Gale, Johan Ling, Alan Williams, Ivana Angelini, Caterina Canovaro, Eva Hjärthner-Holdar, and Kristian Kristiansen. 2018. "Moving Metals III: Possible Origins for Copper in Bronze Age Denmark Based on Lead Isotopes and Geochemistry." *Journal of Archaeological Science* 96: 85–105.

Montero Ruiz, Ignacio, Isabel Martínez Navarrete, and Eduardo Galán. 2016. "Objetos o Materia Prima: Problemas en la Interpretación de Procedencias con Análisis de Isotopos de Plomo." *Boletín del Museo Arqueológico Nacional* 34: 81–98.

Montero Ruiz, Ignacio, María R. Manunza, Fulvia Lo Schiavo, Paolo Valera, José I. Ibarguchi, Nuria Rafel Fontanals, and Pau Sureda. 2018. "The Funtana Coberta-Ballao Hoard: New Copper Provenances in Nuragic Metallurgy." Vol. 56 of *Monographies Instrumentum*, 137–164. Éditions Mergoil.

Murillo-Barroso, Mercedes, and Marcos Martinón-Torres. 2012. "Amber Sources and Trade in the Prehistory of the Iberian Peninsula." *European Journal of Archaeology* 15 (2): 187–216.

Murillo-Barroso, Mercedes, Enrique Peñalver, Primitiva Bueno, Rosa Barroso, Rodrigo de Balbín, and Marcos Martinon-Torres. 2018. "Amber in Prehistoric Iberia: New Data and a Review." *PLOS One* 13 (8): 1–36.

Needham, Stuart, and Claudio Giardino. 2008. "From Sicily to Salcombe: A Mediterranean Bronze Age Object from British Coastal Waters." *Antiquity* 82 (315): 60–72.

Newman, Mark E. J. 2018. *Networks: An Introduction.* 2 edition. Oxford University Press.

Pernicka, Ernst, Bianka Nessel, Mathias Mehofer, and Elvira Safta. 2016. "Lead Isotope Analyses of Metal Objects from the Apa Hoard and Other Early and Middle Bronze Age Items from Romania." *Archaeologia Austriaca* 100: 57–86.

Pernicka, Ernst, Joachim Lutz, and Thomas Stöllner. 2016. "Bronze Age Copper Produced at Mitterberg, Austria, and Its Distribution." *Archaeologia Austriaca* 100: 19–55.

Pétrequin, Pierre, Serge Cassen, Michel Errera, L. Klassen, Alison Sheridan, and Anne Marie Pétrequin. 2012. *Jade: Grandes haches alpines du Néolithique européen, Ve et IVe millénaires av. J.-C.* Centre de Recherche Archéologique de la Vallée de l'Ain.

Pinarelli, Laura. 2004. "Lead Isotope Characterization of Copper Ingots from Sardinia (Italy): Inferences on Their Origins." *Bulletin of the Geological Society of Greece* 36 (3): 1173–1180.

Ramankutty, Navin, Jonathan A. Foley, John Norman, and Kevin McSweeney. 2002. "The global distribution of cultivable lands: current patterns and sensitivity to possible climate change." *Global Ecology and Biogeography* 11 (5): 377–392.

Reguera-Galan, Aida, Tania Barreiro-Grille, Mariella Moldovan, Lara Lobo, Miguel A. de Blas Cortina, and José I. García Alonso. 2019. "A Provenance Study of Early Bronze Age Artefacts Found in Asturias (Spain) by Means of Metal Impurities and Lead, Copper and Antimony Isotopic Compositions." *Archaeometry* 61 (3): 683–700.

Reiter, Samantha Scott, Karin Margarita Frei, Heide Wrobel Nørgaard, and Flemming Kaul. 2019. "The Ølby Woman." *Danish Journal of Archaeology* 8: 1–22.

Sabatini, Serena, and Fulvia Lo Schiavo. 2020. "Late Bronze Age Metal Exploitation and Trade: Sardinia and Cyprus." *Materials and Manufacturing Processes* 35 (13): 1501–1518.

Schauer, Peter. 1971. *Die Schwerter in Süddeutschland, Österreich und der Schweiz I: Griffplatten-, Griffangel- und Griffzungenschwerter.* Vol. 2 of *Prähistorische Bronzefunde IV*. München: Beck.

Schauer, Peter, Andrew Bevan, Stephen Shennan, Kevan Edinborough, Tim Kerig, and Mike Parker Pearson. 2020. "British Neolithic Axehead Distributions and Their Implications." *Journal of Archaeological Method and Theory* 27: 836–859.

Stos-Gale, Zofia A. 2011. ""Biscuits with Ears": A Search for the Origin of the Earliest Oxhide Ingots." Vol. 9 of *Prehistory Monographs*, 221–229. INSTAP Academic Press.

Stos-Gale, Zofia A., and Noël H. Gale. 2009. "Metal Provenancing Using Isotopes and the Oxford Archaeological Lead Isotope Database (OXALID)." *Archaeological and Anthropological Sciences* 1 (3): 195–213.

Stos-Gale, Zofia A., and Noel H. Gale. 2010. "Bronze Age Metal Artefacts Found on Cyprus-Metal from Anatolia and the Western Mediterranean." *Trabajos de Prehistoria* 67 (2): 389–403.

Wang, Shasha, Yuxian Du, and Yong Deng. 2017. "A New Measure of Identifying Influential Nodes: Efficiency Centrality." *Communications in Nonlinear Science and Numerical Simulation* 47: 151–163.

Wang, Yunchuan, Shasha Wang, and Yong Deng. 2019. "A Modified Efficiency Centrality to Identify Influential Nodes in Weighted Networks." *Pramana* 92 (4).

Williams, Ross A., and Cécile Le Carlier de Veslud. 2019. "Boom and Bust in Bronze Age Britain: Major Copper Production from the Great Orme Mine and European Trade, C. 1600-1400 Bc." *Antiquity* 93 (371): 1178–1196.